MOLECULAR CHARACTERIZATION OF INTRINSIC AND TRANSFERABLE GENETIC ELEMENTS HARBORED BY β-LACTAMS AND COLISTIN RESISTANT GRAM-NEGATIVE BACTERIAL STRAINS

RUICHAO LI

Ph.D

The Hong Kong Polytechnic University

2017

The Hong Kong Polytechnic University

Department of Applied Biology & Chemical Technology

Molecular Characterization of Intrinsic and Transferable Genetic Elements Harbored by β-lactams and Colistin Resistant Gram-negative Bacterial Strains

Ruichao Li

A thesis submitted in partial fulfillment of the requirements for the degree of Doctor of Philosophy

November, 2016

CERTIFICATE OF ORIGINALITY

I hereby declare that this thesis is my own work and that, to the best of my knowledge and belief, it reproduces no material previously published or written, nor material that has been accepted for the award of any other degree or diploma, except where due acknowledgement has been made in the text.

_____ (Signed)

____Ruichao Li_____ (Name of student)

Abstract

The increasing prevalence of antimicrobial resistance among bacterial pathogens poses an enormous threat to human health. Although phenotypic resistance can be divided into two distinct categories, namely the intrinsic and acquired phenotypes conferred by intrinsic resistance genes or chromosomal mutations and extrinsic mobile resistance genes, the gravest threat is derived from the mobile genetic elements. However, data regarding the range of genetic elements causing a rapid increase in the prevalence of antibiotic resistance in several key pathogens in recent years are not available. In this study, we selected β-lactam resistant *Vibrio parahaemolyticus* strains and colistin resistant *Escherichia coli* strains as two model systems to investigate the molecular structures of both intrinsic and mobile resistance elements harboured by these newly emerged resistant organisms.

Molecular techniques including isolation and identification of bacteria, PCR, conjugation assay, transformation, S1-PFGE, hybridization, whole genome sequencing and comparative genomics analysis were employed to investigate the range of β-lactam resistance genes harboured by *V. parahaemolyticus*, and characterize the genetic structures of the plasmid-mediated colistin resistance gene *mcr-1* located in plasmids of *E.coli*. This work comprised three sections: First, the intrinsically ampicillin resistance gene $bla_{\text{CARB-17}}$ was identified by genome comparison of all the whole genome sequence data in NCBI and

characterized in *V. parahaemolyticus* to evaluate the function of this genetic element for the first time. A novel detection method targeting this intrinsic resistance gene was developed, conferring robust detection specificity. Second, the genetic features of extended-spectrum β-lactamases (ESBLs) - producing *V. parahaemolyticus* was characterized, with results showing that the resistance elements bla_{VEB}, $bla_{\text{CMY-2}}$ and $bla_{\text{PER-1}}$ were responsible for the resistance observed. The genetic environments of these genes were examined and various mobile elements were found to play a role in accelerating the transmission of the ESBLs genes in conjugative plasmids among *V. parahaemolyticus*. The novel $bla_{\text{PER-1}}$ harboring plasmids were compared from the evolutional perspective and comparative genomics analyses were performed to illustrate the plasmid evolution process. In the third section of this study, a thorough study on *mcr-1*-bearing plasmids was conducted and mechanisms underlying the transmission of the *mcr-1* gene between different genetic loci were elucidated.

Based on findings in this work, several conclusions can be made. The intrinsic $bla_{\text{CARB-17}}$ gene was responsible for causing the ampicillin resistance in *V. parahaemolyticus* by encoding a β-lactamase to hydrolyze the antibiotic; this chromosomal gene is an ideal maker for differentiation between *V. parahaemolyticus* from *V. alginolyticus.* ESBLs genes were found to emerge in *V. parahaemolyticus* in recent years and our works showed that various types of plasmids and mobile resistance elements possessed the ability to transfer the ESBL genes to other species.

Comparative studies of the plasmids concerned confirmed that they were the major facilitators of dissemination of resistance genes in *V. parahaemolyticus*. The types of plasmids harboring the *mcr-1* gene were found to be diverse, and a circular intermediate with the structure IS*Apl1*-*mcr-1*-*orf*-IS*Apl1*(Tn*6330*) was found to play a potential role in the dissemination of *mcr-1* between different genetic loci in plasmids. These findings provide important insight into the structures of genetic elements responsible for mediating an increasing prevalence of antibiotic resistance among Gram-negative bacterial pathogens, facilitating the prevention of emergence of new resistant strains through inhibition of transmission of specific resistance elements.

Publications arising from the thesis

1. Chiou J, Li R, & Chen S (2015) CARB-17 family of beta-lactamases mediates intrinsic resistance to penicillins in *Vibrio parahaemolyticus*. *Antimicrobial agents and chemotherapy 59(6):3593-3595.*
2. Li R, Lin D, Chen K, Wong MH, & Chen S (2015) First detection of AmpC beta-lactamase $bla_{\text{CMY-2}}$ on a conjugative IncA/C plasmid in *Vibrio parahaemolyticus* of food origin. *Antimicrobial agents and chemotherapy 59(7):4106-4111.*
3. Li R, Wong MH, Zhou Y, Chan EW, & Chen S (2015) Complete nucleotide sequence of a conjugative plasmid carrying $bla_{\text{PER-1}}$. *Antimicrobial agents and chemotherapy 59(6):3582-3584.*
4. Li R, Xie M, Lv J, Wai-Chi Chan E, & Chen S (2016) Complete genetic analysis of plasmids carrying *mcr-1* and other resistance genes in an *Escherichia coli* isolate of animal origin. *Journal of antimicrobial chemotherapy 72(3):696-699.*
5. Li R, Xie M, Zhang J, Yang Z, Liu L, Liu X, Zheng Z, Chan EW, &Chen S (2016) Genetic characterization of *mcr-1*-bearing plasmids to depict molecular mechanisms underlying dissemination of the colistin resistance determinant. *Journal of antimicrobial chemotherapy 72(2):393-401.*
6. Li R, Ye L, Zheng Z, Chan EW, & Chen S (2016) Genetic Characterization of a $bla_{\text{VEB-2}}$-carrying plasmid in *Vibrio parahaemolyticus*. *Antimicrobial agents and chemotherapy 60(11):6965-6968.*
7. Li R, Chiou J, Chan EW, & Chen S (2016) A Novel PCR-Based Approach for Accurate Identification of *Vibrio parahaemolyticus*. *Frontiers in Microbiology 7:44.*
8. Li R, Ye L, Wong MH, Zheng Z, Chan EW, &Chen S (2017) Evolution and comparative genomics of pAQU-like conjugative plasmids in *Vibrio* species. *Journal of antimicrobial chemotherapy. doi: 10.1093/jac/dkx193*
9. Li R, Ye L, Zheng Z, Chan EWC, & Chen S (2017) Genetic Characterization of Broad-Host-Range IncQ Plasmids

Harboring *bla*$_{\text{VEB-18}}$ in *Vibrio* Species. *Antimicrobial agents and chemotherapy 61(7).*

Additional publications

1. Lin DC*, et al. (2014)* Selection of target mutation in rat gastrointestinal tract *E. coli* by minute dosage of enrofloxacin. *Frontiers in Microbiology 5:468.*
2. Li R, Chan EW, & Chen S (2016) Characterisation of a chromosomally-encoded extended-spectrum beta-lactamase gene *bla*$_{\text{PER-3}}$ in *Aeromonas caviae* of chicken origin. *International journal of antimicrobial agents 47(1):103-105.*
3. Lin D*, et al. (2016)* IncFII conjugative plasmid-mediated transmission of *bla*$_{\text{NDM-1}}$ elements among animal-borne *E. coli* strains. *Antimicrobial agents and chemotherapy.*
4. Wong MH, *et al.* (2016) IncHI2 Plasmids Are The Key Vectors Responsible for OqxAB Transmission among *Salmonella spp*. *Antimicrobial agents and chemotherapy.*
5. Ye L*, et al. (2016)* Characterization of an IncA/C Multidrug Resistance Plasmid in *Vibrio alginolyticus*. *Antimicrobial agents and chemotherapy 60(5):3232-3235.*
6. Cui M*, et al. (2017)* Prevalence and Molecular Characterization of *mcr-1*-Positive *Salmonella* Strains Recovered from Clinical Specimens in China. *Antimicrobial agents and chemotherapy 61(5).*
7. Liu XB*, et al. (2017)* Molecular Characterization of *Escherichia coli* Isolates Carrying *mcr-1*, *fosA3*, and Extended-Spectrum-beta-Lactamase Genes from Food Samples in China. *Antimicrobial agents and chemotherapy 61(6).*
8. Li R*, et al.* Genetic basis of chromosomally-encoded *mcr-1* gene. Submitted.
9. Li R, et al. Efficient generation of complete sequences of MDR-encoding plasmids by rapid assembly of MinION barcoding sequencing data. Submitted.

Acknowledgments

Above all, I would like to express my sincere and deepest gratitude to my supervisor, Dr. Sheng Chen, for offering me this precious opportunity to pursue PhD study, and his continuous support, encouragement and guidance in the past three years. He is not only a wonderful academic mentor with broad knowledge and great scientific thoughts, but also a career development advisor who enlightened me on my scientific journey. With a harmonious atmosphere, I can always test new ideas with his support and learn from the mistakes. Without his patience and mentoring, it is impossible to complete my thesis on time. His passion to science and generosity to people sets a great role model for me. The training under his supervision will certainly benefit me throughout my life.

I also would like to thank Dr. Edward Chan for his help with manuscript preparation and thesis writing. He always gave me invaluable comments and constructive suggestions on my manuscripts and dissertation, which helped improve my writing skills enormously. Also, I am thankful to Dr. Linfeng Huang in City University of Hong Kong for providing the opportunity to perform whole genome sequencing and collaborating in the small RNAs project; thanks are also due to his PhD student Ms. Yingxue Li.

Additionally, I would like to acknowledge all members of the Chen's lab for their efforts in creating an enjoyable lab ambience. In

particular, I would like to thank Mr. Lianwei Ye and Ms. Miaomiao Xie for their collaboration in bacteria collection and preliminary characterization, and Dr. Jiachi Chiou for her advice in the CARB17 project. I would also thank Mr. Dachuan Lin for his valuable discussion on experimental procedures and findings, Mr. Yuanjie Zhou for sharing his valuable experience in bioinformatics and next-generation sequencing applications, Dr. Marcus Wong, Mr. Kaochao Chen and Ms. Echo Wan for their help in experiments and ordering consumables, Dr. Jiubiao Guo for his assistance in cell culture technique, Ms. Ning Dong for her help in NGS library preparations, and other lab-mates for their teamwork spirit. I would also like to thank the faculty members of the Department of Applied Biology and Chemical Technology for their help in training on equipments.

Moreover, I would like to express my gratitude to my defense committee members Dr. Zhongping Yao, Dr. Yohei Doi and Dr. Xiangdang Du for their instructive comments. Their advice helps improve the quality of this dissertation significantly.

Finally, I would like to give my heartfelt appreciation to my family for their unconditional support and understanding during my study, especially my parents, who have been the root of motivation throughout my upbringing. Furthermore, I thank my friends and

mentors who give me advice in life and career development. This dissertation is dedicated to all of you.

Table of Contents

List of Figures

List of Tables

Chapter One: Introduction

1.1 Background

Since the discovery of penicillin in 1928 by Alexander Fleming, different classes of antibiotics have been developed and put into clinical uses, (**Fig. 1.1**) saving the lives of countless numbers of people globally and significantly reducing the rate of morbidity and mortality of infectious diseases (1). However, overuse of antibiotics in both human and veterinary medicine has gradually led to impairment of the effectiveness of antibiotics by promoting the evolution and transmission of resistance-encoding genetic traits among bacterial pathogens (2, 3). Although Alexander Fleming alarmed the abuses of antibiotics as early as 1945, people only recognized the potential threat that antibiotic resistance can bring about recently. The emergence of antibiotic resistant bacteria is threatening to bring us back to the time when simple infections were often fatal. Contrary to the rapidly increasing prevalence of antibiotic resistance among major bacterial pathogens including *Staphylococcus aureus*, *Enterococcus* spp., *Pseudomonas aeruginosa*, *Acinetobacter* spp. *Enterobacteriaceae*, and *Neisseria gonorrhoeae* , the pace of development of new antibiotics has lagged far behind. To date, antibiotic resistance is not only a clinical or public health issue, it is generally agreed that devising a solution to the problem requires cooperation between academics, public health agencies, political bodies and other related

stakeholders (3, 4). Recently, the United Nations General Assembly's High-level Meeting on Antimicrobial Resistance has been held to allow global leaders to get together to discuss new strategies to fight against antibiotic resistance (AMR), which has been recognized as one of the biggest threats to human health (5). According to a report published by UK government, compared with the 700, 000 deaths recorded every year to date, antimicrobial resistant infections will cause the deaths of ten million annually in the future, a number larger than mortality due to cancer (5). To tackle the global problem of AMR, researchers, policy makers and the industry need to work together in different categories including : to improve awareness and understanding of AMR via education, communication and training, to update knowledge about AMR by surveillance and research, to reduce infections through effective prevention measures, to use antibiotics in human and animal medicine rationally, and to boost investment in development of new medicines, detection technologies, vaccines and other interventions adopted by World Health Organization (6).

Although Methicillin-resistant *Staphylococcus aureus* (MRSA) and Vancomycin-resistant *Enterococci*(VRE) pose great challenges in terms of antibiotics resistance among Gram-positive bacteria, problems due to Gram-negative organisms is more serious because MDR(multidrug resistant) and PDR (pan-drug-resistant) strains are detected among Gram-negative bacteria such as *Pseudomonas aeruginosa*, *Acinetobacter* spp. and *Enterobacteriaceae* (3, 7).

With the emergence of ESBLs (extended-spectrum β-lactamases), KPC (Klebsiella pneumoniae carbapenemases) and NDM (New Delhi metallo-β-lactamase)-producing Gram-negative bacteria (7-9), the choice of effective antibiotics has become limited. Recently, the report of discovery of the plasmid-mediated colistin resistance gene *mcr-1* in animals, food and human specimen around the world signals a further deepening of the AMR crisis (9, 10). To date, much works need to be done to characterize the *mcr-1*, especially of its ability to undergo transmission and evolution.

Bacterial infections constitute an enormous burden on public health and economic development worldwide. Apart from the hospital-acquired infections or those communicable by air, vector and contact, foodborne infections are considered another important public health issue (11). Foodborne infections are usually caused by ingestion of food products including meats, milk, fish and vegetables, which are contaminated by pathogens and lack proper processing. It is estimated that foodborne illness cost between 10-83 billion United States dollars per year in the United States (12), and caused 9.4 million illnesses, 55,961 hospitalizations, and 1,351 deaths each year (13). WHO has released a global estimate of foodborne diseases, showing that 1 in 10 people fall ill every year after eating food contaminated by bacterial pathogens, and 420, 000 die as a result (14). Bacteria including non-typhoidal *Salmonella enterica*, *Campylobacter* spp., *E.coli* (STEC) O157, *Listeria monocytogenes*, *Vibrio parahaemolyticus* and *Clostridium*

perfringens are major foodborne pathogens worldwide (13, 15). In Hong Kong, owing to the high rate of seafood consumption among the population, *V. parahaemolyticus* is listed as the primary cause of foodborne illnesses (16). Although most cases of foodborne illness are self-limiting and antibiotic prescription is not necessary, severe foodborne infections involving diarrhea, fever, abdominal pain, and headache can be fatal in children, the elderly or people with suppressed immune system, for whom antibiotics are necessary for treatment of the diseases. However, food products contaminated with MDR bacteria are rendering treatment challenging; furthermore, foodborne pathogens are able to transfer the resistance genes from farms to clinical settings via food chain (17, 18).

Based on previous works on *V. parahaemolyticus*, this study first characterized the β-lactamases expressed by this pathogen, including ESBLs, AmpC lactamase and intrinsic β-lactamase, followed by the mechanism of transmission and features of evolution of genetic elements encoding these enzymes. In the second part, a thorough study on the molecular characteristics and transmission mechanism of the mobile colistin resistant *mcr-1* gene was conducted, using new sequencing technologies. It should be noted that the antimicrobial resistance in this study focus on Gram-negative bacteria, and do not include Gram-positive bacteria and other microorganisms such as parasites, fungi and viruses. In the next section, a literature review on the characteristics of *V.*

parahaemolyticus and mechanisms of antibiotic resistance among Gram-negative is presented.

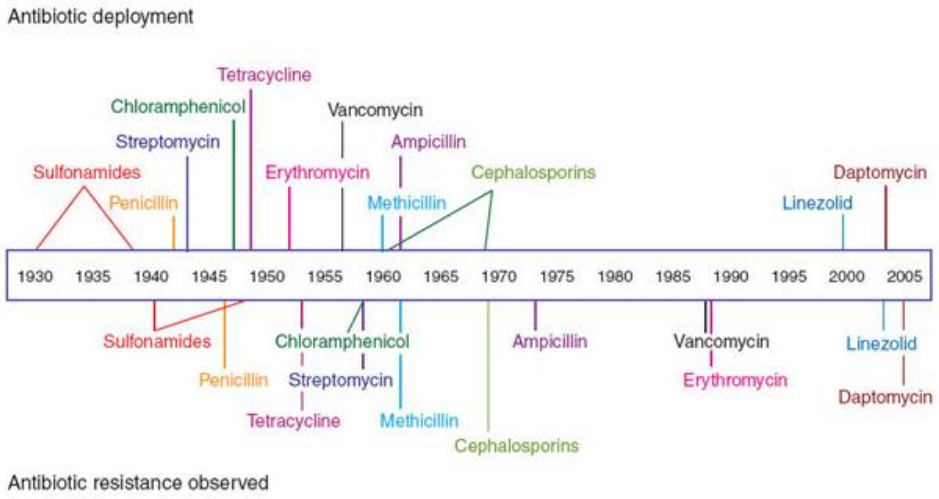

Figure 1. 1 Timeline of key events about antibiotic deployment and antibiotic resistance emergence.(19) Nearly as quickly as life-saving antibiotics are developed, new antibiotic resistant strains emerge.

1.2 Overview of *V. parahaemolyticus*

1.2.1 Introduction of *V. parahaemolyticus*

V. parahaemolyticus is a ubiquitous inhabitant of the marine and estuarine environments, which causes seafood-borne gastroenteritis with characteristic symptoms such as vomiting, diarrhea, abdominal cramps, fever and occasionally wound infections and septicemia (20-22). This bacterium is Gram-negative, halophilic, asporogenous, facultative anerobic, and curved rod-shaped. Recoverable from

brackish saltwater (23), it has a size of approximately 2 μm (**Fig. 1.2**) and typically contains a single, sheathed, polar flagellum when grown in a liquid medium. The bacterium can generate numerous lateral flagella in addition to the polar flagellum, and become swarming cells by surface-induced effect when grown in semi-solid agar medium (24, 25).

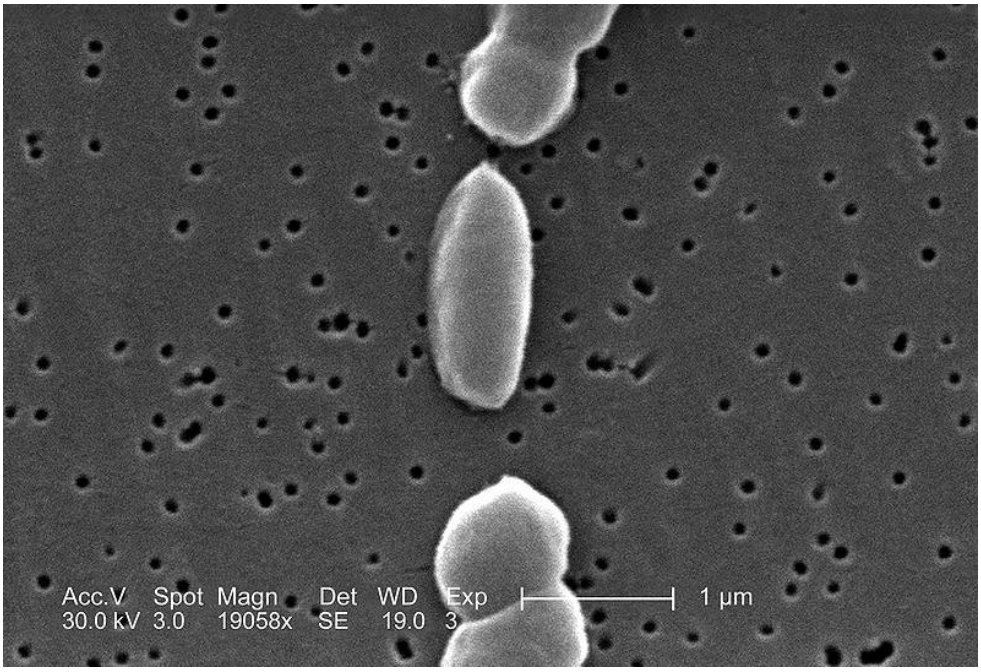

Figure 1. 2 Scanning electron micrograph (SEM) of *Vibrio parahaemolyticus*

(adapted from Wikepedia)

V. parahaemolyticus was first identified as the causative agent of a serious food poisoning epidemic in 1950. The outbreak, due to consumption of semidried juvenile sardines, resulted in sickness of 272 individuals and 20 deaths (26). Since then, this halophile has been a leading cause of human bacterial illness associated with

seafood consumption globally (27). In the United States, the cost of foodborne illness arising from *V. parahaemolyticus* reached up to 40 million dollars and the official record of the number of infection cases caused by this pathogen were 34, 664 in 2013 (28). *V. parahaemolyticus* has been reported to represent 20-30% of food poisoning cases in Japan and recognized as a main cause of seafood-borne illness in many other Asian countries (23). In China, it was reported that 31.1% of the 5770 foodborne outbreaks recorded in a survey were due to *V. parahaemolyticus* during the period of 1991 and 2001 (15). In Hong Kong, *V. parahaemolyticus* accounts for 40% of food poisoning outbreaks and it is recognized as the main cause for food-borne illnesses due to the high rate of consumption of shrimp in this city (29).

According to the Bergey's Manual of Systematic Bacteriology, *V. parahaemolyticus* belongs to the *Vibrio* spp. within the family of *Vibrionaceae*. Along with another two species *V. cholerae* and *V. vulnificus*, these three species are the most important pathogens among the *Vibrio* spp (30). However, not all *V. parahaemolyticus* strains exhibit the same pathogenic potential and they have been divided into environmental and clinical strains according to their differential levels of virulence traditionally (20). Normally, two virulence factors, namely thermostable direct hemolysin (TDH) (responsible for the Kanagawa haemolysis) and TDH-related hemolysin (TRH), which are produced by the majority of clinical isolates yet rarely detectable in environmental strains, are

considered to be the main virulence factors. *V. parahaemolyticus* symptoms typically resolve in less than 72 h. A small number of cases may persist for up to 10 days, but the majority of these cases tend to involve immunocompromised individuals. Almost all clinical isolates of *V. parahaemolyticus* exhibit beta-haemolysis activity when cultured on specialized blood agar (Wagatsuma agar). Virulent *V. parahaemolyticus* strains produce a variety of recognized virulence factors during pathogenesis (31). Apart from the TDH and TRH genetic virulence markers, two distinct type III secretion systems on chromosomes 1 and 2, T3SS1 and T3SS2 respectively, are considered to play a role in the pathogenesis of *V. parahaemolyticus* (32). Based on the epidemiology data, the virulence level of TRH might be less than that of TDH (33). The roles of T3SS1 and T3SS2 are still being investigated.

1.2.2 Prevalence of *V. parahaemolyticus* in environments and different food samples

The distribution of *V. parahaemolyticus* in the marine environments is thought to be related to the water temperature. Studies have shown that the organism was rarely detected in seawater by conventional culture method until water temperatures rose to 15℃ or above. This may be the result of the cells entering a viable but nonculturable (VBNC) state under low temperature (22, 23, 34). This is in agreement with the fact that the frequency of isolation of *V. parahaemolyticus* from environmental samples is much lower during winter. However, the number of *V. parahaemolyticus* in

seawater could increase to 10cells/ml when the temperature rises to around 25℃ (23). A published study conducted in Oregon oyster-rearing environments revealed a positive correlation between the prevalence of *V. parahaemolyticus* and water temperatures (35).

The severity of *V. parahaemolyticus* contamination in shellfish is also known to relate to the water temperatures. Therefore, it is more likely to detect *V. Parahaemolyticus* in shellfish harvested in spring and summer than in winter (23). In a study performed in the eastern coast of China from December 2008 to November 2009, the authors found a disparity in the distribution of *V. parahaemolyticus* between different seasons, and that the highest and lowest levels of abundance were recorded in summer and winter respectively (36). Another study analyzing the prevalence and characteristics of *V. parahaemolyticus* among patients in the southern coastal region of China suggested that this bacterium was the leading causal pathogen for bacterial infections diarrhea during the period 2007-2012 (37). Moreover, cross-contamination between salted food and seafood could occur and salted food might be a vital risk factor associated with *V. parahaemolyticus* outbreaks in Guangdong (38). However, studies on the prevalence of *V. parahaemolyticus* in the environment and food were rare. Although the main cause of food poisoning by this pathogen is via eating raw or undercooked seafood, we believe that other types of food, such as chicken and pork can be contaminated by this bacterium when they are processed with contaminated water; in addition, cross-

contaminations between shellfish and other meat may occur. It is therefore necessary to investigate the prevalence of *V. parahaemolyticus* among different types of meat.

1.3 Major antibiotic classes and corresponding mechanisms of resistance of Gram-negative bacteria

To combat the increasing challenges posed by antibiotic resistant bacterial pathogens, a better understanding of its detailed molecular mechanisms is essential. Although antibiotic resistance of pathogens found in patients results in an adverse effect on the efficacy of antibiotics in treating infectious diseases in last century, the emergence of antibiotic resistance is a natural evolutionary phenomenon that allows bacteria to adapt to antibiotic exposure in ecosystems (39, 40). Most antibiotics used in human and veterinary medicine are derived from natural microorganisms producing antibiotics to enhance their survival fitness. The coexistence of antibiotic-producer, as well as drug resistant and sensitive microorganisms in the same environment is achieved by a competitive trade-off mechanism, which results in a balance between the effects of accumulation of antibiotics and emergence of resistant microorganisms (41). Upon the introduction of antibiotics in medicine, antibiotics underpin modern medicine, increase life expectancy and change the outcome of bacterial infections. However, human activities including misuse and abuse of

antibiotics are disrupting the balance between resistant and susceptible bacteria and an increasing number of multidrug resistance bacteria emerge from the environment amid significant evolutionary pressure. In this process, a number of cellular mechanisms are known to confer resistance to antibiotics, and migration of such resistance-encoding elements between different bacteria, via conjugation, transduction and transformation (**Fig. 1.3**) has become a common event, among which conjugation of plasmid may be regarded as the most important mechanism (39).

Antibiotic resistance in bacteria can be divided into two main categories. First, bacteria can be intrinsically resistant to different antibiotics, a phenomenon often universally found in same bacterial species. The typical example is the insensitivity of Gram-negative bacteria to many classes of antibiotics including vancomycin and linezolide, because of the existence of outer membrane which is impermeable to these antibiotics, or other mechanisms (42). In addition to intrinsic resistance, bacteria can acquire resistance by means of developing chromosomal DNA mutations or acquiring mobile resistance genes with the aid of plasmids, transposons, integrons and mobile elements (43).

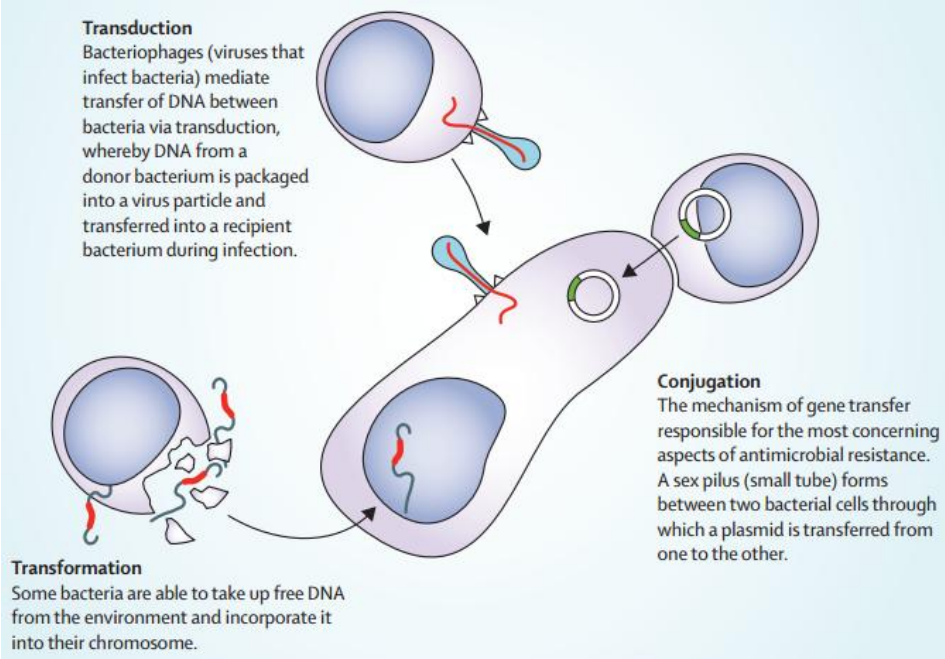

Figure 1. 3 Transmission modes of genetic material including resistance determinant between different microorganisms.

1.3.1 Intrinsic antibiotic resistance

Reduced membrane permeability

In bacteria, the cytoplasmic membrane acts as a barrier between cytoplasm and outer environment that regulates the transport of substances into and out of the cell. Unlike Gram-positive bacteria, Gram-negative bacteria are intrinsically resistant to some antibiotics because of their lower permeability conferred by the outer membrane (40). The elaborate outer membrane in Gram-negative bacteria is composed of lipopolysaccharides (LPS) and phospholipids, where non-specific porin proteins and selective channels are located (44). Antibiotics enter the cytoplasm upon

diffusion across the porin proteins located in the outer membrane. Although the diffusion process is non-specific, the influx of antibiotics can be retarded by various mechanisms including size selection, hydrophobicity, low expression of porin proteins and the generation of more-selective porins (40, 42). It was reported that acquisition of mutant porin genes and change in the patterns of genes regulating porin expression can be achieved after exposure of strains of the *Enterobacteriaceae* family to carbapenems, leading to emergence of antibiotic resistant organisms (40). The important opportunistic pathogen *Pseudomonas aeruginosa* is a typical bacterium which utilizes the low permeability of outer membrane to resist antibiotics (45). Inaccessibility of the antibiotics into the bacterial cell can be enhanced by active efflux of antibiotics bestowed by MDR efflux pumps.

Increased efflux of antibiotics

Intrinsic high-level antibiotic resistance in Gram-negative is attributed not only to the outer membrane, which serves to slow down antibiotic uptake, but also the efflux pumps which actively transport a variety of antibiotics out of the cytoplasm. Antibiotics including tetracycline, quinolones and chloramphenicol could be transported out of cytoplasm via efflux pump, which can result in resistance (46). Efflux pumps are known to broadly exist in all organisms and are encoded by chromosomal genes, including bacteria that do not encounter antibiotics, indicating that this mechanism evolved for the purpose of adaptation other than

conferring resistance to antibiotics (42). In the bacterial membrane, based on the number of components, locations of transporter proteins, the energy utilized and categories of substrates exported by efflux pumps, there are five major types of efflux proteins associated with MDR including small multidrug resistance (SMR), major facilitator superfamily (MFS), multidrug and toxic extrusion (MATE), ATP binding cassette, and resistance-nodulation-division family (RND) (**Fig. 1.4**) (47). Although the resistance level conferred by efflux pumps cannot increase by more than 100-fold in MIC value compared with that caused by enzymes or target mutations, the increases in MIC are sufficient to render bacteria resistant to the antibiotics and result in treatment failure, especially in the case of fluoroquinolones (47, 48). Apart from the function of resistance to antibiotics, certain MDR efflux pumps were found to be involved in bacterial pathogenicity in terms of colonization and persistence of bacteria in the host (47).

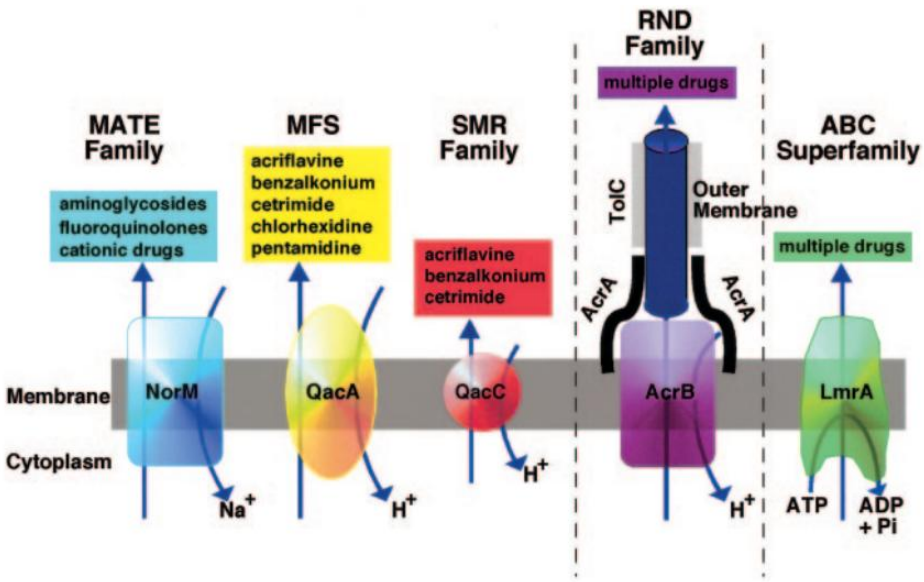

Figure 1. 4 Schematic of the five families of efflux pumps involved in multidrug-resistance.

Additional mechanisms of intrinsic resistance

Additionally, a lack of the bacterial target of antibiotics is another mechanism for resistance. This is another reason why some antibiotics cannot inhibit both Gram-negative and Gram-positive bacteria. As one of antistaphylococcal agents, daptomycin lacks activity against Gram-negative bacteria because of the absence of the lower proportion of anionic phospholipids in cell membrane (49). In addition, chromosomally encoded antibiotic-inactivating enzymes also play a role in intrinsic resistance in bacteria. The intrinsically chromosome-encoded β-lactamase represented by the $bla_{\text{OXA-51}}$-like gene can confer resistance to carbapenems when overexpressed, as a result of incorporating a strong promoter in *Acinetobacter baumannii* (50).

Combined with the aforementioned mechanisms, intrinsic resistance is always derived from a complex network involving a series of elements in cellular pathways, which could be regarded as intrinsic resistome in bacteria (51). With the development of high-throughput sequencing techniques, studying intrinsic resistance can be conducted efficiently to identify the potential intrinsic gene responsible for the resistance. Methods for analyzing intrinsic resistome have been reviewed in detail (51).

1.3.2 Acquired antibiotic resistance

Beta-lactam

Although people utilized remedies such as applying garlic, onions or molds on open wounds to treat infections in the early days, antibiotics began to transform the practice of modern medicine in early 20th century after penicillin was discovered from *Penicillium notatum* (52) by Alexander Fleming. After this ground-breaking discovery, it takes several years for penicillin to be utilized in clinical setting and widely used by physicians. When people realized the power of antibiotics, much investment went to mass production of antibiotics and development of novel agents. Then, different forms of β-lactams were generated, such as cephalosporins, carbapenems, and monobactams, sharing the same core structure β-lactam ring. It is well-known that β-lactams can inhibit the cell wall synthesis of bacteria by covalently binding to penicillin-binding proteins (PBPs), which are enzymes involved in the peptidoglycan

cross-linking process in bacteria, and are the mostly used antibiotics (53). For comprehensive review on various antibiotics belonging to β-lactams and β-lactamase inhibitors, refer to the latest publication by Bush et al. (53).

Although the introduction of β-lactams into clinical setting provides physicians with the tools to prevent specific infections including meningitis and pneumonia, the emergence of resistance to β-lactams is impairing the efficacy of antimicrobial therapy and posing a great concern. The first identified penicillinase enzyme, produced by penicillin-resistant Gram-negative bacteria and *Staphylococcus aureus*, can inactivate penicillin effectively (52). Although there are different ways for bacteria to confer resistance to β-lactams including mutational changes in PBPs encoding genes which cause reduction in the affinity of β-lactams to PBPs, especially in Gram-positive bacteria, the most dominant mechanism in Gram-negative bacteria is the production of β-lactamases which can inactivate the antibiotics by hydrolyzing the β-lactams ring (54). Owing to the combination of widely used β-lactams and surveillance via advanced molecular techniques, the number of known β-lactamases exploded in the past decades according to data provided by the β-lactamases database supported by George Jacoby at Lahey Clinic (http://www.lahey.org/studies/), which has been maintained by NCBI (https://www.ncbi.nlm.nih.gov/pathogens/submit_beta_lactamase/).

Based on the viewpoint by Louis B. Rice, the evolution of β-lactamases occurred in four stages (54). The first stage was presented by the emergence of penicillinases and derivates including TEM-1 and SHV-1. The emergence of resistance to extended-spectrum cephalosporins indicated the second stage mediated by formation of point mutations within the TEM- and SHV-type β-lactamases, conferring resistance to cephalosporins. Then, the third wave involved with the spread of CTX-M family b-lactamases, which were derived from natural cephalosporinases. The latest stage was manifested by the rapid emergence and spread of genetic elements encoding carbapenemases such as the KPC, NDM, and OXA enzymes. It was noted that the novel resistant enzymes could emerge and spread widely after several years of the use of corresponding β-lactams. Based on the molecular characterization including nucleotide and amino acid sequences of the β-lactamases, four categories, namely Ambler class A, B, C, and D, are recognized, which correlate well with the functional scheme (55). Ambler classes A, C, and D β-lactamases possess the amino acid serine at their active site, whereas class B are all metallo-enzymes requiring zinc as a cofactor for their enzymatic activities. For the introduction of different β-lactamases, refer to published reviews (56-59).

CHLORAMPHENICOL

Chloramphenicol and its derivative flofenicol are specifically potent inhibitors of protein chain elongation (biosynthesis) via its affinity to peptidyltransferase of the bacterial 50S ribosomal subunit of both Gram-negative and Gram-positive bacteria (43). The most common mechanism of resistance to chloramphenicol, thiamphenicol and azidamfenicol is the production of various acetyltransferases (CATs), which can inactivate the drug by acetylation (60). Based on the structural differences, two defined CATs are recognized, namely the *catA* and *catB*. However, the flofenicol is non-susceptible to CATs due to the effect of structural modification. The emergence of specific exporters including *floR* and *cmlA* renders resistance to flofenicol and chloramphenicol. These chloramphenicol/ flofenicol resistance phenotypes are transferable among different bacteria via transposon, integron, plasmids and other mobile elements. Furthermore, the *cfr* gene encoding an RNA methyltransferase that modifies 23S rRNA can confer resistance to five classes of antibiotics including phenicols, and has been reported in Gram-negative bacteria including *E.coli* and *Proteus vulgaris*, although the prevalence rate is low (61).

QUINOLONE

The first generation of quinolone refers to nalidixic acid, which was discovered in 1962, possessing activity against Gram-negative bacteria. Addition of fluoride of quinolone generates the fluoroquinolones including ciprofloxacin, norfloxacin and ofloxacin with enhanced bactericidal activity. The development of third-

generation quinolones, such as levofloxacin and sparfloxacin, harbor activity against Gram-positive bacteria as well as Gram-negative bacteria (43). Quinolones can kill bacteria through inhibiting DNA gyrase and topoisomerase IV, both of which are essential for DNA replication in bacteria. The corresponding four genes, *gyrA*, *gyrB*, *parC* and *parE*, can be mutated and confer the bacteria phenotypic resistance to quinolones. Mutations in this so-called quinolone resistance determining regions (QRDR), together with other chromosome-encoded resistance mechanisms including decreased permeability and efflux pump, constitute the conventional quinolone resistance mechanisms (62).

The emergence of plasmid-mediated quinolone resistance determinant *qnrA*, encoding a pentapeptide repeats protein which prevents topoisomerase IV and DNA gyrase from quinolone binding and hence inhibition, and exhibiting low-level quinolone resistance, represents the second major resistance mechanism. Currently, there are six families of *qnr* genes (*qnrA*, *qnrB*, *qnrC*, *qnrD*, *qnrS* , *qnrE* and *qnrVC*) reported (63). Apart from the *qnr* family, another transferable quinolone resistance mechanism via enzymatic inactivation of quinolones was reported as a variant of aminoglycoside acetyltransferase encoding gene *aac(6')-Ib*, *aac(6')-Ib-cr* , conferring low-level resistance to ciprofloxacin (62). The third plasmid-mediated resistance mechanism is conferred by the efflux pump gene *qepA*, which can export hydrophilic fluoroquinolones (64). Another important plasmid-encoded

multidrug efflux pump, OqxAB, can extrude ciprofloxacin and other classes of antibiotics (65, 66). Although plasmid-mediated quinolone resistance is often associated low-level resistance, they can facilitate development of high-level resistance to quinolones by selection of mutants (62, 63, 67).

TETRACYCLINE

Tetracyclines are broad-spectrum antibiotics antibiotics inhibiting the growth of bacteria by blocking protein synthesis. Since the discovery of tetracycline in 1948, several derivates has been developed and widely used to combat infections in humans and as veterinary medicine and growth promoter in animal husbandry (43, 68, 69). Resistance to tetracycline was first found in 1950s, and there are 59 tetracycline resistance determinants reported as of 2016(http://faculty.washington.edu/marilynr/, updated July, 2016). The mechanisms of resistance to tetracyclines are primarily due to acquisition of genes falling in three categories of functions: efflux pumps (33 types), ribosomal protein (12 types), and enzymatic inactivation (13 types) with one unknown mechanisms. The first two mechanisms are the most dominant mechanisms acquired normally via conjugative plasmids, transposons and other mobile elements (70).

AMINOGLYCOSIDES

Aminoglycosides are broad-spectrum antibiotics used to treat Gram-negative and Gram-positive infections. Streptomycin was the first aminoglycoside antibiotic found to be produced by *Streptomyces griseus* in early 1940s, after which additional aminoglycosides, including neomycin, kanamycin, gentamicin and amikacin were developed (43). Aminoglycosides exert antibacterial action through ribosomal binding and blocking of bacterial protein biosynthesis (71). The acquired resistance mechanisms to aminoglycosides mainly fall in two categories: ribosome alteration by 16S rRNA methylases and inactivation of the drugs by modification of enzymes. 16S rRNA methylase was found in bacteria as a plasmid-mediated aminoglycoside resistance mechanism recently, which exhibit high-level resistance to most aminoglycosides through methylation of the aminoglycoside-binding site in 16S rRNA (72). The prevalence of 16S rRNA methylases is increasing and the co-production with other important resistance determinants including ESBLs and carbapenemases are causing a great concern (73, 74). Aminoglycosides are especially susceptible to enzymatic modification due to its large molecules with many exposed hydroxyl and amide groups (40). Correspondingly, inactivation of aminoglycosides by modification of enzymes, which include acetyltransferases, phosphotransferases and nucleotidyltransferases based on the modification types, is the most widespread mechanism of resistance. For the complete list of genes encoding the modification enzymes belonging to N-acetyltransferases (AACs), O-nucleotydyltransferases (ANTs), and O-phosphotransferases

(APHs) and the locations of genes, refer to the review about aminoglycoside modifying enzymes (43, 75).

MACROLIDE-LINCOSAMIDE-STREPTOGRAMIN B

The first macrolide, erythromycin, was found derived from *Streptomyces erythreus* in early 1950s, since then various newer semi-synthetic derivates including azalide and azithromycin, were developed for treatment of infectious diseases (43, 76). Based on the same function of inhibiting bacterial protein synthesis via binding to the 50S ribosomal and blocking peptide elongation, macrolides, lincosamides, streptogramins, ketolides, and oxazolidinones are clustered together as the MLSKO family of antibiotics, although they are distinct chemically (76). The first macrolide-resistant bacteria were described in *staphylococci* shortly after the introduction of erythromycin into clinical use in 1953 (77). Since then, numerous bacteria have been found resistant to antibiotics belonging to MLSKO via various mechanisms. Three main types of genes encoding rRNA methylases, efflux pumps and enzymatic inactivation, account for resistance to MLSKO antibiotics. The detailed information of the genes and their sources are maintained in a specific website of the University of Washington and updated twice a year (http://faculty.washington.edu/marilynr/).

According to data on mechanisms of MLS resistance in the website mentioned above, there are 42 rRNA methylase, 24 efflux, and 26

inactivating enzymes identified by July 8, 2016. Among the rRNA methylases encoding genes, two major types, *erm* and *cfr* , were found in Gram-negative and Gram-positive bacteria (78). The 23S rRNA methyltransferase encoded by the *cfr* gene renders bacteria resistant to lincosamides, oxazolidinones, streptogramin A, phenicols and pleuromutilins, but not macrolides (76). There are 24 different genes with different names that code for efflux pumps which pump the antibiotic(s) out of the plasma. Notably, the recently identified *optrA* can confer transferable resistance oxazolidinones and phenicols in Gram-positive bacteria (79). Currently, there are 2 esterases, 2 lyases, 15 transferases, and 7 phosphorylases identified in inactivating enzymes family. Apart from the three major acquired resistance mechanisms, mutations in 23S rRNA and ribosomal proteins can also result in increased resistance to MLSKO (76).

SULFONAMIDE- TRIMETHOPRIM

As the oldest synthetic antibacterial agent used in 1932, sulfonamides play an important role in treating bacterial infections (43). Currently, the most commonly used sulfonamide derivate is sulfamethoxazole. Owing to the emergence of resistance, sulfonamides are generally combined with other antibiotics, and trimethoprim-sulfamethoxazole (TMP-SMX) which exerts synergetic bactericidal effect is a common drug combination used to treat urinary tract infections (80). As an analogy of p-aminobenzoic acid, sulfonamides can block the biosynthetic pathway of folic acid

by competitively inhibiting the activity of dihydropteroate synthase(DHPS) (81). Acting on the same folate biosynthetic pathway, trimethoprim binds to the active site of the enzyme dihydrofolate reductase (DHFR), which catalyzes the reduction of dihydrofolate to tetrahydrofolate (82). Resistance to sulfonamides results from DHPS gene (*folP*) mutations or more commonly from the acquired alternative DHPS gene (*sul*) (80). To date, three classes of *sul* (*sul1*, *sul2* and *sul3*) genes sharing homologous sequences were identified in different genetic environments, including integrons, IS*CR*s and conjugative plasmids (80, 83). High-level resistance to trimethoprim is bestowed by the acquired gene encoding variants of the chromosomal DHFR, which emerged in Gram-negative bacteria shortly after clinical introduction of the drug. Compared with the *sul* genes, DHFR encoding genes have nearly 30 different alleles within two major types including *dfrA* and *dfrB*, which are usually embedded in integrons as gene cassettes (82, 84). The complete list of *dfr* genes is currently available (43, 85).

1.3.3 Antibiotic resistance in *V. parahaemolyticus*

Normally, *V. parahaemolyticus* associated gastroenteritis is self-limited in most patients and no specific medical therapy is required. Antibiotic therapy usually does not reduce the severity and shorten the course of the illness. However, for prolonged illnesses and life threatening infections caused by *V. parahaemolyticus*, antibiotic therapy (mainly including tetracycline, doxycycline, quinolones and

third-generation cephalosporins) is necessary (86). Trimethoprim-sulfamethoxazole plus an aminoglycoside is used to treat children in whom doxycycline and fluoroquinolones are contraindicated (87). Traditionally, *V. parahaemolyticus* is considered highly susceptible to virtually all antimicrobials. During the past few decades, however, antimicrobial resistance has emerged and evolved in many bacterial genera due to the excessive use of antimicrobials in human, agriculture, and aquaculture systems. Other foodborne pathogens of terrestrial sources have been studied extensively with regard to the development and dissemination of antimicrobial resistance. In contrast, antimicrobial-resistant *V. parahaemolyticus* strains are relatively rare. Recently, several reports have indicated that the prevalence of antimicrobial resistance in *V. parahaemolyticus* has increased, presumably due to extensive use of antimicrobials in clinical treatment and aquaculture systems (87-90). To date, resistance to ampicillin, streptomycin, kanamycin, tetracycline, chloramphenicol and ciprofloxacin have been reported (90). Recent studies also reported resistance to third-generation cephalosporins in *V. parahaemolyticus* strains due to carriage of an extended-spectrum beta-lactamase (ESBL) gene, $bla_{\text{PER-1}}$ (91). However, other ESBL genes or AmpC type genes are not detectable in *V. parahaemolyticus*.

The emergence of ESBLs-producing pathogens is of particular concern due to the limited options for eradicating such organisms in clinical settings. Various ESBLs (including SHV, TEM, OXA, CTX-M, etc.) have been reported in a wide range of bacterial species worldwide (92, 93). As a major class A ESBL, the $bla_{\text{PER-1}}$

gene product confers resistance to penicillins, oxyimino-cephalosporins, and aztreonam, but not oxacillins, cephamycins, and carbapenems, and is susceptible to inhibition by clavulanic acid and sulbactam (94). This *bla* gene was first recognised in the *Pseudomonas aeruginosa* strain RNL-1, which was recovered in France in 1991(95). After that, other closely related variants such as PER-2, -3, -4, -5, -6 and -7 have been identified (96, 97).

Among the repertoire of ESBLs identified, PER-1 β-lactamases were found to belong to a particular class which is confined to relatively few locations and bacterial hosts (*Aeromonas spp*., *Acinetobacter baumannii*, *Alcaligenes faecalis*, *Pseudomonas aeruginosa* and *Enterobacteriaceae*) (98, 99). This phenomenon may indicate either that the dissemination potential of $bla_{\text{PER-1}}$ is limited or that the extent of dissemination of this gene is underestimated. The $bla_{\text{PER-1}}$ gene has been found in plasmids or chromosomes in diverse genetic environments, and is often embedded within Tn*1213* (99, 100). Recently, the IS*CR1* element has been found to play a role in the dissemination of $bla_{\text{PER-1}}$ (99).

$bla_{\text{CMY-2}}$ is the most common reported plasmid-mediated AmpC β-lactamase gene. CMY-2 generally confers reduced susceptibility to cefoxitin and resistance to clavulanic acid; however, cefepime remains unaffected (101). **Fig. 1.2** shows the comparison of regions surrounding $bla_{\text{CMY-2}}$ originated from a study on the genetic context of plasmid-carried $bla_{\text{CMY-2}}$-like genes in *Enterobacteriaceae* (102).

1.4 Transfer mechanism of acquired antibiotic resistance

Different acquired antibiotic resistance genes are often associated with mobile elements and capable of transferring between different genetic loci within the same bacteria (intracellular mobility) or between different bacteria (intercellular mobility), or even among different species by mechanisms independent of homologous recombination. Undoubtedly, the mobile genetic elements play a leading role in facilitating widespread dissemination of antibiotic resistance determinants in different environments worldwide. During the process of horizontal gene transfer (HGT), the major players are the conjugative and mobilizable elements, which refer to the conjugative plasmids or conjugative transposons (integrative conjugative elements, ICE) and mobilizable plasmids or other mobile elements (transposons, integrons and insertion sequences). Apart from the genetic elements, transduction and transformation are two processes involved in the HGT. During transduction, different genetic segments including antibiotic resistance genes can be transferred to a new host and integrated into the chromosome or plasmids after packaging with the bacteriophages (103-105). Furthermore, bacteria can obtain new genetic materials by natural transformation, which indicates the competent bacteria can take up DNA from the surrounding environments and incorporate the naked DNA into the host genome via transposition or recombination (106-108).

Conjugative and mobilizable plasmids

Plasmids are extra-chromosomal DNA replicons in circular or linear forms that can be found in different domains including *Bacteria*, *Archaea* and *Eukaryota* (109). As important vehicles of genetic communication between different bacteria, the role of plasmids in enhancing rapid evolution and adaption to environments has been studied extensively (110, 111). Based on the characterization of mobility, plasmids fall into three categories: conjugative, mobilizable, and nonmobilizable. Apart from the essential genes for plasmid maintenance, some accessory genes including antibiotic resistance genes and other mobile elements can also be found in plasmids. Due to the mobility of conjugative and mobilizable plasmids between different bacterial hosts, they play a vital role in the dissemination of resistance genes in both Gram-negative and Gram-positive bacteria (112, 113). A number of reviews have described the detailed knowledge of resistance genes and associated plasmids (110, 112-114).

Insertion sequences and transposons

Insertion sequences (ISs) are the simplest mobile genetic elements shaping the host genomes. Basically, these elements consist of one or two open reading frames encoding IS-related transposases surrounded by short imperfect terminal inverted repeat sequences (IRs), and normally range from 0.7 to 2.5kb in length (115). The transposases including DDE, DEDD, HUH and Ser transposases are

involved in the DNA mobility by different mechanisms leading to various translocation events (116). IS families are always defined according to the similarity of the encoding transposases, and the number of ISs increase as more genome sequences are available. In order to cope with the large number and diversity of ISs, a specific website (www-is.biotoul.fr) has been developed to deposit and update the information of ISs (117).

Although ISs can mobilize sole genetic elements, combined with accessory genes such as antibiotic genes, they can generate transposons (Tns) which confer different phenotypes to the host (43). Importantly, the ISs are always the basic elements for more complex MGEs, such as Tns, ICEs, and plasmids. Different from the ISs, apart from the transposase-encoding genes, the transposons encode at least one phenotype beneficial to the host, such as the antibiotic resistance phenotype. Two separate IS elements (may or may not be exact replicas) can flank functional genes as direct or inverted repeats to form the simple composite transposons, and the central functional regions can be transferred as one complete DNA intermediate with one IS (113). Another type of transposon is class 2 or complex transposon harboring a tansposases and accessory genes surrounded by short terminal inverted repeat sequences. Newly discovered, fully sequenced transposons are assigned the Tn numbers by a specific UCL website (http://www.ucl.ac.uk/eastman/research/departments/microbial-diseases/tn) (118).

Integrons

Integrons are versatile genetic elements commonly found in bacterial genomes, composing of site-specific recombination system capable of capturing and mobilizing genes, especially antibiotic resistance genes (43). Typically, it encompasses three parts: the *intI* gene encoding the integrase which belongs to the tyrosine recombinase family that catalyzes recombination among different gene cassettes, recombination sites including *aatI* and *attC*, and the integron-associated promoter Pc. The process of acquiring genes via integrons is completed by integrating the circular gene cassettes into integrons with the help of integrases (119). According to the amino acid sequences of integrases, integrons can be divided into five types: class 1 to class 5, with the first three being the most commonly found (119, 120). Notably, circular gene cassettes can be integrated into the same integron to facilitate dissemination of antibiotic resistance genes among plasmids, transopons and chromosomes. There is a database named as INTEGRALL (http://integrall.bio.ua.pt/) to deposit new integrons with different cassettes combinations from 164 bacterial genera (121). For the complete characterization of integrons, a set of reviews are available (119, 122, 123).

Integrative conjugative elements

ICEs or conjugative transposons, similar to conjugative plasmids capable of transferring between different bacteria by direct cell-to-cell contact, are self-transmissible by conjugation but cannot replicate autonomously as a result of lacking origin of replication, and always reside in host chromosomes (124). Normally, the ICEs have a modular organization consisting of genes encoding conjugation, recombination, regulation, and accessory modules (often contain antibiotic resistance genes) (43). There are exhaustive reviews depicting the diversity, evolution, genetics, and biology of different ICEs (124-129). Together with some integrated plasmids, non-replicative but excisable elements, and prophages, these genomic islands structures constitute a larger category in mobile structures (130, 131).

1.5 Application of sequencing technologies in microbial genomics

DNA sequencing is definitely a revolutionized technology in biology and medicine. After the development of Sanger sequencing (chain-termination approach) in 1970s, various novel sequencing technologies with different characteristics including high-throughput and long reads emerged in the last two decades. Based on the characteristics, emerging times and application on the bacterial genomics, sequencing technologies can be divided into three revolutions (generations): the first generation Sanger shotgun sequencing, second generation high-throughput sequencing represented by Illumina and 454 sequencing, and the latest third

generation single-molecule sequencing represented by PacBio and Nanopore sequencing (132). There are several excellent review articles describing different sequencing technologies (132-134). Although DNA sequencing was initially developed in research realm, with the rapid development of technologies and the cost-effective, high-throughput characteristics, whole-genome sequencing is not only extensively utilized in big genome projects, such as 100K Genome Project (http://100kgenome.vetmed.ucdavis.edu/) and 1000 Genomes Project (http://www.internationalgenome.org/), but also has reached for individual research groups, clinical microbiology, and food safety etc. (128, 135).

Following significant improvements in DNA sequencing technologies, WGS (whole-genome sequencing) is increasingly being used by researchers and clinicians to tackle the problem of antibiotic resistance worldwide (136). For the surveillance of pathogens resulting in a variety of infectious diseases, WGS can demonstrate unprecedented resolution in single nucleotide polymorphism (SNP) level compared with other traditional molecular typing methods including PFGE, MLST, and rep-PCR (137). With the availability of WGS, novel antibiotic resistance mechanisms can be identified and elucidated quickly from the DNA sequences, which facilitate the control of emerging MDR pathogens. Furthermore, WGS could be utilized to perform rapid diagnostic tests, predict the virulence level of pathogens and susceptibility to

antimicrobial drugs, and diagnose polymicrobial infections, all of which are more efficient than conventional culture-based methods (135, 138). Although the antibiotic resistance phenotypes are not always associated with genotypes, data on genome sequences are still informative for antibiotic stewardship (139).

Next-generation sequencing (NGS) technology, characterized by short read and high-throughput, is a significant tool for genomics, microbiology and epidemiology study. However, the technology cannot unambiguously identity the positions of repetitive elements and results in many assembled contigs other than one complete sequence (140). When it comes to structures of antibiotic resistance genes, which are always embedded in conjugative plasmids or other mobile genetic elements, NGS fails to produce complete sequences that are important for elucidating the process of evolution and the mechanisms of transmission of resistance genes. To resolve this obstacle, third-generation sequencing technologies were developed to assemble the mosaic genomic regions by long reads more than 10kb (140, 141). With the help of this technology, antibiotic resistance among bacteria can be studied in unprecedented resolution and scale in terms of molecular basis and sample quantity, respectively.

1.6 Summary of the thesis

In order to characterize the antibiotic resistance phenotypes of bacteria from the molecular perspective, we utilized *V. parahaemolyticus* and *E.coli*, both of which can cause serious human infections, as the model organisms of this study. The work in this thesis mainly comprises three parts, ranging from intrinsic resistance to acquired resistance among the two bacteria.

Part 1 (Chapter 2, 3) involves studies on molecular mechanisms of intrinsic resistance to ampicillin in *V. parahaemolyticus*. Based on data that we gathered for an intrinsic resistance gene, a novel detection method was developed to identify *V. parahaemolyticus* accurately.

Part 2 (Chapter 4, 5 and 6) focuses on research into the emerging, transmissible AmpC and ESBLs including CMY-2, PER-1 and VEB in *V. parahaemolyticus*, through various molecular assays, whole genomic sequencing and bioinformatics analysis. The underlying transmission mechanisms of these mobile resistance genes were studied.

Part 3 (Chapter 7) described the transmission mechanism of the acquired colistin resistance gene *mcr-1* which was reported recently. Through comparison of different *mcr-1*-bearing plasmids, the active role of a new transposon in facilitating the spread of *mcr-1* was presented.

Taking the three parts together, basic knowledge regarding antibiotic resistance and its transmission mechanisms has been further advanced.

Chapter Two: CARB-17 family of β-lactamases mediated intrinsic resistance to penicillins in *Vibrio parahaemolyticus*

Part of the content in this chapter is reproduced from the published paper:

Chiou J, Li R, & Chen S (2015) CARB-17 family of beta-lactamases mediates intrinsic resistance to penicillins in *Vibrio parahaemolyticus*. *Antimicrobial agents and chemotherapy 59(6):3593-3595.*

2.1 Abstract

V. parahaemolyticus is most commonly resistant to ampicillin, but the mechanisms underlying penicillin resistance in *V. parahaemolyticus* are not clear. In this study, a novel CARB family of β-lactamases, $bla_{\text{CARB-17,}}$ responsible for penicillin resistance in *V. parahaemolyticus*, was identified. Genetic environment of $bla_{\text{CARB-17}}$ was shown to be highly similar, with no mobile genetic element being detectable. In addition, $bla_{\text{CARB-17}}$-like genes were identified in all 293 *V. parahaemolyticus* genome sequences available in GenBank and detected in all 91 *V. parahaemolyticus* food isolates. A total of 32 novel bla_{CARB} variants were identified in these isolates and were designated as $bla_{\text{CARB-17}}$ to $bla_{\text{CARB-48}}$. These data suggested that $bla_{\text{CARB-17}}$ or its variants were intrinsic in *V.*

parahaemolyticus and responsible for the penicillin resistance. This study depicted the mechanism of intrinsic resistance to penicillin in *V. parahaemolyticus*. Furthermore, based on the reported regulation mechanism of $bla_{\text{CARB-17}}$, termed VbrK/R-CARB system, we conducted a comparative genomics study in *Vibrio* species to probe the system.

2.2 Introduction

Vibrio parahaemolyticus is a major causative agent of gastroenteritis, particularly in areas with high seafood consumptions (26). Major virulence factors such as tdh and trh have been implicated in *V. parahaemolyticus* strains that caused most of the clinical infections. An estimated 45,000 cases of *V. parahaemolyticus* infections occur every year in the United States. In Hong Kong, due to the high rate of seafood consumption among the population, around 40% of food poisoning outbreaks in this city are associated with *V. parahaemolyticus* (142). Antibiotics such as ciprofloxacin can be used for treatment of infections caused by *V. parahaemolyticus*, but the choice of antibiotics should be based on the antimicrobial susceptibilities of the organism. The social cost and risk to the public health related to *V. parahaemolyticus* infections in Hong Kong and other parts of the world are high. Unlike Western countries where infections were often caused by consumption of oysters, food poisoning outbreaks were frequently linked to consumption of shrimps, an extremely popular dietary habit in Hong Kong (142).

Chapter 2 Characterization of CARB-17 β-lactamases in *V. parahaemolyticus*

V. parahaemolyticus is commonly considered highly susceptible to virtually all antimicrobials. Increasing antimicrobial resistance in *V. parahaemolyticus*, probably due to excessive use of antimicrobials in the aquaculture, has recently been reported in some countries (87). *V. parahaemolyticus* from seafood and the environment is most commonly resistant to ampicillin, and it is increasingly resistant to aminoglycosides, tetracycline, sulfamethoxazole/trimethoprim, and chloramphenicol (87). Mechanisms mediating penicillin resistance in *V. parahaemolyticus* are not well defined. Over-expression of β-lactamases is one of the major mechanisms responsible for the ampicillin resistance in *Enterobacteriaceae*. Only one type of β-lactamase, PER-1, which mediates resistance to extended-spectrum cephalosporins, has been reported in *V. parahaemolyticus* strains isolated from seafood in Hong Kong (143). In this study, we identified 33 novel carbenicillin-hydrolyzing β-lactamases (CARBs) from chromosome 2 of *V. parahaemolyticus*, which was proven to be responsible for intrinsic resistance to penicillins in *V. parahaemolyticus*. The underlying mechanism of regulation of this gene was also discussed based on the published paper on our findings (144).

2.3 Materials and Methods

2.3.1 Bioinformatics analysis

A putative class A β-lactamase gene was identified from the genome sequence of *V. parahaemolyticus* V110 after checking the genome annotation report and was designated as bla_{V110}. The sequences of other similar β-lactamase variants were obtained from the search of 294 annotation reports of whole genome sequences of *V. parahaemolyticus* in GenBank as of October 1, 2014 (https://www.ncbi.nlm.nih.gov/genome/691, available WGS items increase in number gradually). The BLAST analyses were performed using the BLAST service provided by the NCBI. The alignment of different β-lactamases, calculation of sequence distances and construction of phylogenetic tree were performed using the DNASTAR Lasergene7 software (Madison, WI, US).

2.3.2 β-lactamase gene cloning

Forward and reverse primers carrying the restriction sites, BamHI and SacI (NEB), were used to amplify the full-length of bla_{V110} from the genomic DNA of *V. parahaemolyticus* V110. The PCR product was digested with the restriction enzymes and ligated to pET28b to generate pET28-bla_{V110}. The signal peptide of novel β-lactamase was predicted to cover the first 19 amino acids using the website SignalP 4.1 server (http://www.cbs.dtu.dk/services/SignalP). The truncated gene containing S^{20} to S^{283} of bla_{V110} was amplified, digested with the restriction enzymes and ligated to the vector to

generate pET28b-mbla_{V110} (m stands for mature). A 6xHis tag was added to the N-terminus of mbla_{V110} for the ease of purification.

2.3.3 Antimicrobial susceptibility testing

Minimum inhibitory concentrations (MICs) of 14 different β-lactams and β-lactam inhibitors including penicillin G, ampicillin, ampicillin/clavulanic acid (2:1), ampicillin/sulbactam (1:1), carbenicillin, pipercillin, pipercillin/tazobactam (10:1), cephalothin, cefuroxime, cefotaxime, cefepime, cefpirome, aztreonam and imipenem were tested on *E. coli* BL21 expressing the recombinant β-lactamases under 1mM of isopropal β-D-1-thiogalactopyranoside (IPTG) using the microdilution method following the CLSI standard (145). *Escherichia coli* strains (ATCC25922 and 35218) were used as quality control.

2.3.4 Expression and purification of β-lactamase

Overnight culture of *E. coli* BL21 (DE3) cells carrying pET28b-mbla_{V110} was inoculated in 500 ml of LB supplemented with proper antibiotic and induced with 1mM of IPTG at 16ºC for 22 h starting from an OD_{595} of 0.6. Cells were lysed using a French press and then spun down at 27,000g for 30 mins. The supernatant were passed through a Ni-NTA column and eluted with elution buffer containing different concentrations of imidazole. The fractions containing the target proteins were pooled, concentrated using a centrifugal filter unit (Millipore, MA, USA) and exchanged the

buffer with 1X PBS, pH 7.4, during the process. The 6xHis tag was then cleaved by incubating the proteins with thrombin at room temperature for 16-20 hours. The reaction mixture was stopped by the addition of PMSF to a final concentration of 1mM and then loaded to Sephacryl™ S-200 gel filtration column (GE Healthcare, PA, US) with the running buffer of 10 mM Tris-HCl, pH 7.9, 50 mM NaCl. The fractions containing the thrombin-cleaved $mBla_{V110}$ were pooled and concentrated with a centrifugal filter unit. The purified protein was analyzed using 12% of Sodium Dodecyl Sulfate-Polyacrylamide gel electrophoresis (SDS-PAGE). The protein concentration was determined using a Nanodrop Lite Spectrophotometer (Thermo Scientific, MA, USA).

2.3.5 Enzymatic kinetics and determination of IC_{50}

The kinetic parameters of novel β-lactamase, Bla_{V110}, were obtained by incubating the enzyme with different concentrations of antibiotics at 25°C in 500 µl of assay buffer (50 mM phosphate buffer, pH 7.0). The rate of hydrolysis of substrates was measured by observing the changes in absorption from the opening of the β-lactam ring at different wavelengths depending on the β-lactam substrates using a spectrometer (Perkin Elmer Lambda Bio20) (146). The initial velocities versus substrate concentrations were measured and fitted to the Michaelis-Menten equation using the GraphPad Prism5 (San Diego, CA, US). The initial velocities were measured in triplicates and averaged to determine K_m and k_{cat}. The effects of different inhibitors including clavulanic acid, sulbactam and

tazobactam on $mBla_{V110}$ were determined by pre-incubation of 100 pM of purified enzyme with various concentrations of inhibitors in the assay buffer at 25°C for 20 min prior to the addition of reporter substrate, nitrocefin. The initial velocity was determined by monitoring the wavelength change at 482 nm over the first 5 min. The IC50 was determined as the inhibitor concentration at which the enzymatic activity was reduced by 50% from the plot of residual activity against inhibitor concentration using GraphPad Prism5.

2.3.6 PCR screening assay

V. parahaemolyticus DNA templates were prepared using the boiling method, in which a loopful of culture was suspended in 200 µl of Phosphate Buffered Saline (PBS) and boiled for 5 mins, cool down in ice and centrifuged at 13,000g for 6 minutes. Amplification of the $bla_{CARB-17}$ gene was performed using primers listed in **Table 2.1** using *V. parahaemolyticus* V110 DNA as the positive control. Briefly, the PCR reaction was carried out in a 25 µl PCR mixture containing 0.5 µM of each primer, 250 µM of dNTP, 1×PCR buffer, 1.5 mM $MgCl_2$, 0.5 U of Taq DNA polymerase (TaKaRa, Dalian , China) and 5 µl of sample DNA, using Amy circle PCR system (Bio-Rad, Hercules, CA) with incubation condition at 94°C for 10 min, followed by 35 cycles of 94°C for 30 s, 64°C for 30 s and 72°C for 30 s, and a final extension of 72 °C for 7 min. The PCR products were further sequenced for confirmation.

Table 2. 1 Primers used to amplify different regions of *bla*$_{V110}$

Primers	Sequence (5'-3')	*bla*$_{V110}$ products
mV110F	CGTAGAGCTCTCCAAATTAAACG	60~852
V110R	CGTAGGATCCTTAACTTTCTTTGTAGTGC	
V110F	GCTGAGAGCTCATGAAAAAGTTA	1-852
V110R	CGTAGGATCCTTAACTTTCTTTGTAGTGC	

2.4 Results and Discussion

2.4.1 Characterization of CARB-17 in *V. parahaemolyticus*

A novel potential β-lactamase gene, *bla*$_{V110}$, with a size of 852bp, was identified through bioinformatic analysis of the whole genome sequence of *V. parahaemolyticus* V110, which was shown to be resistant to ampicillin (29). The novel β-lactamase gene cloned into *E. coli* BL21 exhibited MICs of 256, 512, 256 and 1024 μg/ml towards penicillin G, ampicillin, carbenicillin and pipercillin, respectively. The enzyme appears to be susceptible to β-lactamase inhibitors such as clavulanic acid, sulbactam and tazobactam (**Table 2.2**). Compared to the parental strain *V. parahaemolyticus* V110, *E. coli* BL21 expressing the pET28-*bla*$_{V110}$ exhibited slightly lower MICs to cephalothin, cefuroxime, cefepime and aztreonam, suggesting that *V. parahaemolyticus* V110 may express other mechanisms that account for the elevated MICs to the third and fourth generation of cephalosporins (**Table 2.2**). To verify if the penicillin resistance phenotype was attributed to the expression of *bla*$_{V110}$, we further purified a truncated form of this β-lactamase, in which the signal peptide was removed and designated as mBla$_{V110}$.

The $mBla_{V110}$ protein was purified through several steps including the Ni-NTA column, thrombin treatment to remove the His-tag, and size-exclusion column as described in the materials and methods (**Fig. 2.1**). The purity of this protein was higher than 99% and the yield of the purified $mBla_{V110}$ was about 2.4 mg/L. Kinetic constants determined for $mBla_{V110}$ revealed very high catalytic activities on ampicillin, penicillin G, carbenicillin and pipercillin, whereas very low activities to other β-lactams tested were recorded (**Table 2.3**). The $mBla_{V110}$ exhibited similar K_m on all penicillins, cefepime and cefpirome tested but variable k_{cat} to these penicillins, some cephalosporins, aztreonam and imipenem (**Table 2.3**). The IC_{50} values of $mBla_{V110}$ towards the serine β-lactamase inhibitors were also determined as 113.1, 175.1 and 5.87 nM for clavulanic acid, sultactam and tazobactam, respectively, confirming that $mBla_{V110}$ was not resistant to serine β-lactamase inhibitors (**Table 2.3**). The kinetic data were highly consistent with the MICs of *E. coli* carrying the bla_{V110} gene. Collectively, our data suggested that Bla_{V110} is an active β-lactamase that mediates resistance to penicillins in the *V. parahaemolyticus* V110 strain.

Table 2. 2 MICs of different β-lactams on *V. parahaemolyticus* V110 and *E. coli* carrying pET28-blaV110

Antibiotic	Bacteria Strains		
	V. parahaemolyticus V110	*E. coli* pET28-bla_{V110}	*E. coli* pET-28
Penicillin G	512	256	<1
Ampicillin	128	512	1
AMP/CLA (2:1)	2	<1	<1
AMP/SUL (1:1)	<1	4	<1
Carbenicillin	256	256	2
Pipercillin	256	1024	<1
PIP/TAZ (10:1)	0.0625	1	0.5
Cephalothin	8	1	0.0313
Cefuroxime	8	0.25	0.0313
Cefotaxime	0.0625	0.0039	0.0039
Cefepime	1	0.0625	0.0625
Cefpirome	0.25	0.0156	0.0156
Aztreonam	4	0.0078	0.0039
Imipenem	0.0313	0.25	0.0078

AMP: ampicillin; CLA: clavulanic acid; SUL: sulbactam; PIP: pipercillin; TAZ: tazobactam.

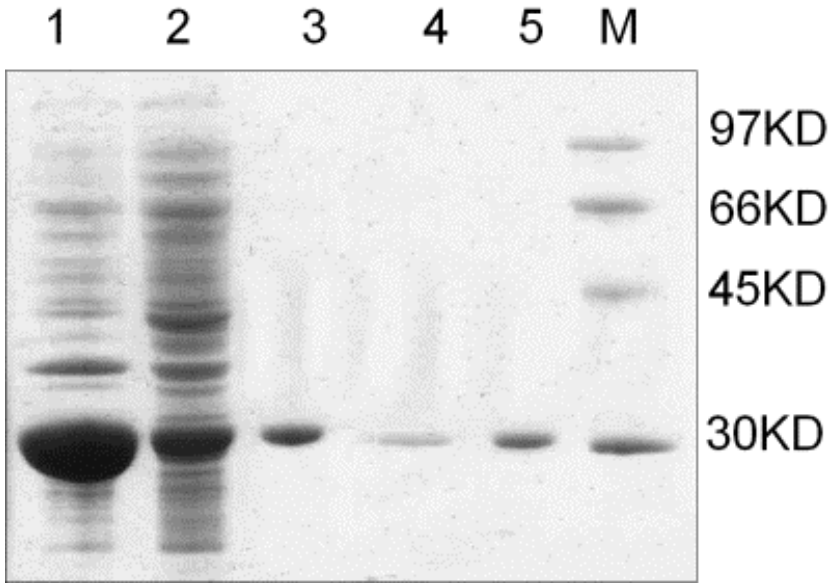

Figure 2.1. **Purification of $mBla_{V110}$.**

E. coli expressing His-$mBla_{V110}$ was broken by French press and separated as the insoluble fraction (lane 1) and soluble fraction (lane 2). His-$mBla_{V110}$ was purified via the Ni-NTA column (lane 3), treated with thrombin to remove the His tag (lane 4) and followed by size exclusion column (lane 5). M: molecular marker.

Table 2. 3 Kinetic constants of $mBla_{V110}$ towards different β-lactams

Antibiotics	**$mBla_{V110}$**		
	K_m (μM)	k_{cat} (s^{-1})	k_{cat}/K_m ($s^{-1}\mu M^{-1}$)
Penicillin G	110.4 ± 19.31	2320 ± 189.2	21.01
Ampicillin	235.8 ± 40.44	2068 ± 170.9	8.77
Carbenicillin	113.9 ± 28.61	1233 ± 177.4	10.83
Pipercillin	32.6 ± 8.87	450.7 ± 50.73	13.82
Cefuroxime	NH	<0.01	
Cefotaxime	NH	<0.01	

Cefepime	104.3 ± 25.67	0.74 ± 0.08	7.10×10^{-3}
Cefpirome	22.6 ± 4.77	0.98 ± 0.07	4.34×10^{-2}
Aztreonam	NH	<0.01	
Imipenem	NH	<0.01	

NH, no detectable hydrolysis was observed with 1 μM of purified $mBla_{V110}$ and up to 500 μM of substrate

Nucleotide BLAST of the bla_{V110} sequence identified 5 similar genes from 5 complete genome sequences of *V. parahemoltyicus* strains in GenBank. Protein BLAST resulted in many other hits of β-lactamases or proteins expressed by *V. parahaemolyticus*, without known functions. The bla_{V110} gene also exhibited 99% homology with PSE-4 from *V. parahaemolyticus* (147, 148) and high homology (54%) to PSE-4 from *Pseudomonas spp.* PSE-4 is an alternative name of CARB-1, which belongs to the CARB-type family originally identified from *P. aeruginosa*, *Acinetobacter* and *V. cholera* (www.lahey.org/Studies/) (149-151). CARBs, also known as carbenicillin-hydrolyzing β-lactamases, have been found to disperse widely among distantly related bacteria, mostly by mobile genetic elements (149, 152, 153). Similarly, the Bla_{V110} enzyme also mediated resistance to ampicillin, penicillin G, carbenicillin and pipercillin. Therefore, Bla_{V110} was designated as a novel member of the CARB family, encoded by $bla_{CARB-17}$ (**Table 2.4**).

Table 2. 4 Novel CARB family of β-lactamases identified in this study

Designation	Accession #	Gene source	Reference
$bla_{CARB-17}$	KJ934265	*V. parahaemolyticus*V110	This study
$bla_{CARB-18}$	KJ934266	*V. parahaemolyticus*V160	This study
$bla_{CARB-19}$	KJ934267	*V. parahaemolyticus*ss24	This study
$bla_{CARB-20}$	CP003973	*V. parahaemolyticus*BB22OP	(154)
$bla_{CARB-21}$	CP006005	*V. parahaemolyticus*O1:Kuk str. FDA_R31	Unpublished
$bla_{CARB-22}$	BA000032	*V. parahaemolyticus* RIMD 2210633	(147)
$bla_{CARB-23}$	CP007005	*V. parahaemolyticus*UCM-V493	(155)
$bla_{CARB-24}$	BK008907	*V. parahaemolyticus* FIM-S1392-	(156)
$bla_{CARB-25}$	BK008888	*V. parahaemolyticus* M0605	(157)
$bla_{CARB-26}$	BK008904	*V. parahaemolyticus* S014	Unpublished
$bla_{CARB-27}$	BK008896	*V. parahaemolyticus* S020	Unpublished
$bla_{CARB-28}$	BK008906	*V. parahaemolyticus* S023	Unpublished
$bla_{CARB-29}$	BK008905	*V. parahaemolyticus* S024	Unpublished
$bla_{CARB-30}$	BK008893	*V. parahaemolyticus* S037	Unpublished
$bla_{CARB-31}$	BK008895	*V. parahaemolyticus* S054	Unpublished
$bla_{CARB-32}$	BK008892	*V. parahaemolyticus* S100	Unpublished
$bla_{CARB-33}$	BK008903	*V. parahaemolyticus* S105	Unpublished
$bla_{CARB-34}$	BK008901	*V. parahaemolyticus* S115	Unpublished
$bla_{CARB-35}$	BK008900	*V. parahaemolyticus* S141	Unpublished
$bla_{CARB-36}$	BK008902	*V. parahaemolyticus* S146	Unpublished
$bla_{CARB-37}$	BK008899	*V. parahaemolyticus* S161	Unpublished
$bla_{CARB-38}$	BK008898	*V. parahaemolyticus* S164	Unpublished
$bla_{CARB-39}$	BK008897	*V. parahaemolyticus* S174	Unpublished
$bla_{CARB-40}$	BK008889	*V. parahaemolyticus* TUMSAT_DE1_S1	(158)
$bla_{CARB-41}$	BK008890	*V. parahaemolyticus* TUMSAT_DE2_S2	(158)
$bla_{CARB-42}$	BK008894	*V. parahaemolyticus* TUMSAT_H03_S5	(158)

$bla_{CARB-43}$	BK008891	*V. parahaemolyticus* TUMSAT_H10_S6	(158)
$bla_{CARB-44}$	Pending	*V. parahaemolyticus* 04.2548	Unpublished
$bla_{CARB-45}$	Pending	*V. parahaemolyticus*T9109	Unpublished
$bla_{CARB-46}$	Pending	*V. parahaemolyticus*CFSAN007448	(159)
$bla_{CARB-47}$	Pending	*V. parahaemolyticus*NIHCB0757	Unpublished
$bla_{CARB-48}$	Pending	*V. parahaemolyticus*VPTS-2009	Unpublished

Analysis of its genetic environment showed that the $bla_{CARB-17}$ gene was located in chromosome 2 of *V. parahaemolyticus* V110. Several putative genes including those encoding transporters and enzymes are located upstream and downstream of $bla_{CARB-17}$ (**Fig. 2.2**). The $bla_{CARB-17}$-like genes could also be identified in chromosome 2 of 5 *V. parahaemolyticus* isolates with completed whole genome sequences in GenBank (**Fig. 2.2**). The genetic environments of the $bla_{CARB-17}$-like genes in these isolates were highly similar, but not identical to that in strain V110. There is no mobile genetic element such as those encoding integrase and transposase within its genetic environment, suggesting that the $bla_{CARB-17}$ gene may be intrinsic to *V. parahaemolyticus*. Further analysis of other 292 whole genome annotation reports of *V. parahaemolyticus* available in the GenBank enabled us to identify $bla_{CARB-17}$-like β-lactamases in 280 out of the 292 *V. parahaemolyticus* strains. Among these 280 $bla_{CARB-17}$-like genes identified from the GenBank, together with two clinical strains sequenced in our lab, a total of 32 CARB variants were identified and designated as $bla_{CARB-17}$ to $bla_{CARB-48}$, in which CARB-18, CARB-22, CARB-20 and CARB-30 contribute to 39.5%, 20.7%,

9.2% and 7.1%, respectively, of the population (**Table 2.4, Figs 2.4 and 2.5**). The 12 out of the 292 *V. parahaemolyticus* strains either had one nucleotide deletion within the full-length of $bla_{CARB-17}$-like genes (10 strains) or exhibited longer nucleotide fragment deletion at the N-termini (2 strains), and hence are designated as undefined (UD) sequences (**Fig. 2.5**). The latter two strains have very low numbers of proteins in their annotation reports, implying that the lack of full-length $bla_{CARB-17}$-like genes may be due to the sequencing coverage issue. Taken together, complete genome analysis suggested that all *V. parahaemolyticus* strains intrinsically harbor $bla_{CARB-17}$ and its variants. To confirm the intrinsic nature of $bla_{CARB-17,}$ 39 and 52 *V. parahaemolyticus* strains isolated from seafood in Shenzhen and Hong Kong, respectively, were screened for the presence of $bla_{CARB-17}$-like genes using primers targeting the full length of $bla_{CARB-17}$. These isolates were confirmed to be *V. parahaemolyticus* through screening for the presence of *tlh* and *atpA* genes, as well as API20E assays. All isolates were resistant to ampicillin with the exception of 10 isolates with ampicillin MIC of 16 μg/ml. All strains were found to possess $bla_{CARB-17}$ (**Table 2.1**). Twenty full length PCR products were sequenced for further confirmation. All PCR products were confirmed to be $bla_{CARB-17}$-like genes and belong to $bla_{CARB-17}$, $bla_{CARB-18}$ and $bla_{CARB-19}$, and the majority of the isolates were found to carry the $bla_{CARB-18}$ gene; such finding is consistent with the results of analysis of the 292 draft genome sequences of *V. prahaemolyticus* (**Table 2.3, Fig. 2.4**). Altogether, these data imply that $bla_{CARB-17}$ like genes are intrinsic to

V. parahemolyticus with the exact genetic sequence being slightly variable among different *V. parahemolyticus* strains.

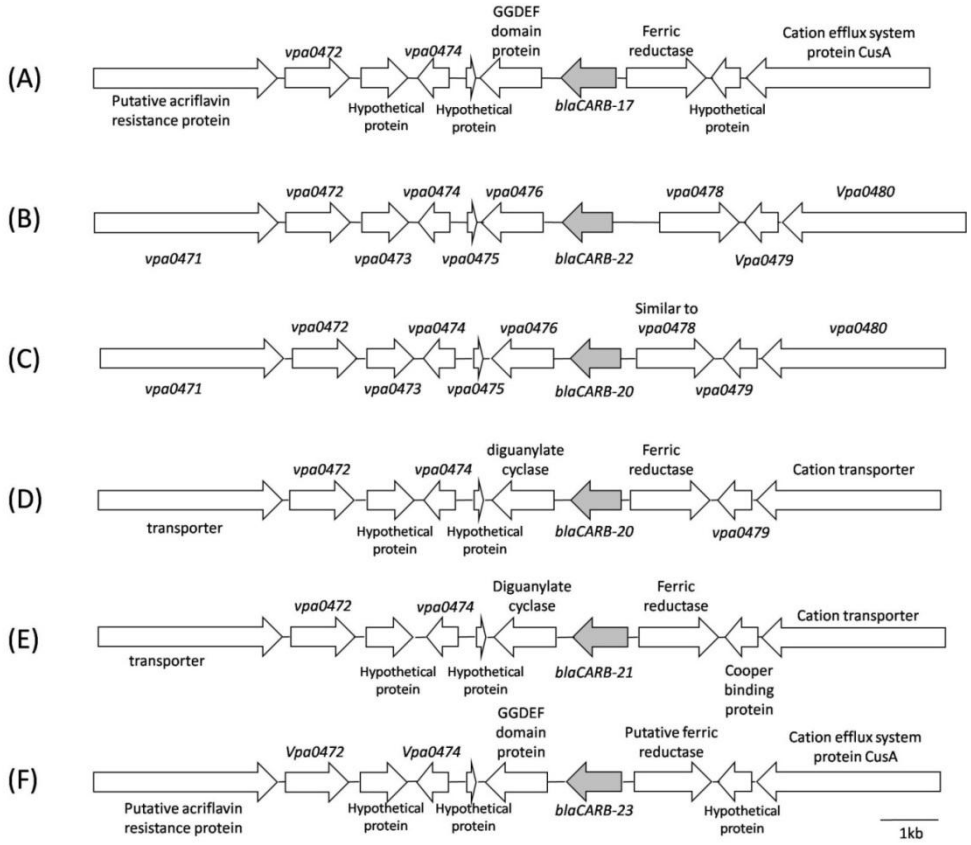

Figure 2.2 Comparison of genetic backgrounds of *bla*$_{\text{CARB-17}}$and *bla*$_{\text{CARB-17}}$-like genes from different *V. parahaemolyticus* strains.

(A) *V. parahaemolyticus* V110 chromosome 2; (B) *V. parahaemolyticus* RIMD 2210633 chromosome 2; (C) *V. parahaemolyticus* BB22OP chromosome 2; (D) *V. parahaemolyticus* O1:K33 str. CDC_K4557 chromosome 2; (E) *V. parahaemolyticus* O1:Kuk str. FDA_R31 chromosome 2; (F) *V. parahaemolyticus* UCM-V493 chromosome 2. *Vpa0471:* multidrug efflux membrane fusion protein; *Vpa0472:* long-chain fatty acid transport protein; *Vpa0473:* hypothetical protein; *Vpa0474:* spermidine n1-acetyltransferase; *Vpa0475:* hypothetical protein (GGDEF family protein with GAF sensor); *Vpa0476:* hypothetical protein*; Vpa0477:* β-lactamase; *Vpa0478:* oxidoreductase*; Vpa0479:* hypothetical protein*; Vpa0480:* cation efflux system transmembrane protein.

The current nomenclature for the CARB family of β-lactamases is confused with the PSE family in the literature. PSE-4 from *P. aerugenosa* shared only 45-49% amino acid sequence homology with the PSE-4 from *Vibrio spp.* except the one from *V. cholerae* (**Fig. 2.3**). CARBs are divided into two subgroups, namely the CARB and RTG subgroups. CARB subgroups, including CARB-1 (PSE-4), CARB-2 (PSE-1), CARB-3, CARB-4, CARB-6, CARB-7, CARB-9, CARB-11 (PSE-5) to CARB-15, are narrow-spectrum β-lactamases that hydrolyze penicillins (160, 161). RTG subgroups, including CARB-5 (RTG-2), CARB-8 (RTG-3) and CARB-10 (RTG-4), consist of an RTG triad as reported for the GN79 (RTG-1) from *Proteus mirabilis* (150, 153, 162, 163). Most of the CARB families were not subjected to functional characterization except CARB-10, which has been shown to hydrolyze cefepime and cefpirome and became extended-spectrum CARB enzyme (153). The CARB-17 exhibited 99% homology to PSE-4 from *V. parahaemolyticus* and approximately 80% to PSE-4 from *V. cholerae henc*, as well as VHW-1 and VHH-1 from *V. harvey* through BLAST analysis (164) (**Fig. 2.3**). The latter two β-lactamases have been shown to be active on penicillins (164). Based upon the functional characterization of novel CARB-17 and its variants, the CARB family of β-lactamase can be separated into three distinct groups through further phylogenetic analysis of all CARB β-lactamases. The first group contains CARB-17 and its closely related variants, the second group contains mainly the previously identified narrow spectrum CARB family from

Pseudomonas spp and *V. Cholerea*, while the third group contains broad spectrum RTG subgroup (**Fig. 2.3**).

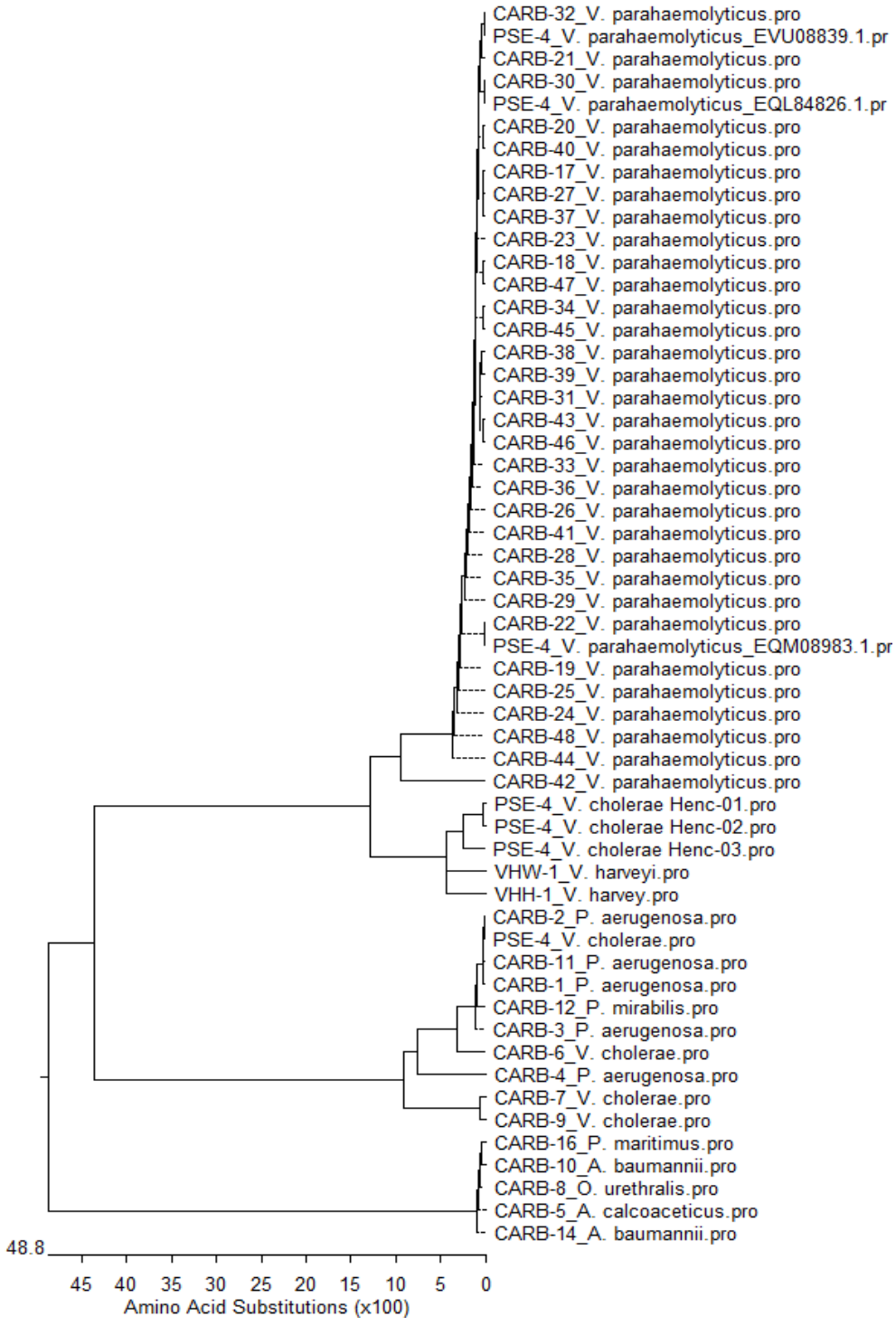

Figure 2.3 Phylogenetic tree of CARB-family and several related β-lactamases. All the protein sequences are extracted from NCBI database. The CARB-family proteins were clustered together.

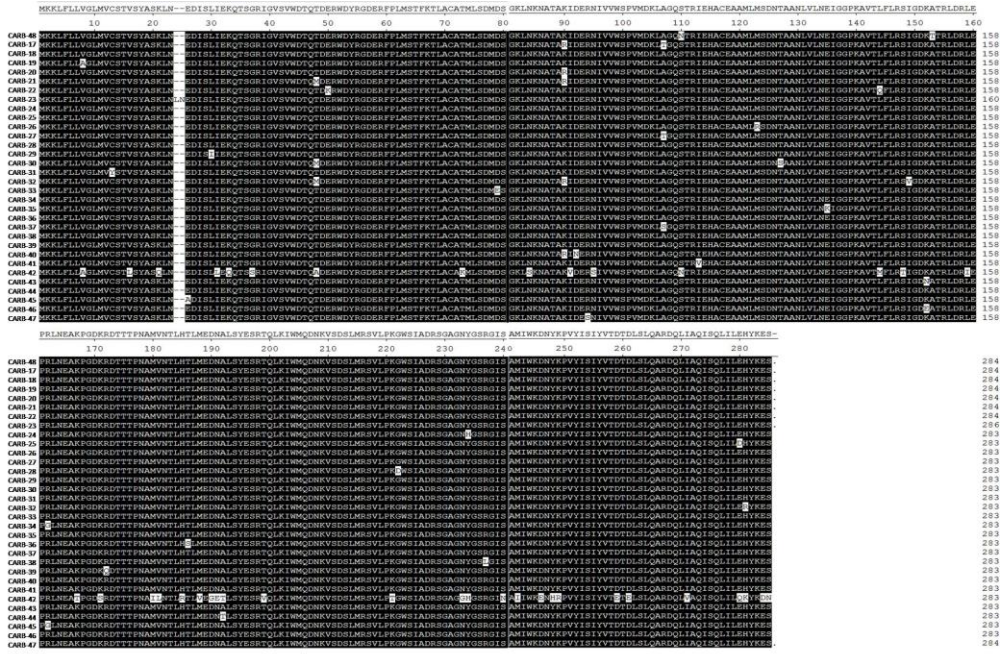

Figure 2.4. Sequence alignment of CARB-17 and other 31 closely related variants. All the variants were extracted from NCBI WGS database.

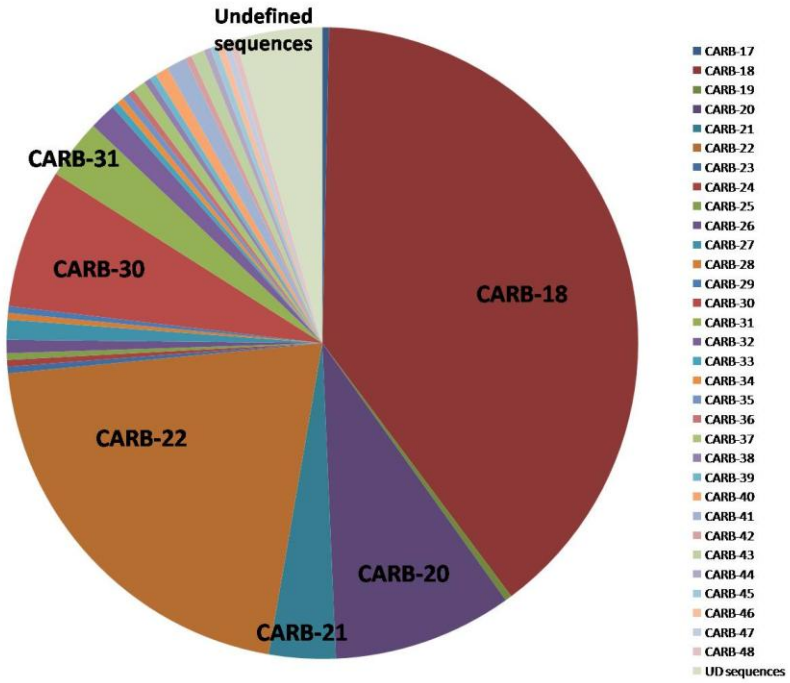

Figure 2.5 Distribution of the 32 CARB variants in 293 *V. parahaemolyticus* strains with draft genome sequence from the GenBank. The area of sectors matched the numbers of strains for each variants.

2.4.2 Comparison of the genetically conserved VbrK/R system in *Vibrio* species

Li *et al* (144) recently reported the discovery of a novel two-component system (TCS) VbrK/VbrR, which regulates the expression of an intrinsic β-lactamase gene in *Vibrio parahaemolyticus*, thereby conferring intrinsic resistance to the penicillin class of antibiotics (**Fig. 2.6**). This intrinsically expressed enzyme was named CARB-17 like β-lactamase by our group (165). As a histidine kinase/response regulator pair, VbrK/R is the only system known to be responsible for sensing and eliciting development of resistance to antibiotics (β-lactams) in Gram-

negative bacteria. An analogous system is known to exist in Gram positive organisms, in which the VanSR TCS was found to mediate vancomycin resistance in *Enterococci* (166). Li *et al*. reported that regulation of expression of the CARB-17 like β-lactamase-mediated intrinsic β-lactam resistance phenotype by the VbrK/R regulatory pathway is well conserved in *Vibrio* species. We suggested that this statement is only true for the *V. harveyi* clade but not other species of *Vibrio* including *V. cholera, V. vulnificus and V. splendidus*.

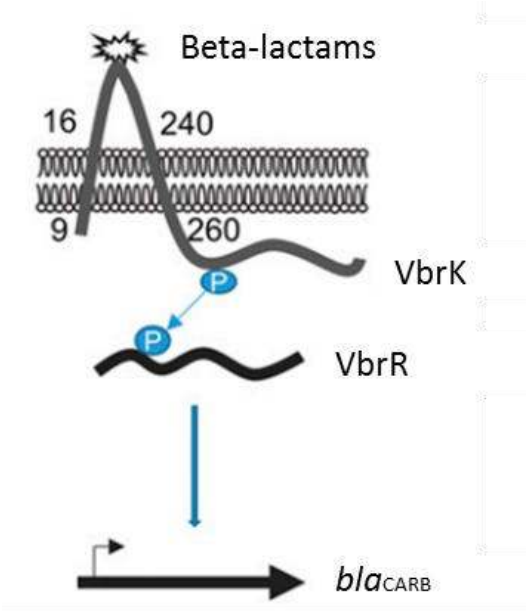

Figure 2.6 Schematic model for VbrK/VbrR-CARB regulation system proposed by Li *et al*.

Upon discovery of $bla_{\text{CARB-17}}$ as the intrinsic penicillin resistance-encoding element in *V. parahaemolyticus*, we searched for homologues of this gene in other species of *Vibrio* (165). Our data showed that CARB-17 like β-lactamase genes were prevalent only in the *V. harveyi* clade with more than 70% homology at the nucleotide sequence level, but not among other species of *Vibrio*

(167). This finding is inconsistent with the idea that the VbrK/R-CARB-17 system is solely responsible for the regulation of $bla_{\text{CARB-17}}$. We then performed phylogenetic analysis for the nucleotide sequences of *vbrK-vbrR* cluster, 16s rRNA, and $bla_{\text{CARB-17}}$ -like genes in different species of *Vibrio* (**Fig. 2.7**). The phylogenetic tree of 16s rRNA showed that the *V. harveyi* clade was more conservative than the other species. Although *vbrK/R* homologues exist in all *Vibrio* species, the *vbrK-vbrR* sequence of *V. harveyi* is also much more conservative than those in other species of *Vibrio* such as *V. cholera, V. vulnificus* and *V. splendidus*. Most importantly, $bla_{\text{CARB-17}}$ like genes could only be detected in the *V. harveyi* clade but not other species of *Vibrio*. The phylogenetic tree also revealed some evolutionary features of *vbrK-vbrR* within different species of *Vibrio*, which confirm that the VbrK/R-CARB-17 system was only conserved within the *V. harveyi* clade. It is therefore likely that the *vbrK-vbrR* homologues in *Vibrio* species other than *V. harveyi* clade play a role in regulating expression of genes other than those encoding β-lactamase, this notion is further supported by fact that *V. cholera, V. vulnificus* and *V. splendidus* are not intrinsically resistant to penicillin.

TCSs are important regulatory systems that are utilized by bacteria to adapt to different environmental conditions, and one TCS may be involved in regulating multiple genes and hence a wide range of physiological functions (166, 168). It is tempting to speculate that the VbrK/R-CARB-17 system, which is well-conserved in the *V.*

harveyi clade, has evolved to become regulators of other genetic components in other *Vibrio* species. In fact, on the basis of the discrepancy between the gene expression patterns of the Δ*vbrK* and WT strains (144), we speculated that $bla_{\text{CARB-17}}$ may not be the only target of VbrK/R in *V. parahaemolyticus* or *V. harveyi* clade. Further works on identifying the range of genes regulated by VbrK/R and its homologues, in the *V. harveyi* clade and other *Vibrio* species respectively, are warranted to comprehensively elucidate the physiological functions of this novel TCS in the *Vibrios*.

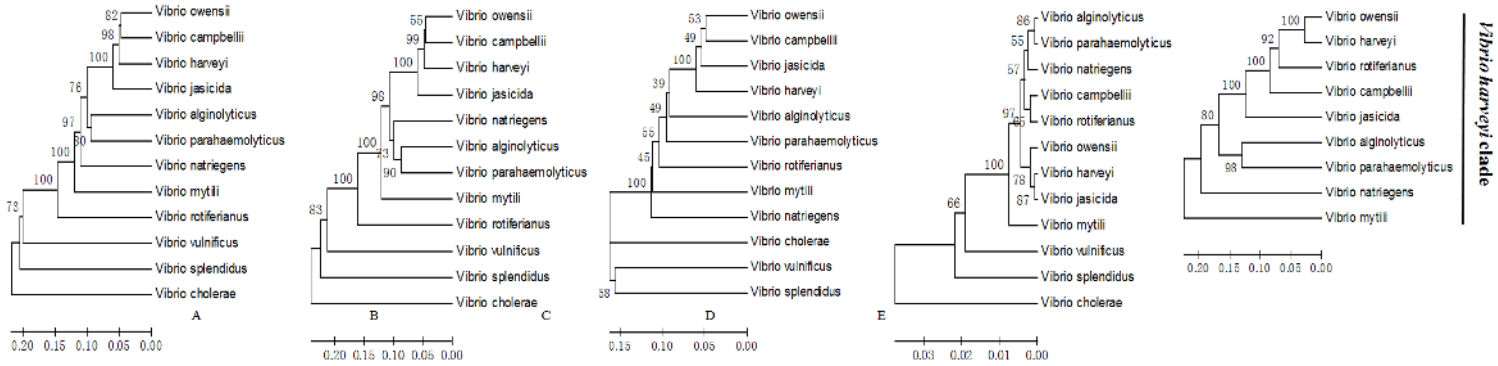

Figure 2.7 Evolutionary relationships of taxa of different genes

The evolutionary history was inferred using the UPGMA method. The bootstrap consensus tree inferred from 100 replicates is taken to represent the evolutionary history of the taxa analyzed(169). The evolutionary distances were computed using the Maximum Composite Likelihood method (170) and are in the units of the number of base substitutions per site. All positions with less than 95% site coverage were eliminated. That is, fewer than 5% alignment gaps, missing data, and ambiguous bases were allowed at any position. Evolutionary analyses were conducted in MEGA6(171). Figure A, B, C, D, E represent the evolutionary relationships of *vbrK*-*vbrR* cluster, *vbrK*, *vbrR*, *16s rRNA* , $bla_{\text{CARB-17}}$ -like genes respectively. *Vibrio harveyi* clade is defined according to the published report (172). All the sequences are extracted from nr, WGS and 16S ribosomal RNA sequences databases in NCBI. No homologous $bla_{\text{CARB-17}}$ -like genes can be found out of V. *harveyi* clade in the databases.

2.5 Conclusion

In conclusion, this study identified 33 novel class A β-lactamases, CARB-17 to CARB-49, which are responsible for intrinsic resistance to penicillins in *V. parahaemolyticus*. The data provide functional information for a large group of β-lacamses identified from *V. parahemolyticus* in the GenBank and clear grouping for the whole family of CARB class of β-lactamases, which may in turn facilitate correct classification of the CARB family of β-lactamases.

Furthermore, the regulation pathways of blaCARB, VbrK/R-CARB-17, should be well-conserved in the *V. harveyi* clade. The functional roles of VbrK/R TCS in other non- *V. harveyi* clade entail further characterization.

Chapter Three: A Novel PCR-Based Approach for Accurate Identification of *Vibrio parahaemolyticus*

Most of the content in this chapter is reproduced from the published paper:

Li R, Chiou J, Chan EW, & Chen S (2016) A Novel PCR-Based Approach for Accurate Identification of *Vibrio parahaemolyticus*. *Frontiers in Microbiology 7:44.*

3.1 Abstract

A PCR-based assay was developed for identification of *Vibrio parahaemolyticus* through targeting the $bla_{\text{CARB-17}}$ like element, an intrinsic β-lactamase gene that may also be regarded as a novel species-specific genetic marker of this organism. Phylogenetic analysis showed that $bla_{\text{CARB-17}}$ like genes were more conservative than the *tlh, toxR* and *atpA* genes, the common markers used for identification of *V. parahaemolyticus*. Our data showed that this $bla_{\text{CARB-17}}$-specific PCR-based detection approach consistently achieved high specificity, whereas PCR targeting the *tlh* and *atpA* genes occasionally produced false positive results. Furthermore, a positive result of this test is consistently associated with an intrinsic ampicillin resistance phenotype of the test organism, presumably encoded by the $bla_{\text{CARB-17}}$ like gene. We envision that combined

analysis of the unique genetic and phenotypic characteristics conferred by $bla_{\text{CARB-17}}$ shall further enhance the detection specificity of this novel yet easy-to-use detection approach to a level superior to the conventional methods of *V. parahaemolyticus* detection and identification

3.2 Introduction

Identification of *V. parahaemolyticus* is conventionally conducted by biochemical testing upon isolation of the organism from selective agar plates (173). However, identification of *V. parahaemolyticus* by phenotypic approaches has some drawbacks in being labor-intensive, time-consuming and not very effective in terms of detection specificity (173, 174). To cope with the problems caused by the conventional microbiological culture method, some rapid detection methods based on genus or species-specific genotypic features have been developed recently (174-180). Many of the targeting genes used in these approaches are phylogenetic markers or those involved in virulence (*tlh*, *toxR*, *atpA* etc.), yet some of which are not highly species-specific as different *Vibrio* species may share similar sequences, thus reducing the accuracy and specificity of such detection methods.

Based on the intrinsic resistant gene $bla_{\text{OXA-51-like}}$ of *Acinetobacter baumannii*, one PCR detection method targeting them has been reported (181). Our laboratory recently identified a β-lactamase that contributed to intrinsic ampicillin resistance in *V. parahaemolyticus*

(182). The gene encoding this enzyme is more conservative in *V. parahaemolyticus* than other gene markers and it bears all the hallmarks of a unique marker suitable for *V. parahaemolyticus* detection and identification. In this study, we took further steps to develop an accurate and simple PCR test for detection and identification of *V. parahaemolyticus* based on this novel genetic marker, a $bla_{\text{CARB-17}}$ like gene, which is 852bp in length.

3.3 Materials and Methods

3.3.1 Bacterial strains

A total of 120 *V. parahaemolyticus* strains and 109 non- *V. parahaemolyticus* strains were used in this study. All strains were identified using 16SrRNA sequencing and API 20E test strips (bioMerieux, Inc.). Genomic DNA extraction was conducted by the boiling method. Briefly, 1 ml of overnight culture was centrifuged and the pellet was resuspended in 400μl of ddH_2O. The bacterial suspension was boiled for 5 min and centrifuged at 11,000g for 6 min. The supernatant was used as DNA template for PCR assay.

3.3.2 Phylogenetic analysis of different genetic markers within the *Vibrio* spp.

V. parahaemolyticus is one member of the *Vibrio harveyi* group, which comprised *Vibrio alginolyticus*, *Vibrio harveyi* and *Vibrio campbellii* etc.. These species exhibited a high degree of genetic relatedness in phylogenetic analysis (183). However, in our routine

identification of *V. parahaemolyticus*, we noticed that PCR often could not differentiate organisms in the *Vibrio harveyi* group, especially *parahaemolyticus* and *Vibrio alginolyticus*. This phenomenon is in agreement with the finding that *tlh* was also distributed among *V. alginolyticus* (184) and that similar genes with *V. parahaemolyticus* virulence-related genes occurred in other Vibrionaceae species(185). Phylogenetic analysis of the *atpA*, *tlh, toxR* and $bla_{\text{CARB-17}}$ genes was then performed with the DNAMAN software (Lynnon Biosoft Corporation, USA, www.lynon.com).

3.3.3 Development of a PCR method targeting $bla_{\text{CARB-17}}$ like genes in *V. parahaemolyticus*

In order to design specific primers for CARB detection in *V. parahaemolyticus*, the conserved regions of this gene in the *V. parahaemolyticus* genome was screened and a PCR-based mismatch amplification mutation assay was developed. Upon sequence alignment, two regions (550-565, 834-852) that correspond to the location of $bla_{\text{CARB-17}}$ (KJ934265) were selected for primer designing. The designed primers were listed in **Table 3.1**. Primer-Blast was used to check primer pair specificity (http://www.ncbi.nlm.nih.gov/tools/primer-blast). The results showed that this set of primers did not have other nonspecific targets in DNA fragments of the nr database.

Table 3. 1 Primers used in comparison of detection specificity of different *V. parahaemolyticus* detection methods

Primer names	Primer Sequences	Product length	Target genes	References
CARB-F	ACC(T)TTGATGGAAGATA	303bp	$bla_{\text{CARB-17}}$	This study
CARB-R	T(C)TAACTTTCTTTGTAGTGC(A)			
TLH-F	AAAGCGGATTATGCAGAAGCACTG	450bp	*tlh*	(186)
TLF-R	GCTACTTTCTAGCATTTTCTCTGC			
atpA-VP-F	TACTAGGCCGCGTAGTA	794bp	*atpA*	(174)
atpA-VP-R	CGCTGGACGTACACCT			
toxR-VP-F	GTCTTCTGACGCAATCGTTG	350bp	*toxR*	(187)
toxR-VP-R	ATACGAGTGGTTGCTGTCATG			

PCR reactions using the designed primers were optimized by testing different annealing temperature, primer concentrations and extension time. Each reaction mixture (20ul) contained 10ul of Premix Ex Taq^{TM} (TaKaRa, Japan), 0.5ul of DNA template, 1ul of forward and reverse primers(10pm) respectively, and 7.5ul of nuclease-free water. The PCR amplification program was as follows:

95℃ for 5min, followed by 30 cycles of 95℃ for 30s, 50℃ for 30s, and 72℃ for 30s, and final elongation at 72℃ for 5min. The PCR products were differentiated on 1.5% agarose and visualized by the Gel Doc System (Biorad). The specificity of the PCR method was tested with 120 *V. parahaemolyticus* strains and 109 non- *V. parahaemolyticus* strains (**Table 2**).

3.3.4 Comparison of the CARB detection approach with other PCR detection methods

Other reported PCR detection methods targeting the *tlh*, *atpA* and *toxR* genes were included in this study to compare the specificity between them. The primers used were listed in **Table 1**. The components of PCR reaction mixtures were identical to the one used in detecting CARB. The PCR amplification program was as follows: 95℃ for 5min, followed by 30 cycles of 95℃ for 30s, 60℃ for 30s, and 72℃ for 30s (1min for *atpA* amplification), and final elongation at 72℃ for 5min. The results were recorded according to the method mentioned above.

3.4 Results and Discussion

With thorough bioinformatics analysis of the putative β-lactamase gene, we identified 32 CARB-like variants among the 293 available whole genome sequences in NCBI as of October 1, 2014. Apart from *V. parahaemolyticus*, CARB-like genes were found to distribute among several other *Vibrio* spp., such as *Vibrio*

alginolyticus, *Vibrio harveyi*, *Vibrio campbellii*, *Vibrio jasicida*, *Vibrio natriegens*, *Vibrio owensii* and *Vibrio rotiferianus*. Upon phylogenetic analysis, we found that the $bla_{\text{CARB-17}}$ like genes in *V. parahaemolyticus* exhibited the highest degree of similarity (78% homology) with that in *Vibrio alginolyticus* (**Fig. 3.1**). In order to compare the uniqueness of this gene with other genetic markers used to detect *V. parahaemolyticus*, we selected the *tlh*. *atpA* and *toxR* genes within the *Vibrio* spp. and compared their genetic relatedness. The results showed that the degree of homology between *V. parahaemolyticus* and *Vibrio alginolyticus* were respectively 86%, 97% and 86% for the *tlh*, *atpA* and *toxR* genes; these percentage values were higher than that of the $bla_{\text{CARB-17}}$ gene, indicating that the $bla_{\text{CARB-17}}$ like gene is the most conservative among these genes in *V. parahaemolyticus*.

The PCR assay designed in this study for detection of the $bla_{\text{CARB-17}}$ like gene in *V. parahaemolyticus* yielded an amplified fragment of 303bp. The efficiency of this PCR method is high (**Fig. 3.2**); the specificity of the developed PCR in this study and other published methods (174, 186) were verified in parallel with different strains (**Table 3.2**), with results showing that PCR methods based on $bla_{\text{CARB-17}}$ yielded 100% specificity and efficiency to all different species of bacteria tested, while the methods based on detecting *atpA* and *tlh* occasionally produced false positive result. The method based on the *toxR* gene has identical specificity with $bla_{\text{CARB-17}}$, however, the original paper about *toxR* detection paper reported

nonspecific amplifications for some *V. vulnificus* strains(187). Primers targeting the *atpA* gene exhibited very high false positive rate (89%) for *V. cholerae* and 2.8% false positive rate for *V. alginolyticus*, whereas primers targeting the *tlh* gene yield 20% false positive rate for *V. alginolyticus* (**Table 3.2**). This indicates that the choice of these two targets is not rigorous enough in terms of detection specificity. Some of the PCR results have been displayed in Supplementary Figure 1. The different *tlh* gene variants in *V. alginolyticus* and *V. parahaemolyticus* were detrimental to the specificity of the primers. All the *tlh* genes in the WGS database for *V. alginolyticus* and *V. parahaemolyticus* were included in Supplementary Sequences. In contrast, the use of $bla_{\text{CARB-17}}$ specific primers did not result in any false positive detection for all the bacteria tested, and consistently maintained 100% detection specificity for *V. parahaemolyticus*. Although many molecular detection methods have been developed to identify *Vibrio parahaemolyticus* rapidly, some do not have a satisfactory level of specificity, hindering extensive application in routine laboratory tests (184, 185). In this work, we showed that the $bla_{\text{CARB-17}}$ gene is a specific *Harveyi* clade (including *V. parahaemolyticus*) gene that can be used as a novel target for detection of *V. parahaemolyticus* by using degenerated primers. Combined with other specific target genes in other *Vibrio* spp., this novel target gene may be used to design multiple-PCR to detect food contamination by *V. parahaemolyticus* rapidly.

Table 3. 2 Result of the specificity of PCR methods targeting different genes in *Vibrio parahaemolyticus* and non-*Vibrio parahaemolyticus* strains.

Species	Source	No. of strains	Positive rate (No. of positive strains)			
			bla$_{CARB-17}$	tlh	atpA	toxR
Vibrio parahaemolyticus	Food, Clinical	120	100%	100 %	100%	100 %
Vibrio cholerae	Food	26	0	0	89% (23)	0
Vibrio vulnificus	Food, Clinical	4	0	0	0	0
Vibrio alginolyticus	Food	35	0	20% (7)	2.8% (1)	0
Vibrio metschnikovii	Food	1	0	0	0	0
Vibrio fluvialis ATCC33809	ATCC	1	0	0	0	0
Vibrio harveyi ATCC33842	ATCC	1	0	0	0	0
Vibrio mimicus ATCC 33653	ATCC	1	0	0	0	0
Vibrio campbellii ATCC33865	ATCC	1	0	0	0	0
Vibrio natriegens ATCC14048	Food	1	0	0	0	0
Aeromonas spp.	Food	7	0	0	0	0
Escherichia coli	Food, Clinical	10	0	0	0	0
Salmonella spp.	Food, Clinical	10	0	0	0	0
Enterobacter spp.	Clinical	2	0	0	0	0
Pseudomonas aeruginosa PAO1	Clinical	1	0	0	0	0
Citrobacter freundii	Clinical	2	0	0	0	0

Klebsiella pneumonia	Clinical	1	0	0	0	0
Proteus mirabilis	Food	2	0	0	0	0
Myroides odoratimimus	Food	2	0	0	0	0
Staphylococcus aureus	Food	1	0	0	0	0

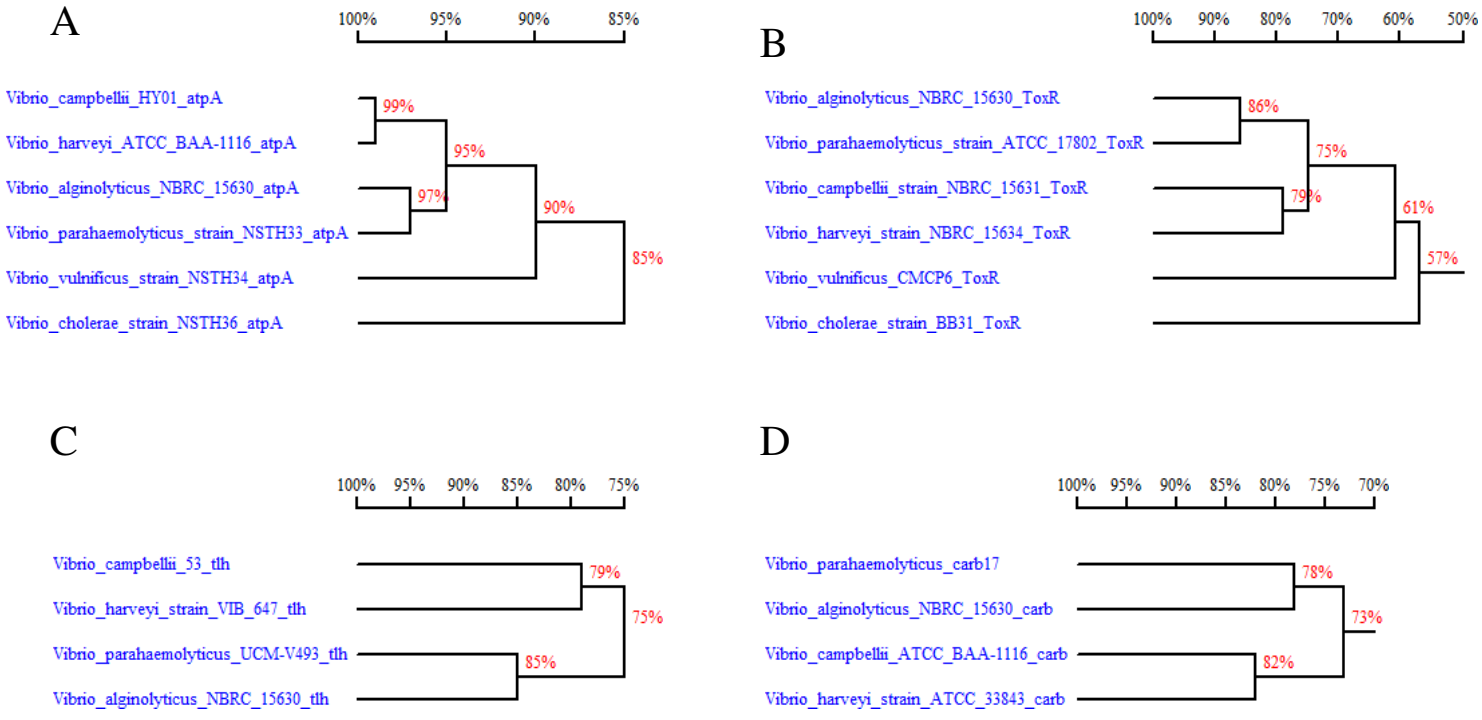

Figure 3. 1 Sequence homology comparison between related *Vibrio* spp. for four different genes used as *V. parahaemolyticus* detection targets.

A. *atpA* gene homology comparison between *Vibrio* spp.; B. *toxR* gene homology comparison between *Vibrio* spp.; C. *tlh* gene homology comparison between species in the *Vibrio harveyi* group; D.$bla_{\text{CARB-17}}$ gene homology comparison between species in the *Vibrio harveyi* group.

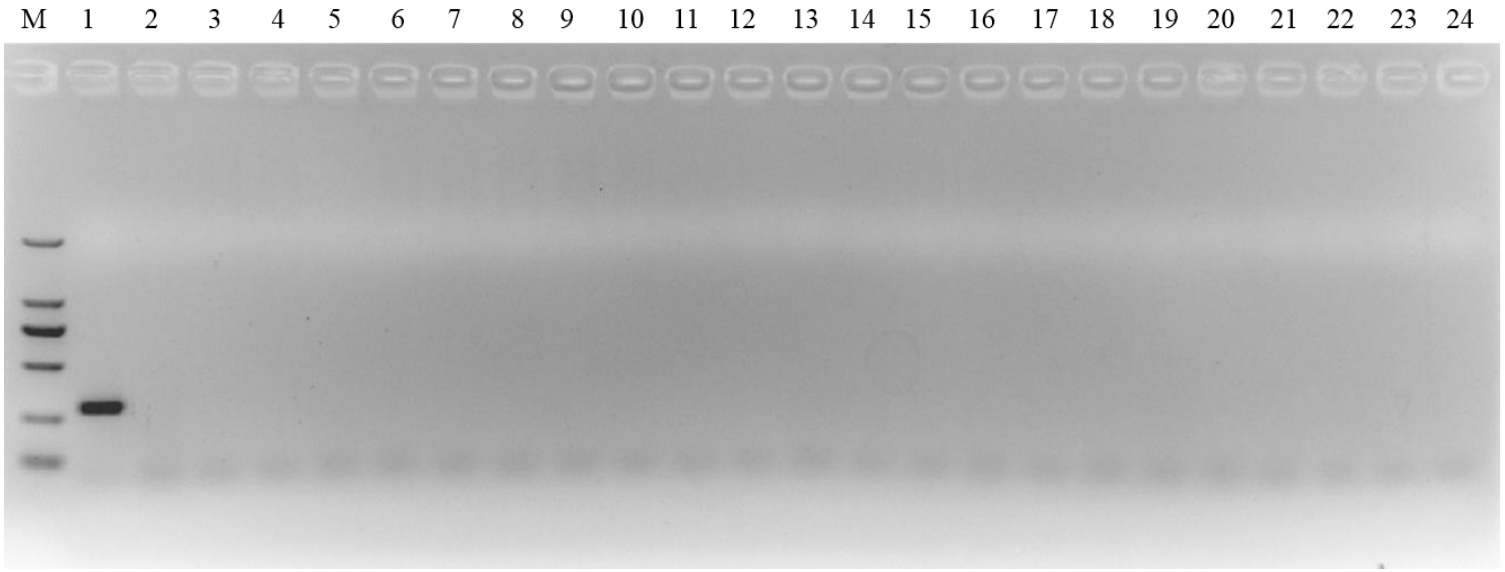

Figure 3. 2 Agarose gel picture of PCR with designed *bla*$_{\mathbf{CARB}}$ primers.

M stands for DL2000 DNA marker, lane 25 is negative controls (no template). Other lanes are the samples of genomic DNA templates of different strains. Lane 1, *V. parahaemolyticus* 17802; land 2, *Vibrio cholera* VC1; lane 3, *Vibrio vulnificus* ATCC27562; lane 4, *Vibrio alginolyticus* ATCC33787; lane 5, Vibrio metschnikovii V18; lane 6, *Vibrio fluvialis* ATCC33809; lane 7, *Vibrio harveyi* ATCC33842; lane 8, *Vibrio mimicus* ATCC33653; lane 9, *Vibrio campbellii* ATCC33865; land 10, *Vibrio natriegens* ATCC14048; land 11, *Aeromonas caviae* A24; lane 12, *Escherichia coli* ATCC25922; lane 13, *Pseudomonas aeruginosa* PAO1; lane 14, *Salmonella typhimurium* LT2; lane 15, *Enterobacter spp*. E1; lane 16, *Citrobacter freundii* C1; lane 17, *Klebsiella pneumonia* 51; lane 18, *Proteus mirabilis* HD4; lane 19, *Myroides odoratimimus* MO12-4; lane 20, *Staphylococcus aureus* ATCC25923; lane 21, *Salmonella enteritidis* SE1; lane 22, *Salmonella derby* SD1; lane 23, *Aeromonas hydrophila* A10; lane 24, negative control.

3.5 Conclusion

In this report, we used the available genome sequences in NCBI to identify a resistance gene known as *bla*$_{\text{CARB-17}}$-like gene that is intrinsic to *Vibrio parahaemolyticus*. Based on the DNA sequences, a set of degenerated primers were designed to detect this major foodborne pathogen. The specificity of this method is better than other published approaches. The *bla*$_{\text{CARB-17}}$ gene can be used as a novel *V. parahaemolyticus* detection marker in combination with other markers to detect different *Vibrio* spp. simultaneously and rapidly. With the increasing amount data of genome sequences, more species-specific genetic markers could be mined *in silico* through bioinformatics techniques, and relieve the laborious works needed to be performed for specificity testing.

Chapter Four: First detection of AmpC β-lactamase *bla*$_{CMY-2}$ on a conjugative IncA/C plasmid in *Vibrio parahaemolyticus* of food origin

Most of the content in this chapter is reproduced from the published paper:

Li R, Lin D, Chen K, Wong MH, & Chen S (2015) First detection of AmpC beta-lactamase *bla*$_{CMY-2}$ on a conjugative IncA/C plasmid in *Vibrio parahaemolyticus* of food origin. *Antimicrobial agents and chemotherapy 59(7):4106-4111.*

4.1 Abstract

Resistance to penicillin is common among *V. parahaemolyticus*, whereas cephalosporin resistance remains rare. In an attempt to assess the current prevalence and characteristics of antibiotic resistance of this pathogen in common food samples, a total of 54 (17%) *V. parahaemolyticus* strains were isolated from 318 meat products and seafood samples purchased from supermarkets and wet markets in Shenzhen, China, in 2013. These isolates exhibited high level resistance to ampicillin, yet they were mostly susceptible to other antimicrobials, except for two which were resistant to extended-spectrum cephalosporins. The β-lactamase gene *bla*$_{PER-1}$ was detectable in one strain, V43, which was resistant to both third and fourth generation cephalosporins. Compared to other *bla*$_{PER-1}$

positive *V. parahaemolyticus* strains reported in our previous studies, strain V43 was found to harbor a ~200kb conjugative plasmid encoding different antimicrobial resistance genes from the previous studies. The β-lactamase gene bla_{CMY-2} was detectable for the first time in another *V. parahaemolyticus* isolate, V4, which was resistant to the third generation cephalosporins. This bla_{CMY-2} gene was shown to be located in an ~150kb IncA/C type conjugative plasmid with a genetic structure of *traB-traV-traA-ISEcp1-*bla_{CMY-2}*-blc-sugE-encR-orf1-orf2-orf3-orf4-dsbC-traC*, which is identical to that of other IncA/C conjugative plasmids in *Enterobacteriaceae*, albeit with a different size. These findings indicate that transmission of ESBL and AmpC β-lactamase genes via conjugative plasmids can mediate the development of extended-spectrum cephalosporins resistance in *V. parahaemolyticus*, thereby posing a potential threat to public health.

4.2 Introduction

V. parahaemolyticus is a halophilic gram-negative bacterium and one of the most important seafood-borne pathogens worldwide. It is widely distributed in estuarine-marine environment and seafood products, often causing infections via consumption of raw or undercooked seafood (188, 189). The most common symptoms of *V. parahaemolyticus* infections include gastroenteritis, diarrhea, headache, nausea, and vomiting. For children, the elderly or people with suppressed immune system, *V. parahaemolyticus* intestinal infections can be fatal (190). The pathogenicity of *V.*

parahaemolyticus is always associated with the presence of the toxin genes *tdh* (encoding the thermostable direct hemolysin) and its homolog *trh* (encoding the TDH-related hemolysin) (191). The U.S. Food and Drug Administration estimates that approximately 4,500 U.S. infections occur per year, and over the past 15 years, outbreaks have been increasing in terms of scale and frequency (190). In recent years, the number of *V. parahaemolyticus* infections in China has increased significantly (188).

For life threatening infections caused by *V. parahaemolyticus*, antibiotic therapy (mainly including tetracycline, quinolones and third-generation cephalosporins) is necessary (86). Increasing prevalence of antimicrobial resistance in *V. parahaemolyticus*, presumably due to extensive use of antimicrobials in clinical treatment and aquaculture systems, has recently been reported (87-90). To date, resistance to ampicillin, streptomycin, kanamycin, tetracycline, chloramphenicol and ciprofloxacin have been reported (90). Recent studies also reported resistance to third-generation cephalosporins in *V. parahaemolyticus* strains due to carriage of an extended-spectrum beta-lactamase (ESBL) gene, $bla_{\text{PER-1}}$ (91). However, other ESBL genes or AmpC type genes are not detectable in *V. parahaemolyticus*.

With the rapid development of aquaculture industry, infections associated with *V. parahaemolyticus* in seafood have become increasingly common in China and Asian countries. In China,

research on the epidemiology and antimicrobial resistance of *V. parahaemolyticus* from food products, in particular meat products, is very rare. This study reported the surveillance of the prevalence and antimicrobial resistance of *V. parahaemolyticus* collected from different food products including shrimps, pork, beef and chicken in Shenzhen, China. The data will provide valuable information for future control of *V. parahaemolyticus* infections in China and neighboring countries.

4.3 Materials and Methods

4.3.1 Isolation and identification of *V. parahaemolyticus*

A total of 318 food samples including shrimps, chicken, pork and beef were collected from supermarkets and wet markets in Shenzhen, China from June to September 2013. The isolation of *V. parahaemolyticus* was conducted as previously described with some modifications (173). Briefly, food samples were purchased and transferred to the laboratory within three hours under low temperature condition (stored in insulated bags containing ice cubes). Five grams of food samples were homogenized in 45 ml alkaline peptone water (APW) and incubated overnight at 37 °C. A loopful of culture was then streaked on thiosulphate citrate-bile salt sucrose (TCBS) agar. After 16 h of incubation at 37 °C, suspicious colonies (blue or green) were picked and streaked on CHROMagar Vibrio plates for identification. The mauve colonies on CHROMagar Vibrio plates, presumptively identified as *V. parahaemolyticus*, were transferred into Brain heart infusion (BHI)

broth with 3% NaCl and incubated overnight at 37 °C. The bacterial culture was stored in 15% glycerol at -80°C for further characterization.

Isolates with typical phenotypes on TSBS and CHROMagar Vibrio plates were confirmed by PCR detection of the thermolabile haemolysin (*tlh*) gene and DNA sequencing. Detection of virulence genes (*tdh* and *trh* genes) was also performed by the PCR approach as previously described (192).

4.3.2 Antimicrobial susceptibility testing and PFGE Typing

Antimicrobial susceptibility testing was performed on *V. parahaemolyticus* isolates by using the standard agar dilution method as described by the Clinical and Laboratory Standards Institute (193). Fourteen antimicrobials were tested including nalidixic acid, ciprofloxacin, ofloxacin, amikacin, gentamicin, tetracycline, ampicillin, amoxicillin-clavulanic acid, cefoxitin, ceftazidime, meropenem, imipenem, trimethoprim-sulfamethoxazole, and chloramphenicol. Resistance breakpoints published by the Clinical and Laboratory Standards Institute were used (194). *Escherichia coli* ATCC25922 was included as the quality control strain.

PFGE was conducted to investigate the genetic relatedness of the identified isolates according to the PulseNet protocol (http://www.pulsenetinternational.org/protocols/) with minor

modifications. In brief, the cell suspensions (OD_{610nm}=0.9) with proteinase K (1 mg/ml) were immobilized into 2% low-melting-point agarose (Amerson, UK) at the ratio of 1:1 before incubation in a lysis buffer including proteinase K (0.1 mg/ml). After five consecutive steps of washing with Tris-EDTA buffer (pH 8.0) at 50 °C in a water bath shaker, the total DNA was digested with 40U of NotI or SfiI (New England Biolabs) for 4 hours at 37 °C, 50°C respectively. Chromosomal DNA of *Salmonella* serotype *Braenderup* (H9812) digested with XbaI was used as reference markers. The DNA bands were separated using a CHEF MAPPER XA pulsed field electrophoresis system (Bio-Rad Laboratories, Hercules, CA, USA) for 19h with switch times of 10-35 seconds at 6 V/cm, 14°C in 0.5× Tris-Boric Acid-EDTA buffer. Gels were stained with GoldView dye and photographed using a Bio-Rad Gel Doc 1000 system. PFGE dendrogram was generated by using the Bionumerics 7.1 software.

4.3.3 β-Lactamase gene screening and analysis of genetic environment

The prevalence of β-Lactamase genes among the test strains was determined by PCR assays that covered most of the known β-lactamase genes as previously described (195). Screening of class 1 integron was also performed as described previously (86). The entire sequence of the bla_{CMY-2} gene was amplified using primers CMY2_F and CMY2_R (**Table 4.1**). The amplified product was cloned into a TOPO pCR2.1 vector (Invitrogen) and sequenced with

universal primers. Primer walking and PCR mapping were performed to investigate the *bla*$_{CMY-2}$ gene environment. A set of primers (**Table 4.1**) were designed based on the published flanking sequence of *bla*$_{CMY-2}$ gene (196). The PCR products were sequenced and subjected to sequence alignment analysis using the BioEdit software.

Table 4. 1 PCR primers used to determine the genetic content of β-lactamase genes.

Primer name	Sequence	Length (bp)	Target	source
CMY2_F	GCTGAGAGCTCATGATGAAAAAATCG	1146	*bla*$_{CMY-2}$	This study
CMY2_R	GGTACGGATCCTTATTGCAGC			
Primers for bla$_{CMY-2}$ genetic environment determination				
TraA-F	ATCAGTTGGCGAATGCCTCA	1417	*traA*-IS*Ecp1*	This study
ISEcp1-R	AACACGGCTTCATTCGCCCAA			This study
ISEcp1-F	ATAAAGACCATGCTCTGCGG	2537	IS*Ecp1*-*bla*$_{CMY-2}$	This study
CMY-2R	ACGGACAGGGTTAGGATA			(195)
ISEcp1-F	ATAAAGACCATGCTCTGCGG	2800	IS*Ecp1*-*bla*$_{CMY-2}$-*blc*	This study
blc-R	TACCAGGTTCCCAGATAGCG			This study
ISEcp1-F(B)	ATAAAGACCATGCTCTGCGG	3465	IS*Ecp1*-*bla*$_{CMY-2}$-*blc*-*sugE*	This study
sugE-R(B)	TTGGCCTGAAATACACCCAC			This study

A-F	CGTAGAGGATCTCAGTTCAG	3700	traB-traV-traA-IS*Ecp1*-bla_{CMY-2}	(197)
A-R	CCTGCCACTGTTTGCCTGTC			
G-F	CGCCTGCTAAAAGCAAGAAT	2700	sugE-ecnR-orf1	(197)
G-R	TGCCATCTGCATGAACAAAT			
H-F	AAGGCTGTTGGCTTCGAGTA	2500	Orf1-orf2-orf3	(197)
H-R	TCAGCAGTATCACCCTGCAC			
I-F	ATGTGTTCAAAGCCGAAACC	2500	Orf3-orf4-dsbC-traC	(197)
I-R	GGTGCCGTAATCGAAGATTT			
Primers for bla_{PER-1} positive plasmids characterization				
PER1-F	GCTCCGATAATGAAAGCGT	520	bla_{PER-1}	(195)
PER1-R	TTCGGCTTGACTCGGCTGA			
TEM1-F	CATTTCCGTGTCGCCCTTATTC	800	bla_{TEM-1}	(195)
TEM1-R	CGTTCATCCATAGTTGCCTGAC			
ISCR1-F	AGACGCCGTGGAAGCGTGTG	509	IS*CR1*	This study
ISCR1-R	GCTCGCTCACACCCTCAGCC			
QnrVC6-F	ATGGAAAAATCAAAGCAATT	657	*qnrVC6*	(86)
QnrVC6-R	TTAGTCAGGAACAATGAT			
Int1-F	GGCATCCAAGCAGCAAGC	variable	Gene cassette (Class 1 Integron)	(198)
Int1-R	AAGCAGACTTGACCTGAT			

4.3.4 Conjugation and plasmid characterization

Filter mating experiment was carried out to study the transferability of resistance phenotypes. Overnight cultures of donors (*V. Parahaemolyticus*) and recipients (sodium-azide-resistant *E. coli* J53) were mixed together to the donor/recipient ratio of 2/1, plated on a filter membrane and selected on MacConkey Agar with ceftazidime (4μg/mL) and sodium azide (100μg /mL) to select transconjugants.

The major incompatibility (Inc) groups of plasmids recovered from transconjugants and parental strains were identified by PCR-based replicon typing (PBRT) method (196). S1-PFGE was used to analyze the plasmids that played a role in conferring resistance to β-lactams according to the standard PFGE protocol described above, except that the use of enzyme in the digestion step was replaced by S1 nuclease. After washing with Tris-EDTA buffer (pH 8.0), the total DNA was digested with 50U of S1 nuclease (Thermal Scientific) for 30 min at 37 °C. The linear plasmids were separated from the chromosomal DNA by electrophoresis for 20h with switch times of 2.16-63.8s at 6 V/cm, 14°C in 0.5×Tris-Boric Acid-EDTA buffer, using a CHEF MAPPER XA pulsed field electrophoresis system (Bio-Rad Laboratories, Hercules, CA, USA). Southern blot hybridization was carried out by following the manufacturer's instructions of the DIG-High Prime DNA Labeling and Detection Starter Kit II (Roche Diagnostics), using the $bla_{\text{CMY-2}}$ and $bla_{\text{PER-}1}$ digoxigenin-labeled probes.

For bla_{PER-1} positive strains, comparison was conducted between a strain from this study and another two bla_{PER-1} positive *V. parahaemolyticus* stains identified in our previous study (91). The primers used to amplify different β-lactamase genes, the *qnrVC* gene and integrons were listed in **Table 4.1**.

4.4 Results and discussion

4.4.1 Prevalence of *V. parahaemolyticus* in different food samples in Shenzhen

A total of 54 (17%) *V. parahaemolyticus* isolates were recovered from 318 food samples in wet markets and supermarkets. Of these isolates, 20 (26%, 20/76), 19 (23%, 19/84), 9(11%, 9/85) and 6 (8%, 6/73) were isolated from shrimps, chicken, pork and beef respectively. *V. parahaemolyticus* was considered the most important pathogen causing seafood-borne infections (23). Reports on *V. parahaemolyticus* strains recovered from other kinds of foods are scarce. In this study, *V. parahaemolyticus* could be detected in all types of meat products such as chicken, pork and beef. The prevalence of *V. parahaemolyticus* in chicken was similar to that of shrimps, whereas its prevalence in pork and beef was slightly lower than that of shrimps. It appears that the chicken, pork and beef food samples might have been contaminated by water containing *V. parahaemolyticus* during the process of handling and storage. More in-depth investigation of the origin of *V. parahaemolyticus* in foods other than seafood should be performed.

In order to determine whether these isolates were virulent, the prevalence of the *tdh* and *trh* genes was screened by PCR. Although the *tdh* and *trh* genes are known to occur in 99% of clinical isolates (188), none of the 54 food isolates contained these two virulence genes. This finding was consistent with those of previous studies indicating low prevalence of *tdh* and *trh* genes in *V. parahaemolyticus* from food samples (87, 90). The relationship between clinical and environmental strains should be investigated further in the future.

4.4.2 Antimicrobial susceptibility profile and PFGE Typing

Antimicrobial susceptibility testing of the 54 *V. parahaemolyticus* isolates showed that a relatively high rate of resistance to ampicillin (100%) and tetracycline (11%) was observed. In addition, five isolates (9%) were found to be resistant to sulfamethoxazole/trimethoprim, and one was resistant to chloramphenicol. Importantly, two isolates exhibited resistance to cefoxitin and ceftazidime. Consistent with a previous study (90), resistance to multiple antimicrobial agents in *V. parahaemolyticus* was not common. Detection of *V. parahaemolyticus* isolates that were resistant to third generation cephalosporins in mainland China has not been reported previously. Our susceptibility testing results indicated that front-line drugs including cefoxitin, ceftazidime and fluoroquinolones remained highly effective against *V. parahaemolyticus* infections. However, our finding that *V.*

parahaemolyticus strains resistant to third-generation cephalosporins have emerged has raised a concern for public health because the transfer of resistance determinants from food isolates to other more pathogenic *Vibrio* strains would have serious consequences (91).

Among the 54 isolates tested, a total of 49 PFGE patterns were identified, and 5 strains were untypable. PFGE dendrogram (**Fig 4.1**) showed that most isolates did not exhibit significant genetic relatedness and no extensive clonal dissemination features were observed. However, there were several clusters in which more than 90% genetic similarity was observed between isolates from different sources. This finding provides evidence of cross-contamination between different types of food in supermarkets.

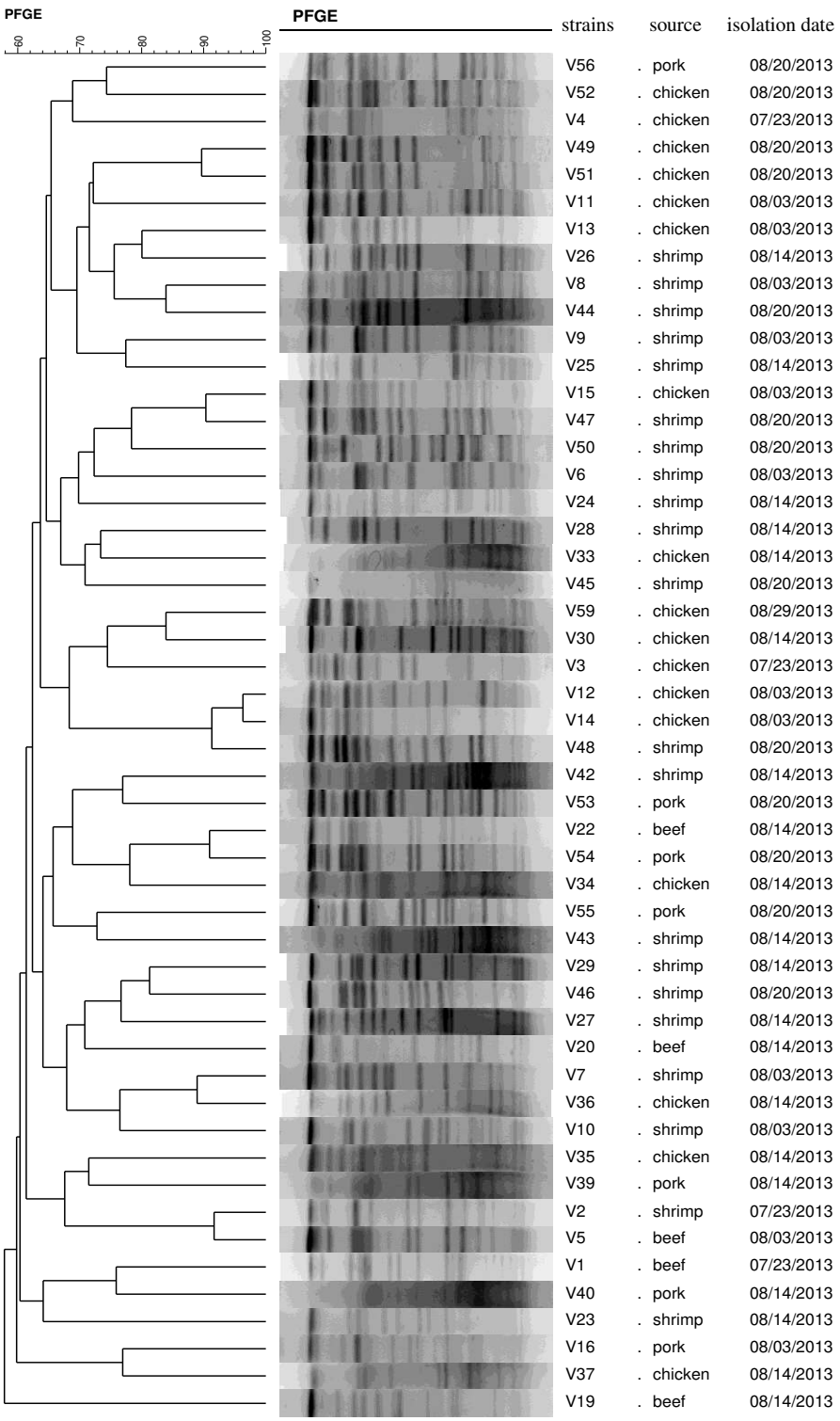

Figure 4. 1 PFGE dendrogram of 49 food *V. parahaemolyticus* isolates

Analyzed by Bionumerics 7.1 software after NotI digestion (5 out of 54 isolates were untypable).

4.4.3 β-Lactamase gene screening

β-lactamase gene screening was performed on two *V. parahaemolyticus* isolates that were resistant to third-generation cephalosporins. For strain V43, which was resistant to all tested β-lactams including cefepime, but not imipenem or meropenem, $bla_{\text{TEM-1}}$ and $bla_{\text{PER-1}}$ were detectable. Since the β-lactamase gene $bla_{\text{PER-1}}$ was previously detectable in *V. parahaemolyticus* isolated from shrimps in Hong Kong in our laboratory (86, 143), this $bla_{\text{PER-1}}$ positive strain was selected for further characterization in this study. On the other hand, the β-lactamase gene $bla_{\text{CMY-2}}$ was detected for the first time in strain V4, which was resistant to ampicillin, amoxicillin/clavulanic acid, cefotaxime, ceftriaxone, and reduced susceptibility to ceftazidime, but not cefepime or carbapenems (**Table 4.2**).

4.4.4 Characterization of $bla_{\text{PER-1}}$ -borne plasmids in *V. parahaemolyticus*

Two genetically unrelated $bla_{\text{PER-1}}$ positive isolates, 2010V36 and 2011V1, which were isolated from our previous studies, were selected for further characterization along with strain V43 recovered in this study (86, 143). Conjugation experiments showed that plasmids carrying $bla_{\text{PER-1}}$ in these three *V. parahaemolyticus* strains were transferrable to *E. coli* J53. Transconjugants V43J-53, 2010V36-J53 and 2011V1-J53 were found to have acquired the ability to exhibit phenotypic resistance to most of the β-lactam

antibiotics tested, including resistance / intermediate resistance to fourth generation cephalosporins such as cefepime, but not carbapenems (**Table 4.2**). Understanding the molecular mechanisms by which *V. parahaemolyticus* exhibits resistance or intermediate resistance to fourth generation cephalosproins, especially those involving acquisition of the ESBL gene bla_{PER-1}, will allow us to define the breakpoint of cefepime for *V. parahaemolyticus* since this is the only report of resistance/intermediate resistance to cefepime in *V. parahaemolyticus*. On the basis of the breakpoints of *E. coli*, as well as comparison between the drug susceptibility levels of transconjugants and the test *V. parahaemolyticus* strains, our data indicated that a breakpoint of 16mg/L or 8mg/L is more appropriate. Apart from the bla_{PER-1} associated phenotypes, other phenotypes such as resistance to tetracycline and trimethoprim in V43, resistance to trimethoprim in 2010V36, and resistance to chlorampenicol, kanamycin and trimethoprim in 2011V1 could also be transferred to *E. coli* J53 through conjugation. These resistance phenotypes were consistent with those conferred by the integrons carrying different resistance genes that were detectable in the conjugative plasmids (**Table 4.3**). S1 nuclease PFGE showed that V43 contained one plasmid with a size of ~200kb that could be transferred to *E. coli* J53. Southern hybridization confirmed the presence of bla_{PER-1} on this plasmid (**Fig. 4.2**). Strain 2010V36 was shown to harbor two plasmids with sizes of ~175kb and ~110kb respectively, the ~175kb plasmid being transferrable to *E. coli* J53. The plasmid size in 2010V36 here was different from that of the previous study, presumably because the use of S1-PFGE method

offered more accurate plasmid size determination in this study. Southern hybridization also confirmed the presence of a bla_{PER-1} on the ~175kb plasmid. Strain 2011V1 was found to contain three plasmids with sizes of ~200kb, ~70kb, and ~45kb respectively. The ~200kb plasmid was shown to be self-transmissible (**Fig. 4.2**). Southern hybridization also confirmed the presence of bla_{PER-1} in the ~200kb plasmid.

In our previous study, partial genetic environment of bla_{PER-1} was determined for strain 2011V1 (86). To check whether bla_{PER-1} in V43 and 2010V36 also contained similar genetic structures as that of strain 2011V1, further characterization of plasmids recovered from V43, 2010V36 and 2011V1 was performed using primers to amplify the flanking region of bla_{PER-1}, with bla_{PER-1} of 2011V1 as a template for primer design (**Table 4.1**). The results, as summarized in **Table 4.3**, showed that the genetic structures of these plasmids were different, despite the fact that both plasmids recovered from strains V43 and 2011V1 were about 200kb in size. In addition to bla_{PER-1}, plasmid from V43 also contained a bla_{TEM-1} gene, IS*CR1* and an integron carrying the *arr-3* and *dfrA27* genes; although the conjugative bla_{PER-1} positive plasmid from strain 2010V36 contained IS*CR1* and an integron carrying the *arr-3* and *dfrA27* genes, it was slightly smaller in size (~175kb) than the other two plasmids. The conjugative plasmid from strain 2011V1 contained IS*CR1* and a new integron carrying the *aacA3*, *catB2*, *dfrA1* and *aadA1* genes. In addition, it also carried a novel PMQR gene *qnrVC6* (86). These

data indicated that all three bla_{PER-1} -borne plasmids recoverable from three different *V. parahaemolyticus* strains were genetically different. Further sequencing approach will be applied to understand the evolution features of these three plasmids in *V. parahaemolyticus*.

4.4.5 Characterization of plasmids carrying the bla_{CMY-2} gene in *V. parahaemolyticus*

Conjugation experiments were also performed on the V4 strain, with results showing that the plasmid containing the bla_{CMY-2} gene in this strain could be transferred to *E. coli* J53. Transconjugant V4J53 exhibited slightly higher MICs to various β-lactam antimicrobials than the original V4 strain (**Table 4.2**). Interestingly, V4 did not exhibit resistance to chloramphenicol, whereas V4J53 became resistant to chloramphenicol, presumably due to the fact that some resistance genes might be better expressed in *E. coli* (**Table 4.2**). This phenomenon was also observable in our previous study (143). S1 nuclease PFGE and Southern hybridization analysis showed that the V4 strain harbored 4 plasmids with sizes ranging from ~45kb to ~150kb. The conjugative plasmid detected in transconjugant V4J53 was ~150kb. Southern hybridization confirmed that the bla_{CMY-2} gene was located in this transmissible plasmid in both V4 and V4J53 (**Fig. 4.3**). Plasmid typing indicated that the transmissible plasmid belonged to the IncA/C type plasmid. Plasmids harboring bla_{CMY-2} have been found to belong to different plasmid types (IncA/C, IncI1, etc.) detectable in members of

Enterobacteriaceae recovered from various sources. The sizes of the plasmids varied from ~45kb to ~200kb (199-202). IncA/C plasmids carrying bla_{CMY-2} with similar size (~150kb) were mainly reported in *Escherichia coli* and *Salmonella enterica* (201). It is likely that the bla_{CMY-2}-borne IncA/C plasmid in this strain originated from *Enterobacteriaceae*; alternatively, formation of this plasmid may be due to mobilization of bla_{CMY-2} gene to different plasmid backbones through *ISEcp1*-mediated transposition activities (197).

The flanking sequence of bla_{CMY-2} was amplified by PCR mapping according to published sequences and confirmed by sequencing. It was found that the arrangement of genetic environment of bla_{CMY-2} was in the order of *traB-traV-traA-ISEcp1-*bla_{CMY-2}*-blc-sugE-encR-orf1-orf2-orf3-orf4-dsbC-traC* (**Fig. 4.4**). The β-lactamase gene bla_{CMY-2} is the most commonly reported plasmid-encoded AmpC β-lactamase gene in *Salmonella* spp., *Escherichia coli*, and other species of *Enterobacteriaceae* worldwide (56). This gene renders the host organism resistant to a variety of β-lactams, including oxyimino-cephalosporins and cephamycins (56). The genetic content in the vicinity of the bla_{CMY-2} gene usually comprised the *ISEcp1* and *blc-sugE* elements in its upstream and downstream regions respectively (197). Hence the *V. parahaemolyticus* V4 strain is genetically similar to those described in several other reports (197, 203). Comparison with other published sequences in NCBI database indicated that the genetic segment in which the bla_{CMY-2} gene is

located has been identified in plasmids of *Salmonella* spp., *Escherichia coli*, *Klebsiella pneumonia, Providencia stuartii* and *Shigella sonnei* (56, 197, 203). However, the sizes of these previously reported plasmids were different from that of the V4 strain.

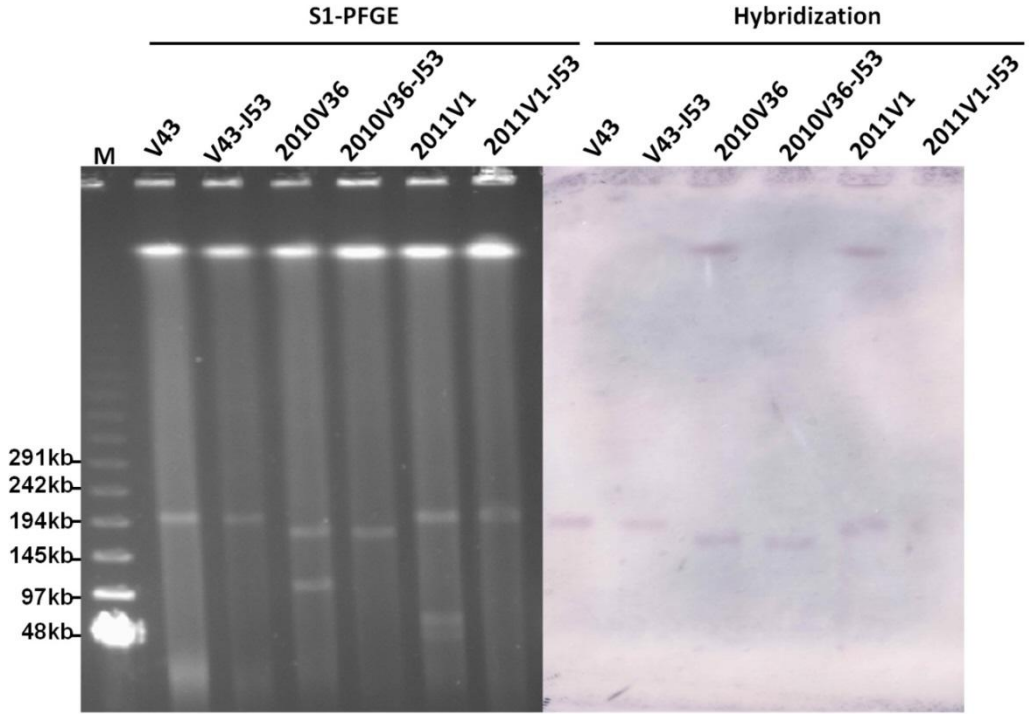

Figure 4. 2 S1-PFGE and southern blot hybridization of *bla*$_{PER-1}$ positive strains and the corresponding transconjugants.

M, Lambda Ladder PFGE Marker (New England Biolabs).

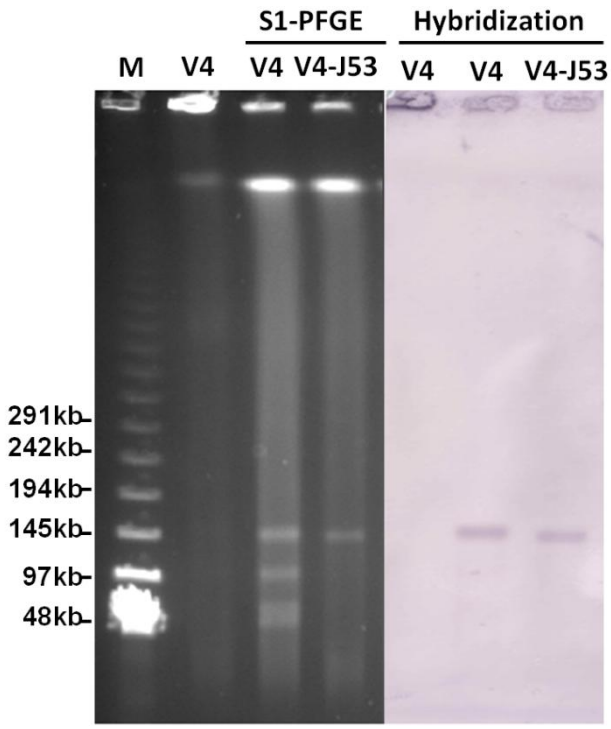

Figure 4. 3 S1-PFGE and southern blot hybridization of V4 and transconjugant V4J53.

M, Lambda Ladder PFG Marker (New England Biolabs); V4, V4 genomic DNA without S1 digestion.

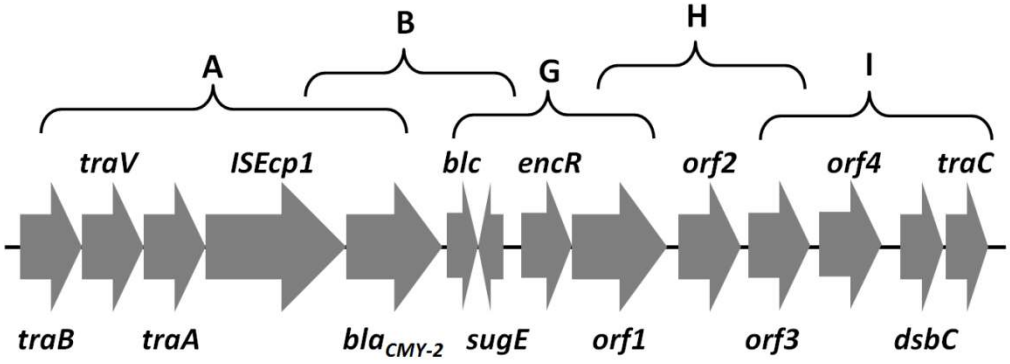

Figure 4. 4 Genetic structure of *bla*$_{CMY-2}$ -borne IncA/C conjugative plasmid in *V. Parahaemolyticus* strain V4.

A~I represent the primers' target regions. Primer sequences are shown in **Table 4.1**.

Table 4. 2 MICs of ESBL-producing *V. parahaemolyticus* strains and the corresponding transconjugants

Strain	β-lactamase gene	MICs(mg/L)											
		AMP	**CTX**	**CRO**	**CAZ**	**CEP**	**TET**	**GEN**	**NAL**	**CIP**	**CHL**	**KAN**	**TRI**
J53		1	≤0.125	≤0.125	≤0.125	≤0.125	2	1	2	≤0. 125	2	0.25	≤0. 125
V4	$bla_{\text{CMY-2}}$	128	8	32	8	0.5	32	1	0.5	≤0. 125	2	8	16
V4-J53	$bla_{\text{CMY-2}}$	>128	16	64	64	0.5	64	1	2	≤0. 125	64	1	>64
V43	$bla_{\text{PER-1}}$	>128	>128	>128	>128	32	32	8	1	≤0. 125	2	8	32
V43-J53	$bla_{\text{PER-1}}$	128	128	128	>128	16	64	8	2	≤0. 125	32	0.5	>64
2010V36	$bla_{\text{PER-1}}$	>128	>128	>128	>128	32	1	1	0.25	≤0. 125	0.25	2	16
2010V36-J53	$bla_{\text{PER-1}}$	>128	>128	>128	>128	16	2	1	2	≤0. 125	2	2	>64
2011V1	$bla_{\text{PER-1}}$	>128	>128	>128	>128	16	1	4	0.5	≤0. 125	16	64	>64
2011V1-J53	$bla_{\text{PER-1}}$	>128	>128	>128	>128	32	2	4	4	≤0. 125	16	64	>64

AMP, Ampicillin; CTX, Cefotaxime; CRO, Ceftriaxone; CAZ, Ceftazidime; CEP, Cefepime; TET, Tetracycline; GEN, Gentamicin; NAL, Nalidixic acid; CIP, Ciprofloxacin; CHL, Chloramphenicol; KAN, Kanamycin; TRI, Trimethoprim.

Table 4. 3 Comparison of genetic contents of *bla*$_{PER-1}$-borne plasmids recovered from three *V. parahaemolyticus* strains and the corresponding transconjugants

Strain	V43	V43-J53	2010V36	2010V36-J53	2011V1	2011V1-J53
bla$_{PER-1}$	+	+	+	+	+	+
bla$_{TEM-1}$	+	+	-	-	-	-
IS*CR1*	+	+	+	+	+	+
qnrVC6	-	-	-	-	+	+
class 1 Integron	arr-3, dfrA27	arr-3, dfrA27	arr-3, dfrA27	arr-3, dfrA27	aacA3, catB2, dfrA1and aadA1	aacA3, catB2, dfrA1and aadA1
Number of plasmids detectable and their respective sizes	1(200kb)	1(200kb)	2 (175kb ,110kb)	1 (175kb)	3 (200kb,70kb, 45kb)	1(200kb)

4.5 Conclusion

In this study, we reported the isolation of *V. parahaemolyticus* from meat products other than seafood. These isolates were susceptible to most of the antimicrobials tested, except that two were resistant to extended spectrum cephalosporins. The β-lactamase gene bla_{PER-1} was detectable in one *V. parahaemolyticus* isolate, V43, which was resistant to both third and fourth generation cephalosporins. The conjugative bla_{PER-1}-borne plasmid recoverable from this strain was structurally different from those reported previously. On the other hand, the β-lactamase gene bla_{CMY-2} was detected for the first time in another *V. parahaemolyticus* isolate, V4, which was resistant to the third generation cephalosporins. The bla_{CMY-2} gene was shown to be located on an ~150kb IncA/C type conjugative plasmid with the genetic structure of *traB-traV-traA-ISEcp1-*bla_{CMY-2}*-blc-sugE-encR-orf1-orf2-orf3-orf4-dsbC-traC* which has been reported in other IncA/C conjugative plasmids in *Enterobacteriaceae*, albeit with slightly different size. This finding indicated that the transmission of ESBL and AmpC β-lactamase genes via different conjugative plasmids mediated the development of resistance to extended-spectrum cephalosporins and other drugs in *V. parahaemolyticus*. Such plasmid is transferable to *Enterobacteriaceae* and possibly other pathogenic *Vibrio* spp., thereby posing a significant threat to public health.

Chapter Five: Genetic Characterization of *bla*$_{VEB}$-carrying plasmids in *Vibrio* species

Part of the content in this chapter is reproduced from the following papers:

Li R, Ye L, Zheng Z, Chan EW, & Chen S (2016) Genetic Characterization of a *bla*$_{VEB-2}$-carrying plasmid in *Vibrio parahaemolyticus*. *Antimicrobial agents and chemotherapy 60(11):6965-6968.*

Li R, Ye L, Zheng Z, Chan EWC, & Chen S (2017) Genetic Characterization of Broad-Host-Range IncQ Plasmids Harboring *bla*$_{VEB-18}$ in *Vibrio* Species. *Antimicrobial agents and chemotherapy 61(7).*

5.1 Abstract

In this chapter, we present three *bla*$_{VEB}$-bearing plasmids recovered from *V. parahaemolyticus* and *V. alginolyticus*, one of which belongs to a new conjugative plasmid (338, 538bp) encoding class 1 integron with *bla*$_{VEB-2}$ embedded and other resistance genes. This conjugative plasmid pVPS92-VEB only exhibit similarity to another *bla*$_{NDM-1}$-bearing plasmid pNDM-116-14 in *V. cholerae*, which represented a novel type of MDR plasmid in aquatic pathogens. Another two plasmids belong to small IncQ plasmids (7, 831bp, 9,

159bp) and encode a MDR encoding fragment in which a new *bla*$_{VEB-18}$ was found located between the *aac(6')-II* and *aadB* cassettes. This is the first description of *bla*$_{VEB}$ in *Vibrio* species, which implied that this class of lactamase has spread in water environment.

5.2 Introduction

Resistance to the third-generation cephalosporins in *V. parahaemolyticus* strains due to carriage of an extended-spectrum beta-lactamase (ESBL) gene, *bla*$_{PER-1}$, and the AmpC β-lactamase gene *bla*$_{CMY-2}$, has been reported in last chapter. Apart from these two resistance elements, however, no other ESBL genes have been reported in *V. parahaemolyticus* to date. VEB-type β-lactamases can be classified into different subtypes from VEB-1 to VEB-17, with one to four amino acid substitutions in VEB-1(204-206) (**Fig. 5.1**). The *bla*$_{VEB}$ genes have been identified in various *Enterobacteriaceae*, *Proteus mirabilis*, *Pseudomonas aeruginosa* and *Acinetobacter baumannii* (207, 208). To date, no research studies on VEB expressed by *V. parahaemolyticus* have been conducted. In order to fill this knowledge gap, we performed this work with a focus on the genetics of *bla*$_{VEB}$ in *V. parahaemolyticus* and genetically related *V. alginolyticus*.

Figure 5. 1 Sequence alignment of eighteen different VEB variants. *bla*$_{VEB-1a}$ and *bla*$_{VEB-9}$, *bla*$_{VEB-1b}$ and *bla*$_{VEB}$-16 encodes the same VEB bariants.

5.3 Materials and Methods

5.3.1 Strains and identification

Two cephalosporin-resistant *V. parahaemolyticus* (VPS72 and VPS92) and one *V. alginolyticus* (VAS24) harboring *bla*$_{VEB}$ were isolated from a shrimp sample collected from a supermarket during our foodborne pathogen surveillance in Shenzhen, China in 2015. The genetic identity of this isolate was further confirmed by MALDI-TOF (Bruker) identification, amplification and sequencing of *bla*$_{CAR-17}$ and *tlh* genes, and by API20E strip (165). The isolates

were subjected to screening of β-lactamase genes using PCR and DNA sequencing as previously described (195). Antimicrobial susceptibility tests were performed by broth microdilution method according to the CLSI guideline (209).

5.3.2 Conjugation and hybridization

Conjugation assay was performed using azide-resistant *E. coli* J53 as recipient strain and recovered by screening on LB agar supplemented with 16 μg/ml cefotaxime as previously described (210). Plasmid was extracted from VPS72, then introduced into TG1 by electroporation and positive transconjugates were obtained by screening on LB agar plates supplemented with cefotaxime (4ug/ml). PFGE and Southern hybridization were performed as previously described (210).

5.3.3 Plasmids sequencing and comparison

To understand the genetic features of the plasmid harboring *bla*$_{VEB-2}$, the plasmid recovered from the transconjugant was extracted using the Qiagen plasmid midi kit (QIAGEN) and sequenced using Illumina NextSeq 500 and PacBio RSII single-molecule real-time (SMRT) sequencing platforms (Wuhan Institute of Biotechnology, China). Illumina reads were aligned to PacBio contigs to improve the accuracy of the plasmid sequence data, and obtain the complete sequence of the plasmid. The complete plasmid sequence was confirmed by PCR and then annotated with RAST tool and the

NCBI Prokaryotic Genome Annotation Pipeline (PGAP). Plasmid comparison was performed with the BRIG software(211).

Nucleotide sequence accession numbers. The completed plasmid sequences for pVAS24-VEB, pVPS72 and pVPS92-VEB was deposited in NCBI with accession numbers KX575838, KX539265 and KU356480 respectively.

5.4 Results and discussion

Three strains were resistant to ampicillin and cefotaxime (**Table 5.1**). The bla_{VEB-2} gene was detected for the first time in *V. parahaemolyticus*. S1-PFGE and hybridization showed that the bla_{VEB-2} gene was located on a plasmid with size of ca. 320kb in VPS92. Sequencing result of PCR products with bla_{VEB} primers shown that the bla_{VEB} in VPS72 and VAS24 was a new VEB subtype, designated as bla_{VEB-18}. Both bla_{VEB-2} in VPS92 and bla_{VEB-18} in VAS24 could be transferred to J53 AzR receipt strain after confirmation with PCR.

Table 5. 1 MICs of VPS92, VPS72, VAS24 and their transconjugates or transformant to different drugs.

Strain	TET	AMP	AMK	SXT	CTX	NAL	CIP	AMC	CHL
J53	0.5	1	0.5	0.25/4.75	0.03	1	0.03	4/2	2
VPS92	2	>64	4	>8/152	>16	4	1	4/2	4
VPS92-J53	8	>64	0.5	>8/153	>16	16	0.25	8/4	32
VAS24	0.5	>64	4	0.25/4.75	>16	2	1	8/4	1

VAS24-J53	0.5	>64	0.5	0.25/4.75	>16	8	0.003	4/2	2
TG1	0.25	1	0.5	0.25/4.75	<0.015	2	0.0075	1/0.5	1
VPS72	1	>64	4	0.25/4.76	>16	1	0.5	16/8	0.25
VPS72-TG1	2	>64	0.5	0.25/4.77	8	4	0.015	4/2	1

The *bla*$_{VEB-2}$ -bearing plasmid in VPS92, designated as pVPS92-VEB, was found to be 338, 538bp in length, contain 390 predicted CDSs and exhibit a GC content of 44.3% (**Fig. 5.2**). The plasmid harbored different genes including resistance and mobile elements, conjugative transfer related genes and hypothetical genes. Annotation results showed that *bla*$_{VEB-2}$ was located in a class 1 integron with the structure *bla*$_{VEB-2}$-*aadB-arr2-cmlA-bla*$_{OXA-10}$-*aadA1-sul1*. After conducting BLASTN, the *bla*$_{VEB-2}$ genetic environment was found to be similar to that of the *bla*$_{VEB-1}$ gene in an integron of *Acinetobacter baumannii* (CU459141), *Pseudomonas aeruginosa* (GQ388247) and *Escherichia coli* (AF205943) (212). This indicates that similar integrons harboring *bla*$_{VEB-2}$ could mobilize between different plasmids in different species of bacteria and that the *bla*$_{VEB}$ gene could be evolved into different alleles. Owing to the fact the *bla*$_{VEB}$ is always embedded in class 1 integrons, the formation of the *bla*$_{VEB-2}$ -bearing integron could accelerate the rate of transmission of *bla*$_{VEB-2}$ among plasmids and chromosomes (213, 214). A mercury resistance operon downstream of the *bla*$_{VEB-2}$ -bearing integron, in which the *floR*, *tetA-tetR*, *strA-strB* genes were clustered into a MDR region, was found to be

flanked by mobile elements. This structure may facilitate the transmission of multiple resistance genes in one single mobilization event. In the upstream region of the *bla*$_{VEB-2}$ bearing integron, one *qnrVC4* gene cassette was found to be inserted into the plasmid backbone, implying that the integron related *qnrVC4* cassette can migrate between integrons and other genetic loci (215, 216). BLASTN analysis showed that the backbone of pVPS92-VEB was similar (99% identity in 78% coverage) to a single plasmid, namely pNDM-116-14 (LN831184), which was isolated from a *V. cholerae* strain isolated in India (**Fig. 5.2**). After comparing with the plasmid replicon database, the predicted replication initiation gene *repE* was shown to be novel, with no homology to any of the known replicon genes. The pNDM-116-14 plasmid was known to contain two MDR regions: class 1 integron with different gene cassettes including *bla*$_{NDM-1}$, and one gene cassette in which the *bla*$_{CMY-4}$ gene was inserted into the backbone of the plasmid (**Fig. 5.2**). The major differences between these two plasmids were the mobile elements that carried different antimicrobial resistance genes. In addition, some additional insertion sequences other than those in the MDR region could be seen in pNDM-116-14 (**Fig. 5.2**).

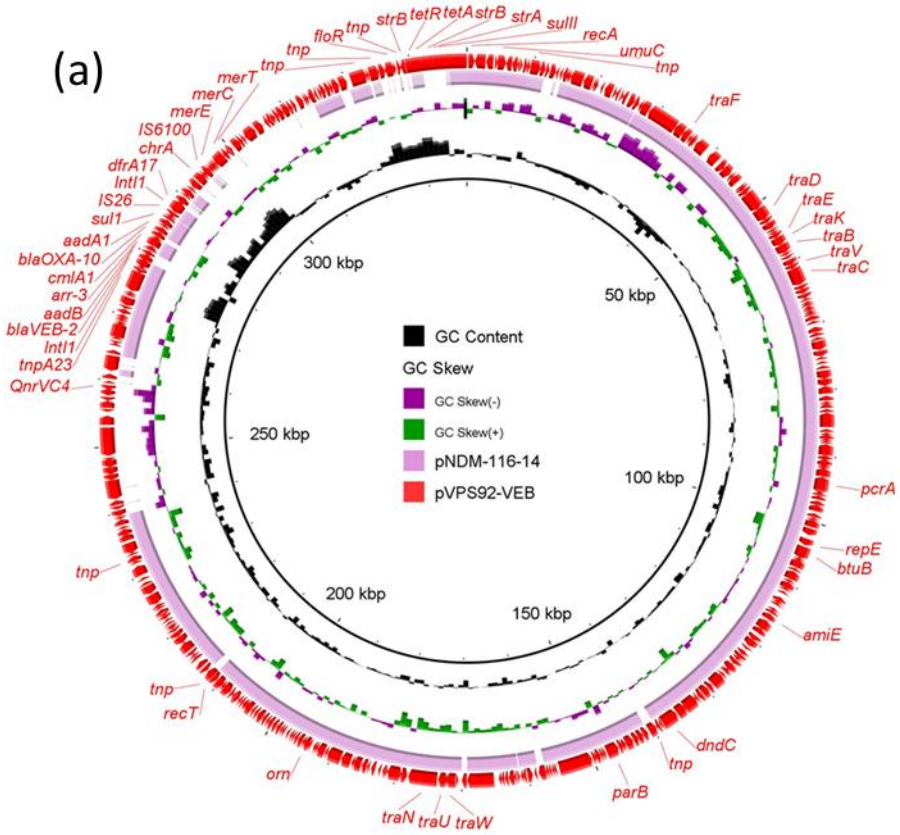
(a)
300 kbp
50 kbp
250 kbp
100 kbp
200 kbp
150 kbp
GC Content
GC Skew
GC Skew(-)
GC Skew(+)
pNDM-116-14
pVPS92-VEB
floR
tnp
strB
tetR
tetA
strB
strA
sulII
recA
umuC
tnp
traF
traD
traE
traK
traB
traV
traC
pcrA
repE
btuB
amiE
dndC
tnp
parB
traN
traU
traW
orn
tnp
recT
tnp
tnp
QnrVC4
tnpA23
IntI1
blaVEB-2
aadB
arr-3
cmlA1
blaOXA-10
aadA1
sul1
IS26
IntI1
dfrA17
chrA
IS6100
merE
merC
merT
tnp
tnp

338

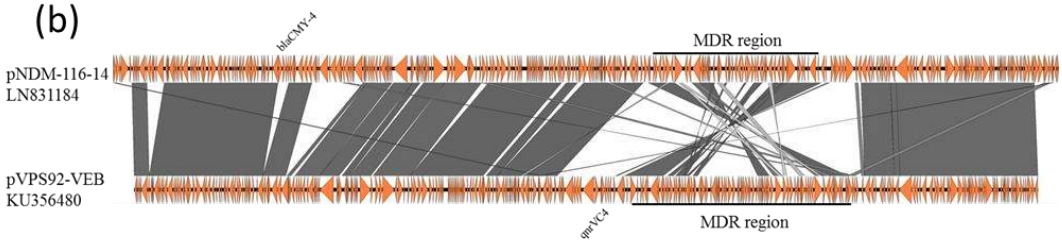
(b)
blaCMY-4
MDR region
pNDM-116-14
LN831184
pVPS92-VEB
KU356480
qnrVC4
MDR region

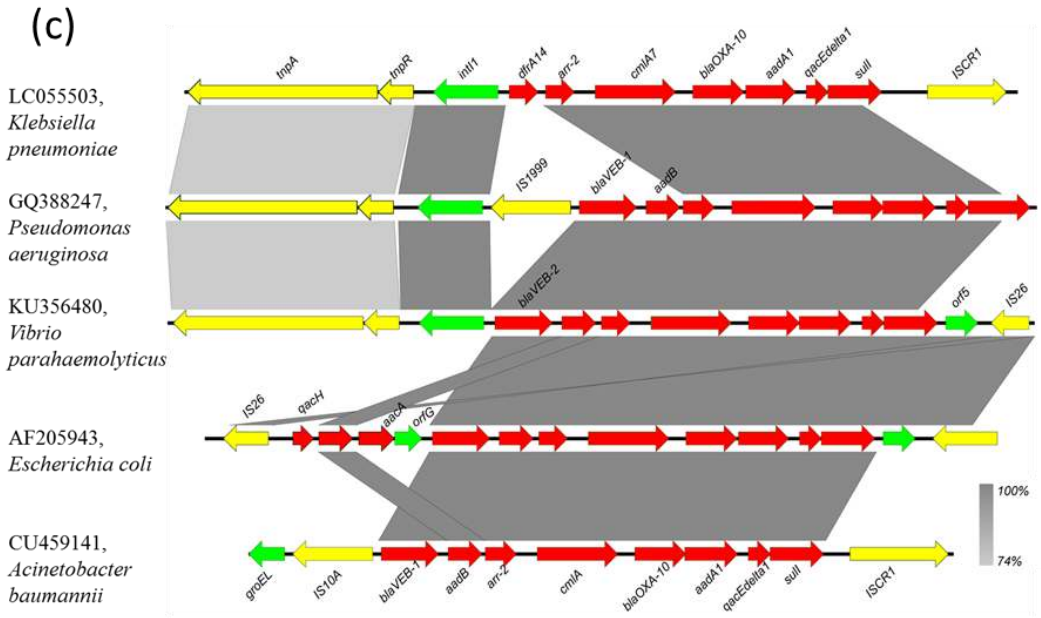

Figure 5. 2 Plasmid comparison between pVPS92-VEB (338, 538bp) and pNDM-116-14 (354, 308)

(a) Circular map representation of the plasmid comparison results. The outer red circle indicates the plasmid maps of pVPS92-VEB, which was used as the reference for BLASTN. Inner pink circle represents the homologous alignment of pNDM-116-14 to pVPS92-VEB. Variation was mainly seen in the MDR region of these two plasmids. (b) Linear representation of the plasmid comparison data. Some additional insertion sequences other than those in the MDR region could be seen in pNDM-116-14. (c) Genetic alignment of class 1 integron harboring *bla*$_{VEB-2}$ and other similar integrons from different bacteria. The red arrows indicate the resistance genetic cassettes embedded in integrons. The yellow arrows denote the mobile elements. The green arrows represent other genes and predicted CDSs. The right bottom legend shows the percentage of sequence alignment when conducting BLASTN.

Sequencing results showed that VPS72 and VAS24 harbored a new *bla*$_{VEB}$ variant, designated as *bla*$_{VEB-18}$, which contained three substitutions (V19A, T104M and N294D) compared with *bla*$_{VEB-1}$, and one amino acid substitution when compared with VEB10 (V19A) and VEB17 (Y64F). According to the MICs, *bla*$_{VEB-18}$ and *bla*$_{VEB-2}$ have similar function in conferring resistance to ampicillin

and cefotaxime, but susceptibility to amoxicilin/clavulanic acid. This indicated that the amino acid substitutions did not affect the enzymatic activity of VEB-18 compared with other VEB types. The new *bla*$_{VEB-18}$ gene was surrounded by *aadB* and *aac(6')-II* in a small plasmid pVPS72-VEB with 7, 831bp in length and encoding 10 CDSs (**Fig. 5.3**). BLASTn of the *bla*$_{VEB-18}$ environment against the nr database demonstrated *bla*$_{VEB-18}$ genetic arrangement was novel and similar *bla*$_{VEB}$-*aadB* sequences were found in reported integrons in NCBI database. This cassette combination may be co-transferred between different genetic loci. The backbone of pVPS72-VEB encoded plasmid replication and mobilization related functions and was structurally similar to the IncQ-like plasmids, which were very small in size (5.1-14.2kb) (217). The most similar backbone structure with 86% identity to pVPS72-VEB and pVAS24-VEB was found from one resistance genes encoding IncQ plasmid pMS260 in *Actinobacillus pleuropneumoniae*, which is a common swine pathogen (218) (**Fig. 5.3**). Similarly, *bla*$_{VEB-18}$ in pVAS24-VEB was also IncQ-like plasmid exhibiting homology with pVPS72-VEB, with IS*186* inserting into pVAS24-VEB between *aadB* and *repA* (**Fig. 5.3**). It has been reported that IncQ plasmids are highly mobilizable with the help of large conjugative plasmids and promiscuous for capturing resistance genes in environments (217). pVAS24-VEB can be obtained through conjugation assay, however, no transconjugant could be harvested for pVPS72-VEB. The presence of conjugative plasmids in the original strain may explicate this phenomenon. This report is the

first description of IncQ-like plasmid harboring *bla*$_{VEB-18}$ in *V. parahaemolyticus* and *V. alginolyticus*. Because IncQ plasmids are usually found in environments, the incorporation of resistance genes may facilitate its transmission to clinical pathogens under exposure to antimicrobials.

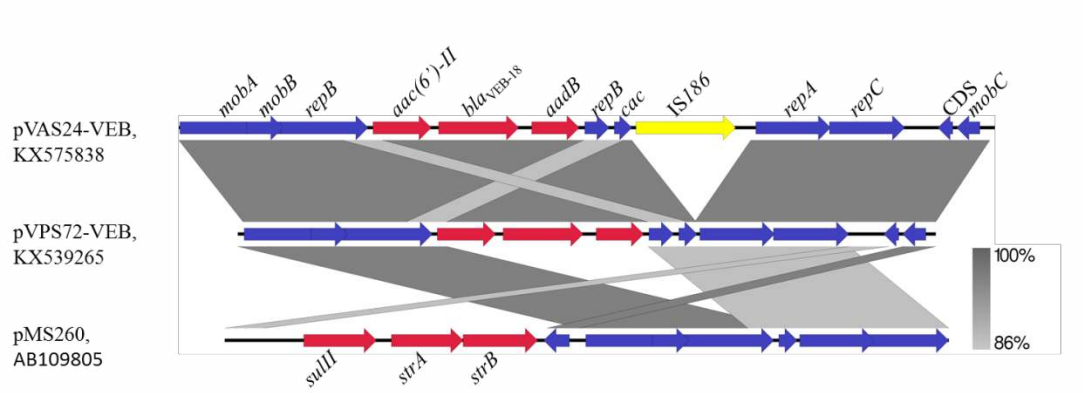

Figure 5. 3 Plasmid sequence alignment of pVAS24-VEB, pVPS72-VEB and pMS260 sharing similar IncQ plasmid backbone

The dissemination of extended-spectrum-β-lactamase (ESBL) genes among pathogens and opportunistic pathogens pose a serious concern to public health (204). VEB-type β-lactamases can be classified into different subtypes, from VEB-1 through VEB-17, with one to four amino acid substitutions when compared to VEB-1 (204-206). The *bla*$_{VEB}$ genes have been identified mainly in *Pseudomonas aeruginosa* and in other bacterial species such as *Proteus mirabilis* and *A. baumannii* (207, 208). The nature of the novel backbone of pVPS92-VEB and pNDM-116-14 suggested that this type of plasmid may originate from the aquatic environment

since it was only reported in the *Vibrio* species twice, yet has not been reported in other bacteria including those in the family of *Enterobacteriaceae*. Although similar plasmids were only reported in *Vibrio* species, the plasmid could be transferred to *E. coli* according to results of the conjugation experiment. In addition, the presence of the *qnrVC4* gene cassette in this plasmid is further suggestive of its aquatic origin since *qnrVC* gene was typically found in marine organisms. However, it is difficult to get conclusion on the sources of the integrons bearing *bla*$_{VEB-2}$ or *bla*$_{NDM-1}$ because of their existence in both *Enterobacteriaceae* and marine bacteria and their high mobility among different genetic loci.

5.5 Conclusion

In conclusion, this study reported the first detection of the *bla*$_{VEB-2}$ gene in a large conjugative plasmid pVPS92-VEB, the backbone of which may have originated in the aquatic environment, whereas the integron carrying *bla*$_{VEB-2}$ may be obtained through non-aquatic bacteria such as *A. baumannii*, through HGT. New *bla*$_{VEB-18}$ gene was supposed to originate from integron structure and recombine into new IncQ-like plasmid by *bla*$_{VEB}$-*aadB* circular cassette, then captured *aac(6')-II* cassette and evolved into pVPS72-VEB and pVAS24-VEB. The acquisition of various types of ESBL-encoding elements such as *bla*$_{PER-1}$, *bla*$_{VEB}$ and AmpC β-lactamase gene in *Vibrio* spp. constitutes an increasing public health threat posed by the aquatic pathogens.

Chapter Six: Evolution and Comparative Genomics of Novel Incompatibility Type Conjugative Plasmids in *Vibrio* species

Some of the content in this chapter is reproduced from the published papers:

Li R, Wong MH, Zhou Y, Chan EW, & Chen S (2015) Complete nucleotide sequence of a conjugative plasmid carrying bla_{PER-1}. *Antimicrobial agents and chemotherapy 59(6):3582-3584.*

Li R, Ye L, Wong MH, Zheng Z, Chan EW, &Chen S (2017) Evolution and comparative genomics of pAQU-like conjugative plasmids in *Vibrio* species. *Journal of antimicrobial chemotherapy*. *doi: 10.1093/jac/dkx193*

6.1 Abstract

Conjugative plasmids play a key role in the transmission of antimicrobial resistance genes among organisms inhabiting in different environmental niches. In this study, we performed comparative genomic analysis of conjugative, multidrug resistance-encoding (MDR) plasmids recently recoverable from aquatic bacteria, which exhibit a similar core structure. The plasmids ranged from 16.3 to 20.6kb in size and were found to harbor as many as 111 core elements encoding conjugative, replication and

maintenance functions. Importantly, all test plasmids were found to comprise a typical MDR region which contained various accessory and resistance genes including IS*CR1*-*bla*$_{PER-1}$-bearing complex class 1 integrons, IS*CR2*-*floR*, IS*CR2*-*tet(D)*-*tet(R)*-IS*CR2*, *qnrVC6*, a Tn*10*-like structure, the *mer* operon, *mph* operon, and others embedded within a variety of mobile elements. Comparison between an empty vector without resistance genes and different MDR plasmids showed that integration of different mobile elements such as IS*26*, IS*CR1*, IS*CR2*, IS*10* and IS*6100* into the plasmid backbone was the key mechanism by which foreign resistance genes were acquired during the evolution process. These findings suggest that aquatic bacteria constitute a major reservoir and site of dynamic evolution of a wide range of mobile resistance elements, which may be transmissible to other human pathogens during food production and processing.

6.2 Introduction

The emergence of ESBLs-harboring pathogens is of particular concern due to the limited options for eradicating such organisms in clinical settings. As a unique class A ESBL, the *bla*$_{PER-1}$ gene product confers resistance to penicillins, oxyimino-cephalosporins, and aztreonam, but not oxacillins, cephamycins, and carbapenems, and is susceptible to inhibition by clavulanic acid and sulbactam (94). The *bla*$_{PER-1}$ gene was first recognized in the *Pseudomonas aeruginosa* strain RNL-1, which was recovered in France in 1991 (95). After that, other closely related variants such as PER-2, -3, -4,

-5, -6 and -7 have been identified (96, 97). PER-1 β-lactamases were confined to relatively few locations and bacterial hosts (*Aeromonas spp*., *Acinetobacter baumannii*, *Alcaligenes faecalis*, *Pseudomonas aeruginosa* and *Enterobacteriaceae*) (98, 99). The $bla_{\text{PER-1}}$ gene has been found in plasmids or chromosomes in diverse genetic environments, and is often embedded within Tn*1213* (99, 100). Recently, the IS*CR1* element has been found to play a role in the dissemination of $bla_{\text{PER-1}}$ (99). In a previous study, we reported the detection of $bla_{\text{PER-1}}$ in *Vibrio parahaemolyticus* strains from seafood in Hong Kong (91). In order to further delineate the genetic background and dissemination mechanism of the $bla_{\text{PER-1}}$, we first obtained the complete nucleotide sequences of the plasmid pVPH1 harboring $bla_{\text{PER-1}}$ and determined its mechanisms of transmission. Based on pVPH1, we characterized all the similar plasmids from our samples.

Plasmids play a pivotal role in bacterial adaptation to changing environments by conferring new phenotypic characteristics to the host organism, such as resistance to antimicrobials and heavy metals, as well as expression of virulence factors (111, 219-221). Acquisition of multiple resistance genes, especially via uptake of conjugative and mobilizable plasmids, poses a significant health threat worldwide (111). To tract multiple-drug-resistance-encoding (MDR) plasmids and study the epidemiological characteristics of organisms harboring such elements, different plasmid typing methods based on PCR assays targeting the replicon or relaxase

genes, have been devised (196, 222). With the advent of whole genome sequencing technology, complete plasmid sequences have become available. Accordingly, novel plasmid families that were previously undetectable by conventional replicon typing methods can now be identified.

Bacteria inhabited in the aquatic environment are an important reservoir of antibiotic resistance genes; to the population size of drug resistant marine microorganisms has expanded dramatically as a result of abused usage of antimicrobial agents in aquaculture (223). Resistance-encoding mobile genetic elements, such as the plasmid-mediated quinolone resistance genes (PMQR), were found to be originated from aquatic environment and have spread to human pathogens (224). Recently, a novel type of MDR plasmids, namely pAQU1 and pAQU2, was identified in marine pathogens in Japan (225, 226). Since then, our laboratory has recovered a plasmid, pVPH1, which shared similar backbone with the pAQU type plasmid but contained different resistance genes (227). Sequence analysis indicated that the backbone of this type of plasmid was not available in the NCBI database, suggesting a need to investigate the origin of these elements. Although scattered data regarding the prevalence of resistance genes in aquatic environments are available (228), there have been no systematic studies aimed at identifying and delineating the genetic characteristics of the typical plasmids that harbor multidrug resistance (MDR)-encoding elements in aquatic organisms. In order to characterize the range of mobile

resistance genes in *Vibrio* spp. systematically, we utilize the third generation sequencing approach to obtain complete plasmid sequences in five pAQU type plasmids, followed by analysis by comparative genomics methods, and delineation of the route by which such plasmid evolved from a vector without resistance genes to one which has acquired MDR-encoding elements.

6.3 Materials and methods

6.3.1 Bacterial strains

V. parahaemolyticus strain V36 was isolated from a shrimp sample in Hong Kong in 2010 (143) and used for $bla_{\text{PER-1}}$ genetic characterization in the first part of this chapter.Then, a total of 154 *Vibrio parahaemolyticus* and 23 *Vibrio alginolyticus* isolates obtained from different food samples from the Foodborne Pathogen Surveillance Program, conducted during the period of 2013 to 2015 in Shenzhen, China (215, 229), and were used to characterize the epidemiological features and evolution routes of pAQU type plasmids in these isolates. Strains were cultured in Brain heart infusion (BHI) broth or agar plates supplemented with 3% NaCl routinely. Antimicrobial susceptibility test was performed to test the MICs of different antimicrobials by using microbroth dilution method according to CLSI standard (209). *Escherichia coli* strain ATCC25922 was used as the control.

6.3.2 Conjugation assay and S1-PFGE

In order to determine the transferability of plasmids harbored by *Vibrio* spp., conjugation experiments were performed by filter mating assay using azide-resistant *Escherichia coli* J53 as the recipient strain. Transconjugants were recovered from LB plates supplemented with 100μg/ml sodium azide and 4μg/ml ceftazidime. Carriage of pAQU type plasmid was confirmed by PCR targeting the *traI* gene, which was specific for this type of plasmid. S1-PFGE was performed on both parental strains and transconjugants as previously described (229).

6.3.3 Plasmid sequencing

The nucleotide sequence of the plasmid pVPH1 from V36 was determined by the whole-genome shotgun approach, utilizing the Illumina HiSeq 2000 sequencing platform following the manufacturer's recommendation. The sequencing reads were assembled into contigs with Velvet (http://www.ebi.ac.uk/~zerbino/velvet/). Gaps were closed using a PCR based strategy and Sanger sequencing. Gene predictions and annotations were conducted by RAST tool and modified manually by BLAST online (230). Sequence comparisons and alignment were performed by Mauve software (231).

One hundred milliliter overnight cultures were subjected to plasmid extraction using the Qiagen Plasmid Midi kit (Qiagen) following the

manufacturer's instructions. The quantity and quality of plasmid samples were determined by the dsDNA High Sensitivity (HS) Assay Kit (Thermo), with measurement being made in the Nanodrop and Qubit 3.0 machines. The plasmid DNA samples were sheared with a Covaris Adaptive Focused Acoustic instrument and used for library preparation with NEBNext Ultra DNA Library Prep Kit and the Multiplex Oligos Kit for Illumina (NEB). The libraries were quantified by employing the Agilent 2100 Bioanalyzer and by performing qPCR with P5-P7 primers, and pooled together and sequenced on the Illumina NextSeq 500 platform with the pair-end (PE) sequencing method (2 × 150bp) according to the manufacturer's protocol (Illumina). Single-molecular real-time sequencing on PacBio RS II sequencer was utilized to generate long reads spanning possible repetitive regions in plasmids by constructing 20K libraries with P5-C3 chemistry (Pacific Biosciences). De novo assembly of Illumina short pair-end reads was performed with SPAdes 3.5 (232). PacBio long reads were used to close gaps in Illumina assembly results, and closed plasmid contigs were corrected with Illumina reads and circularized with in-house scripts.

6.3.4 Plasmid annotation and alignment

All plasmid sequences were submitted to online RAST tool for automatic annotations and modified manually by BLAST (230). Linear alignment of plasmid sequences were conducted by Easyfig

tool with local BLASTN (233). BRIG software with embedded BLASTN was used to compare plasmids with a reference (211). ISFinder, ResFinder and PlasmidFinder were used to analyze the plasmid sequences *in silico* after obtaining the complete sequences (117, 234). The INTEGRALL database was used to annotate and designate class 1 integron (121). All complete plasmid sequences were submitted to the NCBI database with accession numbers listed in **Table 1**.

6.3.5 Core-genome and pan-genome of plasmids

After obtaining the complete sequences of six new pAQU type plasmids and three other previously reported plasmids with similar backbones, their core genomes were analyzed by bioinformatics tools. Prokka was used to annotate the plasmid sequences (235), and the gff files generated were analyzed with the pan genome pipeline Roary (236). CLC Genomics Workbench was used to create phylogenetic tree with UPGMA and 100 bootstraps based on multiple core gene alignment (concatenated core genes) file, which was the output file from Roary process. Combining formed tree file and the gene_presence_absence file, roary plots were utilized to generate the plasmid phylogeny tree with a matrix with the presence and absence of core and accessory genes, pie chart of distribution and core and accessory genes, and a frequency plot.

6.4 Results

6.4.1 Characterization of pVPH1 and the circular intermediate

The plasmid carrying bla_{PER-1} was able to be conjugated into *E.coli* J53. The complete plasmid sequence of pVPH1 was 183,730bp in size and had an average G+C content of 45.2%, which is similar to that of the chromosome of *V. parahaemolyticus* (45.1%-45.6%). Annotation results revealed that pVPH1 harbored 114 predicted coding sequences; among them, several functional regions could be identified. After conducting the BLASTN alignment search against NCBI database, the sequence organization of pVPH1 was found to be similar to that of pAQU1 (72%) and pAQU2 (76%). Both pVPH1 and pAQU type plasmids belonged to group of self-transmissible plasmids known as $MOB_{(H12)}$, which is prevalent in *Enterobacteriaceae* and *Vibrionaceae* (225, 226, 237). Although they harbored similar backbone sequences, the MDR regions which constituted the remaining parts of the plasmid were structurally diverse (**Fig. 6.1**). This may indicate that the different MDR regions can be disseminated in plasmids with similar backbone structure.

Figure 6. 1 Plasmid sequence alignment of the pVPH1 and pAQU1, pAQU2 by Mauve software

The upper panel is the sequence of pVPH1 obtained in this study. The representation of each sequence from Mauve contains, from top to bottom, the local collinear blocks (LCBs), forward CDs, reverse CDs, and annotated features. Lines are used to link similar LCBs, and a colored similarity plot is drawn for each sequence, the height of which reflects the level of sequence identity respectively. The unique region for pVPH1 has been labeled in the upper part of this picture.

6.4.2 Epidemiology of pAQU type plasmids

Screening of ESBL genes in 154 *Vibrio parahaemolyticus* and 23 *Vibrio alginolyticus* strains showed that three strains (VPS43, VAS114 and VAS19) harbored the $bla_{\text{PER-1}}$ element (238). The plasmids in these three *V. parahaemolyticus* strains were conjugative (**Table 6.1**). S1-PFGE and hybridization with the $bla_{\text{PER-1}}$ probe indicated that the size of such plasmids ranged from ca. 160k to 210k. To assess the degree of genetic similarity between these three plasmids and a previously reported $bla_{\text{PER-1}}$ positive plasmid, pVPH1, primers targeting the conserved relaxase gene *traI* (traI-F, TCATGCCTGTAATTGGCCGT; traI-R, TTGCGGATGCTTTAGGCTGA) were designed and used to determine if this gene was present in the $bla_{\text{PER-1}}$ -bearing plasmids. All the three plasmids were found to be positive for *traI*, suggesting that they comprised a structure similar to pVPH1. Interestingly, screening ceftazidime-susceptible strains with these primers enabled us to identify two other strains (VPS62 and VPS91) that carried *traI* gene, but without $bla_{\text{PER-1}}$ (**Table 6.1**). These five plasmids together with a $bla_{\text{PER-1}}$ positive plasmid identified from a *V.*

parahaemolyticus strain, VPH2, in Hong Kong, a city adjacent to Shenzhen, were subjected to plasmid sequencing in an attempt to construct the evolution route of this novel type of plasmids (**Table 6.1**) (227).

Table 6. 1 The sources and genetic characteristics of pAQU type plasmids analyzed in this work

Strain	Bacterial species	Plasmid name	Size(bp)	Accession number	Location	Year of isolation	Sources	Complex class 1 integron
VPS62	*V. parahaemolyticus*	pVPS62	184,719	KX957971	Shenzhen, China	2015	chicken, supermarket	-
VPS91	*V. parahaemolyticus*	pVPS91	163,005	KX957972	Shenzhen, China	2015	shrimp, supermarket	-
VAS19	*V. alginolyticus*	pVAS19	187,130	KX957968	Shenzhen, China	2015	shrimp, wet market	+
VAS114	*V. alginolyticus*	pVAS114	206,274	KX957969	Shenzhen, China	2015	shrimp, wet market	+
V36	*V. parahaemolyticus*	pVPH1	183,730	KP688397	Hong Kong, China	2010	shrimp, supermarket	+
V43	*V. parahaemolyticus*	pVPS43	201,098	KX957970	Shenzhen, China	2013	shrimp, supermarket	+
2011VPH2	*V. parahaemolyticus*	pVPH2	198,487	KP791968	Hong Kong, China	2011	shrimp, supermarket	+
04Ya311	*Photobacterium damselae*	pAQU1	204,052	AB571865	Japan	2004	seawater, coastal aquaculture site	-
04Ya090	*Vibrio spp.*	pAQU2	160,406	AB856327	Japan	2004	sediment, coastal aquaculture site	-

Complete sequence of these six plasmids were successfully obtained and subjected to sequence analysis together with pVPH1, pAQU1 and pAQU2, which were previously reported plasmids of similar core structure (227). These plasmids ranged from 163,005 bp to 206, 274 bp in size and were obtained in a wide timeframe spanning 2004 to 2015 (**Table 6.1, Fig. 6.2**). Alignment of the nine complete pAQU type plasmids demonstrated that they contained two conserved regions responsible for plasmid conjugation and maintenance. Two mosaic regions were detected within these plasmids, one of which contained a Multidrug Resistance Region (MDR) in which various antimicrobial resistance genes were found (**Fig. 6.3**). *In-silico* resistance genes search using the antibiotic resistance gene database indicated that the number of genes within the MDR region ranged from 0 to 10 (**Fig. 6.4**). Heatmap was plotted to show the distribution of different resistance genes and insertion sequences. For pVPS91, no resistance genes and insertion sequences were found, suggesting that it may be the prototype of this type of plasmids. The MDR regions were extracted from the other eight plasmids which harbored resistance genes. Based on the existence of the complex class 1 integrons which contained IS*CR1*-$bla_{\text{PER-1}}$, the MDR regions could be divided into two categories: the first type harbored the typical complex class 1 integron, and the second one harbored a Tn*10* -like structure (**Fig. 6.5**).

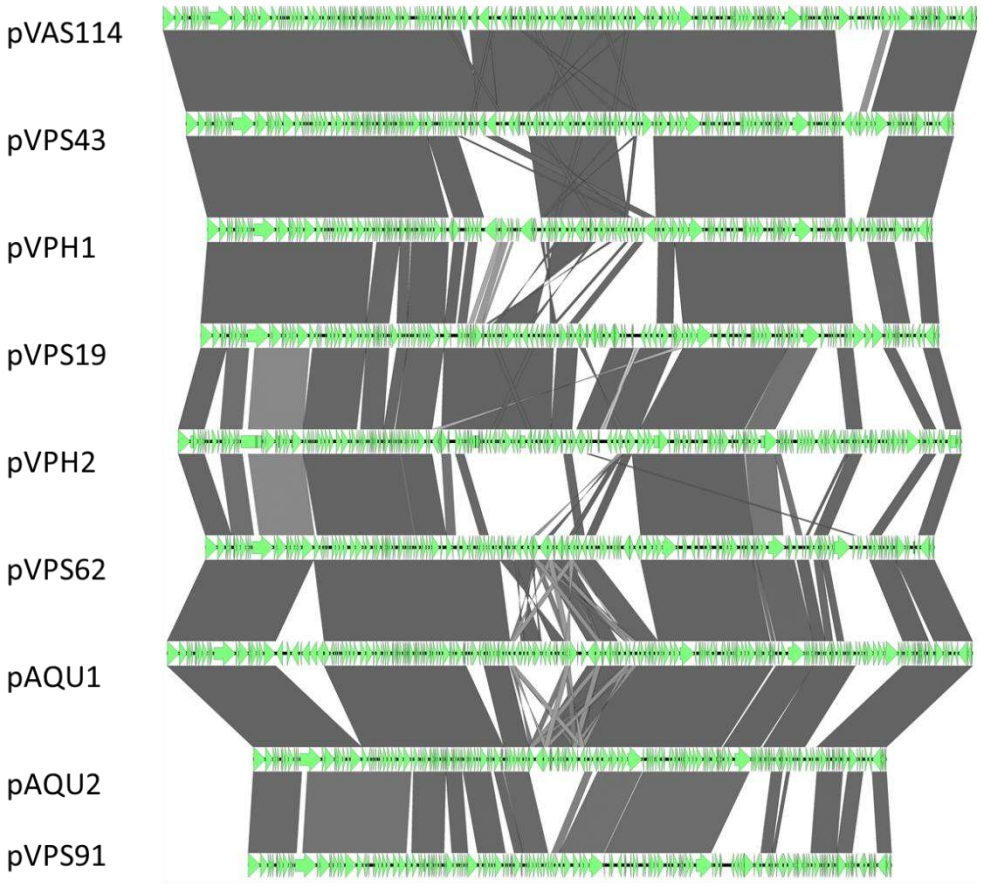

Figure 6. 2 Linear alignment of nine pAQU type plasmids with similar core structures

The meta information of plasmids is provided in **Table 1**, and sequences can be found in NCBI database using accession numbers listed in **Table 1**. The mosaic regions in the middle of alignment belong to MDR regions, which contained all the resistance genes in plasmids, except *qnrVC6*-dfrA31 in pVPS62 which is located in the second plastic region at the end of the alignment.

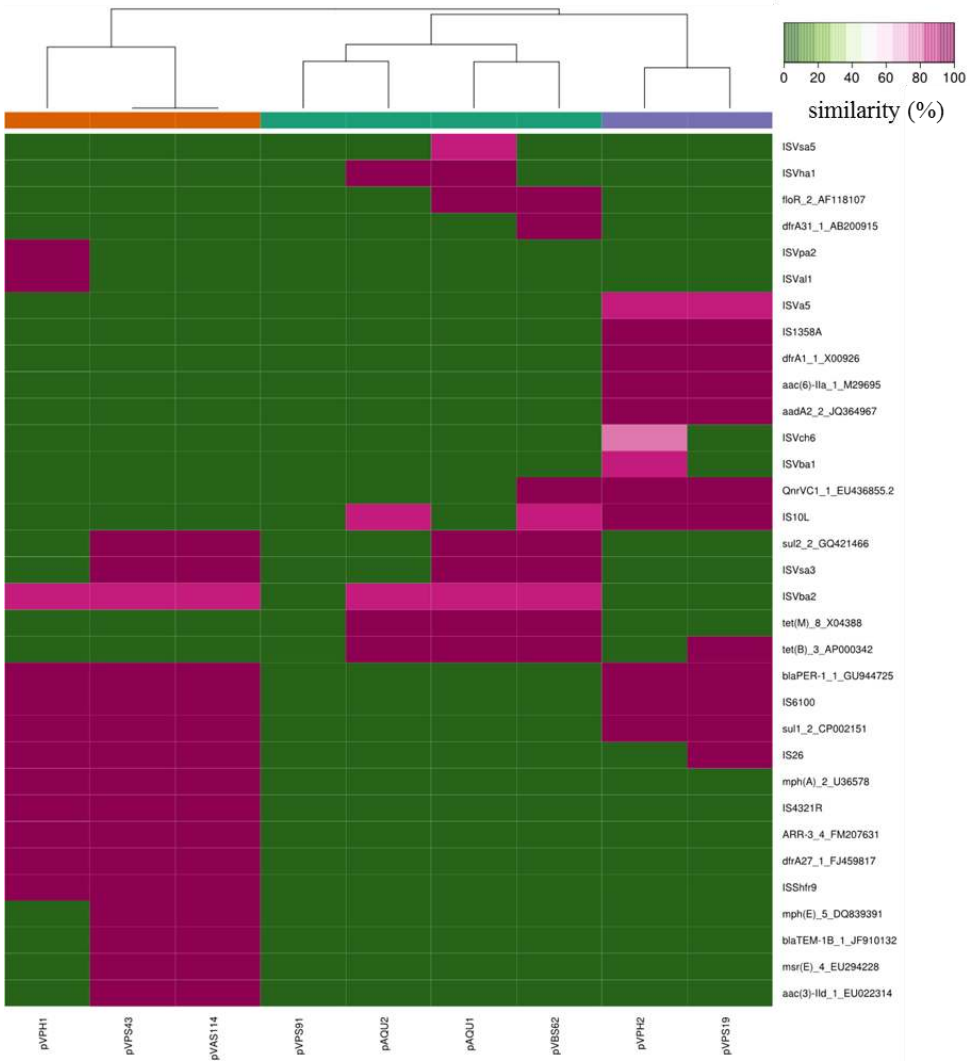

Figure 6. 3 Heatmap depicting the existence of different antimicrobial resistance genes and insertion sequences in the nine plasmids

The plasmids can be clustered into three groups based on the distribution of resistance genes and insertion sequences. The number of resistance genes range from 0 to 10.

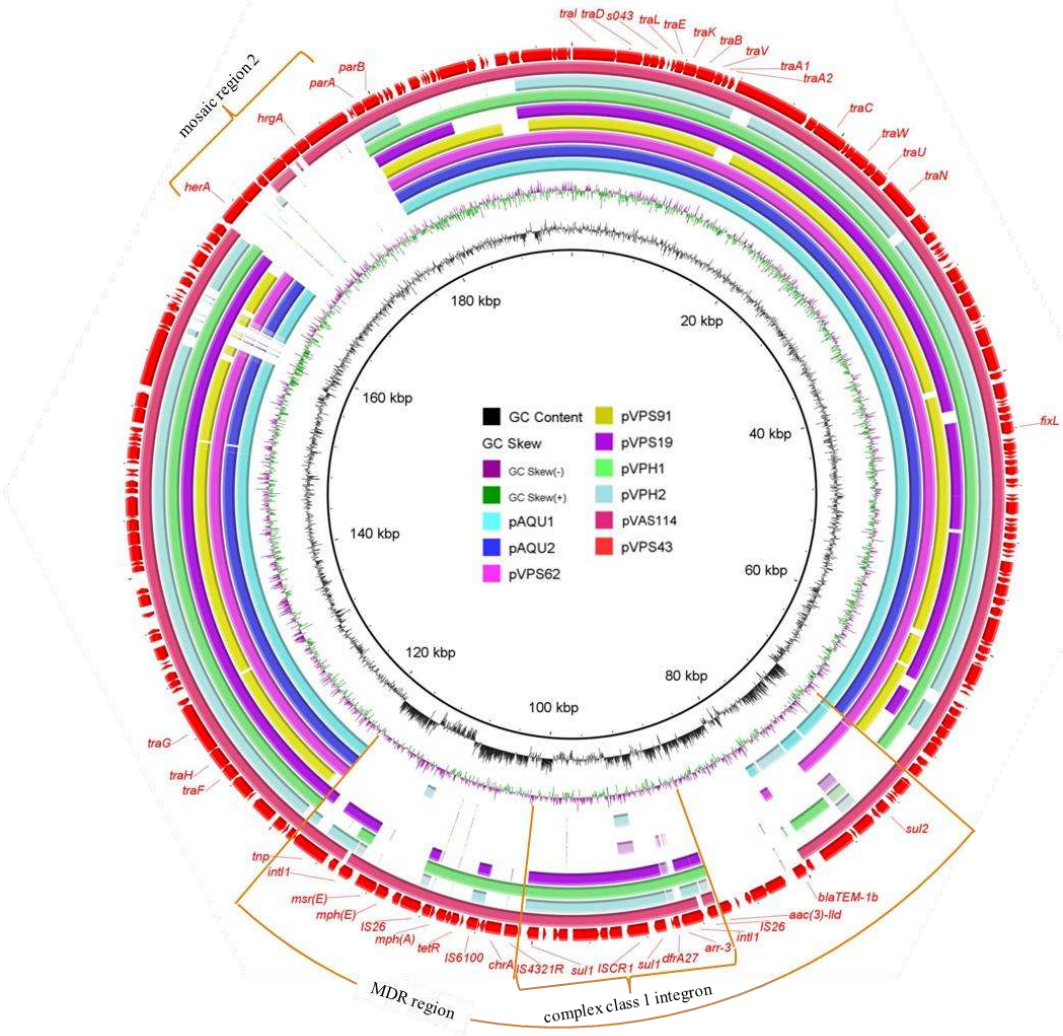

Figure 6. 4 Circular maps depicting the plasticity of pAQU type plasmids

The plasmid, pVPS43 with the largest number of resistance genes (10), was used as the reference to compare with eight other plasmids. The outer circle depicted by red arrows represents annotations of pVPS43. With two mosaic regions (MDR region and mosaic region 2) inserted, the plasmids can be divided into four parts, among which two core plasmid genome regions are responsible for plasmid conjugation and maintenance. In the MDR region, complex class 1 integrons with $bla_{\text{PER-1}}$ exist in five plasmids. Alignment of the five complex class 1 integrons is shown in **Fig. 6.5**.

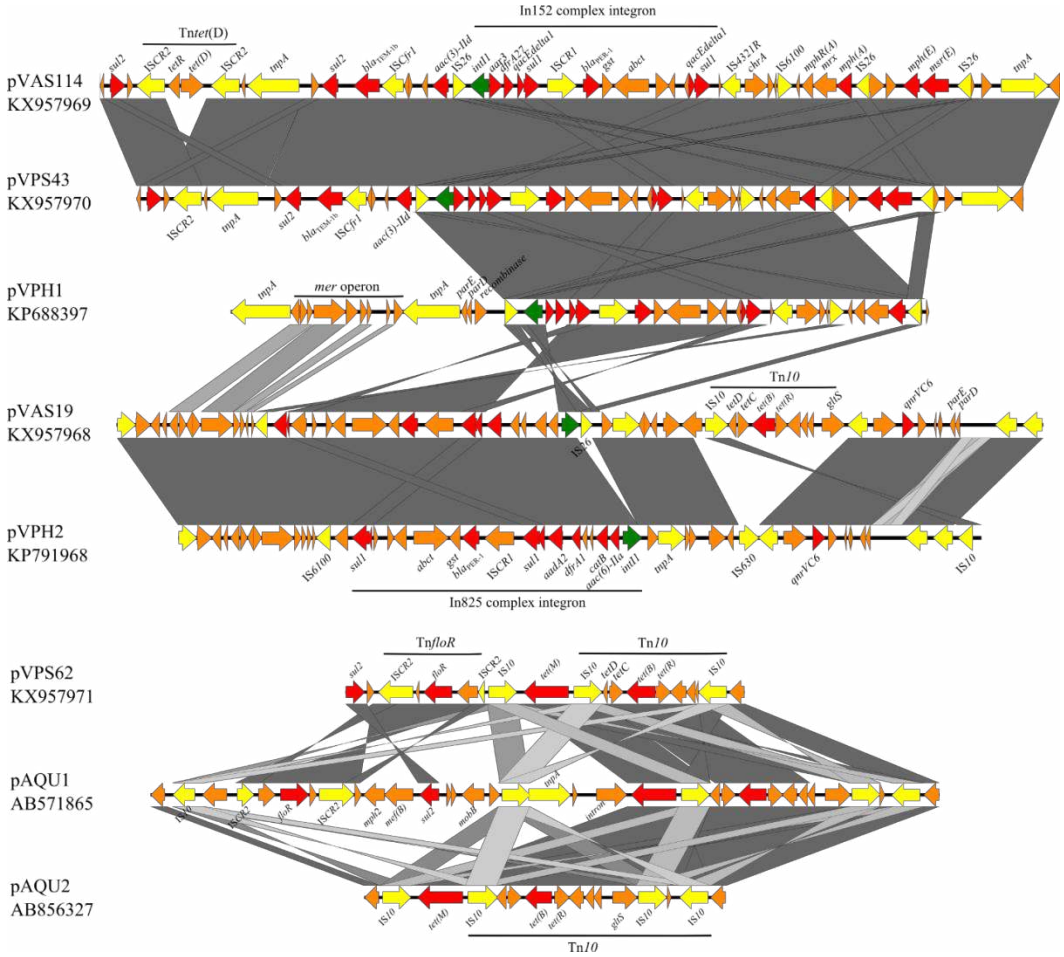

Figure 6. 5 Alignment of eight pAQU type plasmids containing different MDR regions

Two main types of plasmids were divided based on the presence of IS*CR1* mediated $bla_{\text{PER-1}}$**.** The upper five plasmids with complex class 1 integrons can be further categorized into two types differed by existence of the resistance gene cassettes in class 1 integron. The lower three plasmids were characterized by the presence of Tn*10* similar structures.

6.4.3 Structure of complex class 1 integron-bearing plasmids

According to data of the previous studies regarding $bla_{\text{PER-1}}$, apart from the Tn*1213*- related structure, complex class 1 integron also played an important role in dissemination of $bla_{\text{PER-1}}$ (239, 240). In this study, two typical complex class 1 integrons which contained

different class 1 integrons such as IS*CR1*, *bla*$_{PER-1}$ -*gst- abct* and duplicated 3'CS regions, were found among the five *bla*$_{PER-1}$-bearing plasmids. The complex class 1 integrons in the five plasmids were compared by using Easyfig (**Fig. 6.5**). The two different complex class 1 integrons were found to differ only in genetic cassettes embedded in class 1 integrons. The first type had the structure *intI1- aar3- dfrA27- qacE*Δ*1-sul1*-IS*CR1- bla*$_{PER-1}$*-gst-abct-qacE*Δ*1-sul1* shared by pVAS114, pVPH1 and pVPS43. On the other hand, pVAS19 and pVPH2 contained another complex class 1 integron with the structure *intI1-aac(6)-IIa-catB-dfrA1-aadA2- qacE*Δ*1-sul1*-IS*CR1- bla*$_{PER-1}$*-gst-abct- qacE*Δ*1-sul1*. Compared with the nr database in NCBI, integron of the first type comprised the structure In152 (5'- CS-*aar3-dfrA27*- 3'CS), which was first identified in *Aeromonas* spp. (HQ386839); integron of the second one contained the fragment In825 (5'- CS- *aac(6)-IIa-catB-dfrA1- aadA2*-3'CS), which was found in the chromosome of *Shewanella xiamenensis* (KR780673), as well as IS*CR-1-qnrA1*-3'CS, thereby constituting a complex class 1 integron (241).

It has been reported that complex class 1 integron in pVPH1 can generate a circular intermediate (IS*CR1- bla*$_{PER-1}$*-gst-abct-qacE*Δ*1-sul1*) with 8997bp in size (227). Furthermore, a similar circular structure was detected in a *Vibrio cholerae* strain harboring an In4 integron-bearing conjugative IncA/C plasmid (242). Prior to these two studies, IS*CR1*-mediated *bla*$_{PER-1}$ has been found in a complex Tn*402*-like integron and surrounded by two copies of 3'CS region

of class 1 integron in *Acinetobacter johnsonii* , which usually inhabits the aquatic environment (240). The ability of the other four plasmids to form the circular intermediate was tested as previously described (227), with results showing that all contained the IS*CR1* mediated circular structure. This finding indicates that this circular form is activated among bacteria and can be integrated into the classical class 1 integron to form a new complex class 1 integron.

According to the plasmid alignment result, pVAS114 and pVPS43 exhibited a high degree of sequence homology (**Fig. 6.2, Fig. 6.5**). The structure of the MDR regions in the two plasmids were nearly identical (*sul2*-IS*CR2-sul2-bla*$_{\text{TEM-1b}}$-*aac(3)*-IS*26*-complex class 1 integron-IS*4321R-chrA*-IS*6100-mphR(A)-mrx-mph(A)*-IS*26-mph(E)-msr(E)*-IS*26*), except that the IS*CR2-tet(D)-tetR* fragment was found to have integrated into the existing IS*CR2* element in pVAS114, forming the structure IS*CR2-tet(D)-tetR*-IS*CR2* (designated as Tn*tet*(D)) , whereas only one copy of IS*CR2* was found in pVPS43. This new transposon therefore comprised two intact IS*CR2* in direct repeats. A similar structure, IS*CR2-tet(D)-tetR*-ΔIS*CR2*, was known to be present in the SXT element in a *V. cholerae* strain (243). This phenomenon indicated that IS*CR2-tet(D)-tetR* may exhibit the ability to mobilize between the SXT element and plasmids, generating structurally similar transposons. Beyond the complex class 1 integron, the *mph* operon was bounded by IS*6100* and IS*26*, followed by the *mph(E)-mrs(E)*-IS*26* structure. In comparison, *mph(E)-mrs(E)*-IS*26* was absent in plasmid pVPH1,

which prompted us to hypothesize that IS*26* played an important role in the dissemination of *mph(E)-mrs(E)*. Furthermore, the mercuric resistance operon and *parDE* type II toxin-antitoxin system were located upstream of complex class 1 integron in pVPH1. In pVAS19, another type of mercuric resistance operon was followed by a complex class 1 integron that was in a reverse orientation when compared with pVPH1, then the *tet(B)-tet(R)*, *qnrVC6* and *parDE* systems were surrounded by insertion sequences. In pVPH2, the MDR region was nearly identical to pVAS19 except that the 8K Tn*10* region (244) comprising *tet(B)-tet(R)* and *jemABC* was absent.

6.4.4 Structure of Tn*10* bearing plasmids

Based on the absence of complex class 1 integron, another three plasmids were grouped and compared (**Fig. 4**). Plasmids pAQU1 and pAQU2, found in Japan, are known to contain different resistance genes, both of which do not have class 1 integron and IS*CR1*- $bla_{\text{PER-1}}$. The *tet(B)-tet(R)-jemABC* elements, surrounded by IS*10L* and IS*1R* within the Tn*10*-like cluster, were found to be present in both pAQU1 and pAQU2. Compared with the original Tn*10* (AF162223), one more copy of IS*10* was inserted into the extreme 3' end of *jemA* in pVPS62. The plasmid pVPS62 was characterized by having the structure *sul2*-IS*CR2-floR*-ΔIS*CR2*-Tn*10*. The structure IS*CR2-floR*-ΔIS*CR2* has been described as Tn*floR* in *Escherichia coli* (245). This structure was shared by

pVPS62, and pAQU1 in a reverse manner (**Fig 6.5**). In the boundary between Tn*floR* and Tn*10* in pVPS62, IS*10*-tet*(M)* was inserted.

Another mosaic region was the areas encoding hypothetical proteins upstream of the type I restriction-modification system, and this plastic region were found to exist in all pAQU plasmids. Three *qnrVC6* positive plasmids were identified out of the nine pAQU type plasmids (**Fig. 6.3**). Although *qnrVC* genes are always associated with class 1 integrons, the three *qnrVC6* genes in plasmids pVPS62, pVPH2 and pVAS19 were distributed in two locations. Both pVPH2 and pVAS19 have an identical *qnrVC6* gene located between the 3' extremes of MDR regions and the *parD*E system. Comparatively, *qnrVC6- dfrA31* was located in the mosaic region 2 in plasmid pVPS62. Sequences harboring *qnrVC6* were extracted from the NCBI database and alignment with these two genetic arrangements was performed (**Fig. 6.6**). Apart from class 1 integron related *qnrVC6*, *qnrVC6* can be mobilized and integrated into different loci of plasmids, together with its *attC* site. This indicted that *qnrVC6* cassette was still active in the potential circular gene cassettes (246). Although a previous report (226) suggested that pAQU type plasmids contributed to the widespread of tetracycline resistance gene *tet(M)*, only one plasmid pVPS62 was positive for this gene in our seven identified pAQU plasmids (**Fig. 6.3**). This may indicate that the association between *tet(M)* and pAQU plasmids was restricted regionally.

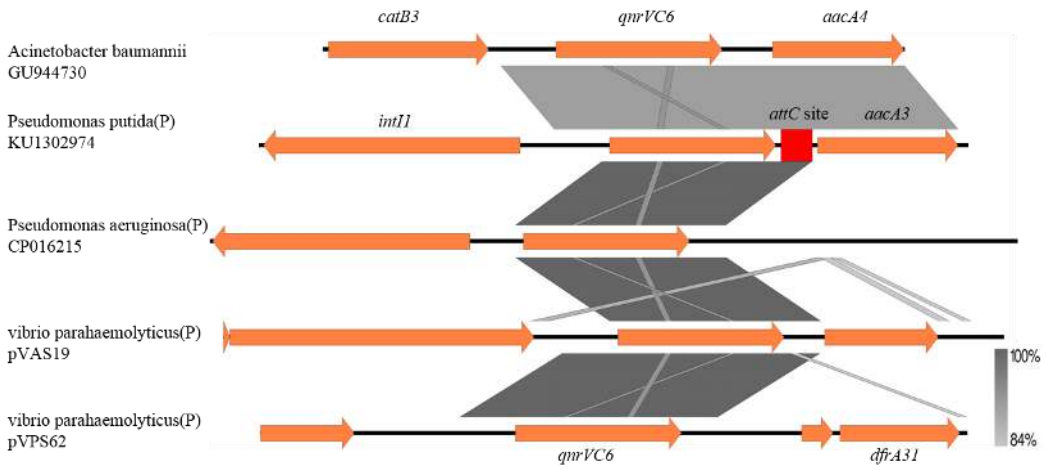

Figure 6. 6 Alignment of *qnrVC6* positive DNA segments in both pAQU plasmids and other available *qnrVC6* positive sequences in NCBI

The letter P in brackets indicates that the DNA segments are derived from plasmids. Arrows without annotation labels represent the predicted coding sequences without known functions. The legend at the right bottom corner depicts percentage of DNA homology.

6.4.5 Characterization of core-genome and pan-genome of plasmids

With the help of the Roary pan genome pipeline, we analyzed the nine pAUQ type plasmids collectively. After annotation with Prokka and analysis of roary, there were 511 genes identifiable from 1916 predicted genes in the nine plasmids. A total of 111 genes were found to be shared by all the plasmids and regarded as core genes. Another 400 genes existed as accessory genes in less than 9 plasmids. The 111 core genes comprised of plasmid maintenance genes such as *tra* genes and hypothetical genes. The 400 accessory genes are composed of resistance genes, insertion sequences, toxin-antitonxin system and hypothetical genes of unknown functions.

Through alignment of the 111 core genes, a phylogenic tree was constructed and matrix with the presence and absence of core and accessory genes were combined with the tree (**Fig. 6.7a**). The evolutionary tree indicated that two major clusters were generated, which matched the distribution of resistance genes among the plasmids. Plasmid pVPS91, which harbored no resistance genes and insertion sequences, was distinguished from the other eight MDR plasmids. As a MDR cluster, the MDR plasmids could be further divided into several subgroups: pAQU1 and pAQU2 were clustered together, and other six plasmids were clustered into three different groups that did not match the distribution of resistance genes. For the five $bla_{\text{PER-1}}$-bearing plasmids, three groups were generated with pVPS43 and pVAS114 clustering together (**Fig. 6.7b**). The plasmid pVPS62 without complex class 1 integron was in the middle of the $bla_{\text{PER-1}}$-bearing plasmids in the phylogenic tree, which may indicate that the complex class 1 integrons were active and mobilizable between plasmids harboring similar backbone. The clusters generated by distribution of resistance genes and insertion sequences (**Fig. 6.3**) and by homology of shared core genes (**Fig. 6.7**) were not strictly matched. This implied that the evolution features of the MDR plasmids are highly dependent on the results of evolution of the core genes and accessory genes.

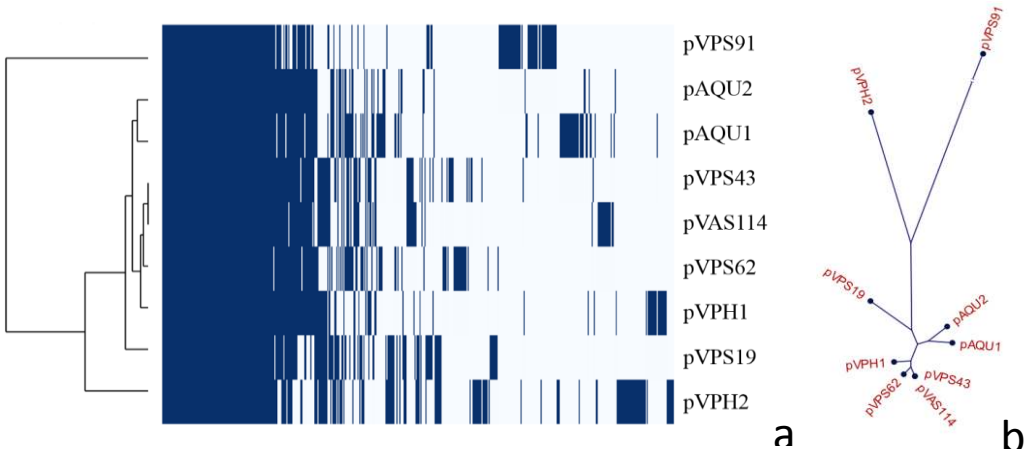

Figure 6. 7 Phylogram of pVQU plasmids based on SNP of core genes

a, phylogram of core genes of pAQU plasmids against matrix with the presence and absence of core and accessory genes; b, unrooted radial phylogram of core genes of the nine plasmids.

6.5 Discussion

The MDR regions of pVPH1 are centralized in a region of ~40kb in size, which is flanked by two different Tn3 family transposase genes. There were many different genetic mobile elements in this mosaic region, such as IS*26*, Class 1 Integron, IS*CR1*, IS*4321* and IS*6100*. A mercuric resistance operon (*mer* operon) was also found between the Tn3 and TniA transposase elements, which was similar to that of plasmid pR148 from *Aeromonas hydrophila* (247). Downstream of the mercuric resistance operon was a ParDE type II toxin-antitoxin system (248).

A class 1 integron with an arr3-dfrA23 cassette flanked by IS*26* and IS*CR1* was also found with *bla*$_{PER-1}$ being located downstream of IS*CR1* in an area including *gst* (encoding a glutathione S-transferase), *abct* (encoding an ABC-type transporter) and three hypothetical genes, followed by the *qacEdelta1* and *sul1* genes. A similar *bla*$_{PER-1}$ genetic arrangement has been described in a previous study (99) with slight difference as shown in **Fig. 6.8**. IS*CR1* was always found to be linked with a class 1 integron, which played an important role in the mobilization of various antibiotic resistance genes (249). Resembling IS*91*-like elements that can generate free circular intermediates, IS*CR1* mediated resistant genes were supposed to be translocated via rolling-cycle transposition with the help of *oriIS* and *terIS* (99, 249, 250). The genetic arrangement around *bla*$_{PER-1}$ can be divided into two major groups, one is the conventional *bla*$_{PER-1}$-*gst* structure surrounded by IS*Pa12* and IS*Pa13* of Tn1213 (100), the other being IS*CR1*-*bla*$_{PER}$-gst-abct structure in a class 1 integron. The first group may be derived from the chromosome in *P. aeruginosa* RNL-1 (AY779042) where *bla*$_{PER-1}$ was first detected (100, 251). It has been detected in different pathogens and was found to disseminate mainly among European countries. However, the second group was always found to be fused with class 1 integron and distributed only in China to date (91, 99, 252, 253). This phenomenon indicates that the dissemination of *bla*$_{PER-1}$ among bacteria populations undergoes different pathways in different geographical sites. In order to verify if this IS*CR1* element can generate circular DNA segment (254), a

pair of primers (C-F, TTCGGCTTGACTCGGCTGA; C-R, TGCAGTAGAGGGTGCTGTTG) were designed to amplify the hypothetical circular intermediate with the reverse PCR method (**Fig. 6.9**). The result showed that it can be circularized, the diagrammatic representation of which is shown in **Fig. 3**. It was speculated that IS*CR1* may act like IS*91* to generate circular intermediates and mobilize genes immediately upstream of IS*CR1* (255). However, the sequencing results showed that the IS*CR1* element in this plasmid can form the circular intermediate for the downstream region of IS*CR1* (IS*CR1-per1-gst-abct-qacEdelta1-sul1*). Examination of the nucleotide sequence revealed that the recombination site that triggered the excision of the circular intermediate was probably the 3'-CS area (*qacEdelta1-sul1*) of the class 1 integron (**Fig. 6.9**). The results also suggested that this type of the circular intermediate may actually mediate the formation of the complex class 1 integron.

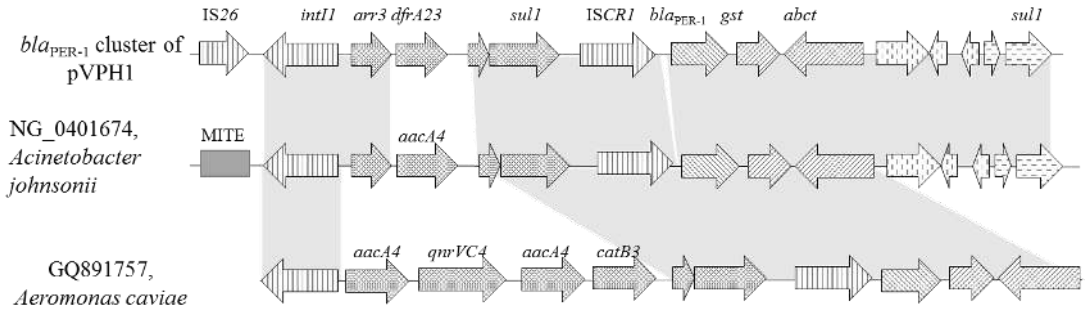

Figure 6. 8 Comparative analysis of complex class 1 integron harboring *bla*$_{PER-1}$ from different bacterial species

Annotated coding sequences are displayed as arrows. The shadow quadrangles indicate the consensus sequences among different organisms. The arrows without gene names represent the hypothetical open reading frames.

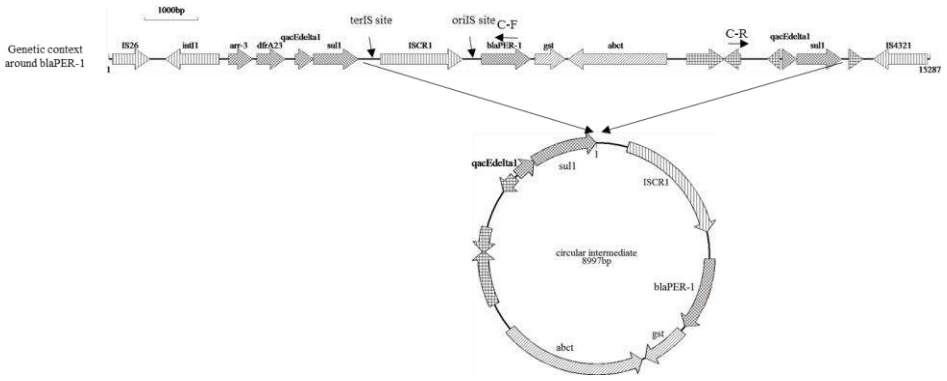

Figure 6. 9 Circular intermediate generated by IS*CR1* using the reverse PCR method

The 3'-CS area (*qacEdelta1-sul1*) of class 1 integron probably was the homologous region for the excision of the circular intermediate. OriIS and terIS are origin and termination sites of ISCR element respectively.

With the advent of revolutionary sequencing technology, especially the availability of third-generation sequencing methods such as single-molecular real-time sequencing (SMRT) and nanopore sequencing (256), an increasing number of completed bacterial genomes have become available. Likewise, the number of fully-sequenced plasmids has increased rapidly. As an important vehicle utilized by bacteria to evolve and adapt to external environments, data regarding fully-sequenced plasmids will be immensely usefully for studies of evolution and functions of plasmids. As a consequence, novel plasmids that cannot be typed by conventional methods have been discovered (109). In our previous study on ESBLs-producing *V. parahaemolyticus* strains recovered in Hong Kong, we showed that $bla_{\text{PER-1}}$ was located in plasmids designated as pVPH1 and pVPH2, with a backbone similar in structure to pAQU1 and pAQU2 (227). In this study, we sequenced six different

plasmids with a backbone similar to the pAQU plasmids recently recovered from marine bacteria (225-227). Analysis showed that this type of plasmids were vehicles that comprised multiple resistance genes and that the MDR regions in these plasmids were active in acquiring different resistance elements.

Among the nine plasmids analyzed, typical MDR regions with different resistance genes were found conserved in the backbones of eight MDR plasmids, albeit from various bacteria such as *V. parahaemolyticus*, *V. alginolyticus and Photobacterium damselae* of different locations year of isolation. The ESBL-encoding gene $bla_{\text{PER-1}}$ was first found preceded by IS*CR1* in *Acinetobacter johnsonii*, the same phenomenon was observable in *Vibrio cholerae*, *Vibrio parahaemolyticus* and other species (227, 240, 257). IS*CR* family was a very important mobile element first found associated with class 1 integron, facilitating the transmission of various resistance gene by rolling-cycle transposition (258). Based on this hypothesis, the circular intermediate with the structure IS*CR1*-$bla_{\text{PER-1}}$-*gst-abct- qacE*Δ*1-sul1* was detectable among the five plasmids which harbored complex class 1 integrons. Furthermore, IS*CR2*, which shares 65% protein identity with its IS*CR1* equivalent, was found in a plasmid containing IS*CR2-tet(D)-tetR*-IS*CR2* , which may form by recombination of IS*CR2-tet(D)-tetR* and *ISCR2*, in a manner similar to the result of mobilization of the IS*CR2-tet(B)* element (259). In *V. cholerae*, a similar structure with IS*CR2-tet(D)-tetR*-ΔIS*CR2* was found in the SXT elements (243). This

implied that IS*CR2* was active in mobilizing *tetA-tetR* among pAQU plasmids and SXT elements. Two plasmids were found to harbor ΔIS*CR2-floR*-IS*CR2* in the MDR regions, this element was able to generate IS*CR2-floR* intermediate circles by which *floR* can be mobilized between different bacteria within SXT elements and plasmids(including pAQU plasmids) (245, 258). Taken together, pAQU plasmids play an important role in dissemination of IS*CR1-bla*$_{PER-1}$, IS*CR2- tetA-tetR*-IS*CR2* and ΔIS*CR2-floR*-IS*CR2*. A previous study suggested that pAQU plasmids contributed to dissemination of the tetracycline resistance gene *tet(M)* (226). Apart from *tet(M)*, *tet(B)* and *tet(D)* in this kind of plasmid should also be able to confer resistance to tetracycline.

Based on the source of strains harboring pAQU type plasmids, these plasmids should have the tendency to inhabit in bacteria of aquatic environment. Upon increasing exposure to antimicrobials, this type of conjugative plasmids is expected to be transmissible between different bacteria, and possess the ability acquire diverse resistance genes with the help of different mobile elements, rendering the host organisms adaptable to adverse environments. According to results of comparative analysis of MDR regions of different plasmids (**Fig. 6.5**), IS*26*, IS*CR1*, IS*CR2*, IS*10* and IS*6100* were the most important mobile elements in shaping the plasticity of pAQU plasmids, along with the accessory and resistance genes.

Many types of conjugative plasmids harboring a variety of resistance genes, such as IncA/C, IncHI2 and IncQ, were reported and compared to identify the MDR region, which were always found to be clustered together by multiple events of integration with the help of mobile elements (217, 221, 260-262). In pAQU type plasmid, similar MDR regions were found to be highly conserved, located in a specific region and exhibit the ability to evolve and comprise different combinations of resistance genes. Most importantly, this plasmid category could be conjugated from the donor aquatic strains to *E.coli* strains, and this raised the concern that the resistance genes can be transmitted from the aquatic ecosystem to clinical pathogens via this kind of novel conjugative plasmids.

6.6 Conclusion

In summary, we first determined the first complete nucleotide sequence of $bla_{\text{PER-1}}$ carrying plasmid from *Vibrio Parahaemolyticus* and revealed its transmission mechanism mediated by mobile elements. Then, we conducted a systematic study on the conjugative pAQU plasmids which harbor resistance genes by using the third-generation sequencing technology and bioinformatics methods. This type of plasmid represents a newly emerged MDR plasmid which may be transmissible to other human pathogens through the food chain or other routes. The different types of resistance genes distributed among pAQU plasmids prompted us to hypothesize that abuse or overuse of antimicrobials

in aquaculture may continue to select for organisms harboring pAQU plasmids and that introduction of new resistance determinants into the MDR region of such plasmids with the help of mobile elements is a common event.

Chapter Seven: Molecular Mechanisms Underlying Dissemination of the Colistin Resistance Determinant

The content in this chapter has been published in following papers:

Li R, Xie M, Zhang J, Yang Z, Liu L, Liu X, Zheng Z, Chan EW, &Chen S (2016) Genetic characterization of *mcr-1*-bearing plasmids to depict molecular mechanisms underlying dissemination of the colistin resistance determinant. *Journal of antimicrobial chemotherapy 72(2):393-401.*

Li R, Xie M, Lv J, Wai-Chi Chan E, & Chen S (2016) Complete genetic analysis of plasmids carrying *mcr-1* and other resistance genes in an *Escherichia coli* isolate of animal origin. *Journal of antimicrobial chemotherapy 72(3):696-699.*

7.1 Abstract

The recently discovered colistin-resistance gene, *mcr-1*, threatens to compromise the effectiveness of colistin as a last-resort antimicrobial agent. This work aimed to understand the mechanisms of transmission of this novel resistance determinant in order to develop countermeasures to arrest its transmission among major pathogens. Thirty-five out of 97 ESBL-producing *E. coli* strains isolated from pig farms in China were shown to contain the *mcr-1*

gene. Fifteen strains exhibiting different PFGE types were subjected to characterization of the profiles and genetic features of the plasmids that they harbored. Three major types of *mcr-1*-bearing plasmids were recovered: IncX4 (~33kb), IncI2 (~60kb) and IncHI2 (~216-280kb), among which the IncX4 and IncI2 plasmids were found to harbor the *mcr-1* gene only, whereas multiple resistance elements including $bla_{\text{CTX-M}}$, bla_{CMY}, bla_{TEM}, *fosA*, *qnrS*, *floR* and *oqxAB* were detectable, in various combinations, alongside *mcr-1* in the IncHI2 plasmids. The profiles of *mcr-1*-bearing plasmids in the test strains were highly variable, with co-existence of two plasmids being a common phenomenon. Comparative analysis of plasmids maps showed that these plasmids contained a *mcr-1* gene cassette with varied structural components, with the IncHI2 type being the most active in acquiring foreign resistance genes.

Apart from the widespread IncHI2 plasmids, one phage P7-like plasmid (pHYEC7-*mcr1*) was also found to harbor Tn*6330*, a novel transposon Tn*6330* with the structure IS*Apl1*-*mcr-1*-*orf*-IS*Apl1* found to be the key element which mediates the translocation of *mcr-1* into various plasmid backbones through formation of a circular intermediate. Further study indicated the circular intermediate can be excised by retaining one copy of IS*Apl1* and generating the circular intermediate. These findings provided important insights into the transmission mechanisms of *mcr-1*, and lay the foundation for development of novel intervention measures.

7.2 Introduction

The continuous emergence of novel antibiotic resistance-encoding genetic elements among the major bacterial pathogens in recent years has undermined current efforts to devise new antimicrobial strategies, and pose enormous threat to public health (40, 263). Polymyxins including polymyxin B and colistin are cationic antimicrobial peptides which act on Gram-negative bacteria by disrupting the outer membrane (264). Polymyxins were discovered in the late 1940s but deemed unsuitable for treatment of bacterial infections because of its neurotoxic effects; however, emergence of multidrug-resistant Gram-negative bacteria have prompted a renewed interest in this old antibiotic, which is currently regarded as a possible last resort agent to eradicate multidrug resistant organisms (265, 266). Resistance to colistin has been reported among different bacterial species, the underlying mechanism of which is mainly intrinsic in nature. On the other hand, acquired resistance due to modifications of the bacterial outer membrane, efflux pumps, and capsular polysaccharides formation (264, 267) have also been reported. Recently, the pioneering work performed by Liu et al. (268) described the recovery of a conjugative plasmid-mediated polymyxin resistance gene *mcr-1*, which encodes an enzyme belonging to phosphoethanolamine transferase enzyme family, in both animals and human (268). Following this discovery, a number of studies have reported the presence of *mcr-1* among different species of *Enterobacteriaceae* which exhibited multidrug-

resistant phenotypes in veterinary farms, food samples, and clinical settings around the world (269, 270). The emergence of *mcr-1* has been traced back to *E. coli* strains isolated in the 1980s when colistin was first introduced in veterinary practice in China (271), indicating that this gene has long-existed in food animals.

Plasmids harboring *mcr-1* have been reported to include the IncX4, IncI2, IncP and IncHI2 types (269, 272-274). The prevalence of *mcr-1* in plasmids harbored by different bacterial species highlights its potential of being transferred horizontally. Notably, *mcr-1* was often found located downstream of IS*Apl1* (273), which is an insertion sequence belonging to the IS*30* family (275). The close genetic association between IS*Apl1* and *mcr-1* indicates that IS*Apl1* may play a pivotal role in the dissemination of *mcr-1*. The complete sequences of *mcr-1*-bearing plasmids are limited and there is lack of data on the role of IS*Apl1* in mediating *mcr-1* transfer among different plasmids. In this study, we characterized the *mcr-1*-bearing plasmids in *E. coli* isolated from different parts of China, and discovered a *mcr-1*-bearing transposable element which can form a circular intermediate that plays a key role in genetic translocation and hence transmission of the *mcr-1* element in bacteria.

7.3 Materials and Methods

7.3.1 Bacterial strains and identification

Cefotaxime resistant *E. coli* strains were isolated from feces of healthy pigs in various farms located in six provinces in China, including Guangdong, Fujian, Jiangsu, Shandong, Henan and Liaoning, during the period of September 2014 to March 2015, by using MacConkey agar plates supplemented with 4μg/ml cefotaxime. Strain HYEC7 was isolated from a fecal sample collected from a pig farm in Guangdong, China in December 2015, and identified as *Escherichia coli* by using API 20E strip (bioMerieux). The strains were identified as *E. coli* by MALDI-TOF MS using a Bruker MicroFlex LT mass spectrometer (Bruker Daltonics) and confirmed using API20E strips (bioMérieux).

Table 7. 1 Primers used in this study

Primers	Sequence (5'-3')	Target gene	Size
MCR1-F	CGGTCAGTCCGTTTGTTC	*mcr-1*	309bp
MCR1-R	CTTGGTCGGTCTGTAGGG		
MCR1-RC-F	ACGCACAGCAATGCCTATGA	circular form	2672bp
MCR1-R	CTTGGTCGGTCTGTAGGG		
IncI2-F	GCTGCTTGACGCAATATGGG	IncI2 replicon	427bp

IncI2-R	CTGCGCATACCAGCGTTTAC		
IncHI2-F	CTTTAAGTGCTGGCTCGGGA		
		IncHI2 replicon	187bp
IncHI2-R	TGAGAAGGCAAGCACTACCG		
IncX4-F	TCTCGCGCGAATAGTTTTGA		
		IncX4-*mcr-1*	2800bp
MCR1-RC-F	ACGCACAGCAATGCCTATGA		

7.3.2 Prevalence of *mcr-1* positive *E. coli* strains

All *E. coli* strains were subjected to a screen for the presence of *mcr-1* gene by PCR using primers (**Table 7.1**) as previously described (9) . The PCR products were purified and sequenced by Sanger sequencing to confirm the genetic identity.

7.3.3 Antimicrobial susceptibility testing

Minimum inhibitory concentrations (MICs) of fourteen antimicrobial agents as listed in **Table 7.2** were determined using the agar dilution method; results were interpreted according to recommendations of CLSI (276). *E. coli* strain ATCC25922 was used as a quality control strain.

7.3.4 XbaI-PFGE, S1-PFGE and Southern hybridization

E. coli strains that carried the *mcr-1* gene were subjected to further characterization. Pulsed-field gel electrophoresis (PFGE) with XbaI

digestion were performed to assess the genetic relatedness of isolates, using the CHEF-MAP-PER System (Bio-Rad); genomic DNA of the *S. Braenderup* H9812 strain restricted with XbaI was used as the reference standard. Cluster analysis of PFGE patterns was typically performed by the BioNumerics (Applied Maths) system. S1 nuclease -PFGE was performed to characterize the plasmid profiles; the location of *mcr-1* was identified by Southern hybridization with digoxigenin-labeled *mcr-1* probe according to the manufacturer's instructions of the DIG-High Prime DNA Labeling and Detection Starter Kit II (Roche Diagnostics).

7.3.5 Plasmid sequencing and bioinformatics analyses

Plasmids extracted from the 15 bacterial strains using the QIAGEN Plasmid Midi Kit were used to prepare the sequencing libraries, which were constructed by the NEBNext® Ultra™ II DNA Library Prep Kit for Illumina® (NEB) and sequenced by the NextSeq 500 Illumina platform, with 2×150bp paired-end reads. De novo assembly of the reads was conducted with SOAPdenovo2 (277), followed by the use of ResFinder(278) and PlasmidFinder (279) to identify resistance genes and plasmid types among the scaffolds. Construction of complete or partially complete plasmid sequences was accomplished by using available plasmids reference sequences to align the contigs and mapping reads and cover the gaps. In an attempt to obtain the complete gene map of *mcr-1* -bearing plasmids for which *in-silico* analysis failed to produce, PacBio RSII single-molecule, real-time (SMRT) sequencing was performed to create

libraries of 20Kbp in Wuhan Institute of Biotechnology, Wuhan, China. The library preparation work was conducted according to manufactures' instructions of Pacific Biosciences. Illumina contigs were joined together by using the PacBio long contigs after assembly with HGAP 3.0. The annotations of the plasmids sequences were conducted by RAST (230) and edited manually. Alignments with highly homologous complete plasmid sequences available in NCBI for these three type plasmids were depicted by using the BRIG tool (211). Comparison of four complete *mcr-1* IncHI2 plasmids was performed and visualized with Easyfig (233). The representative *mcr-1*-bearing plasmid sequences pECJS-59-244, pECJS-B60-267, pECJS-61-63 and pECGD-8-33 were submitted to NCBI with accession number KX084394, KX254341, KX254342 and KX254343 respectively.

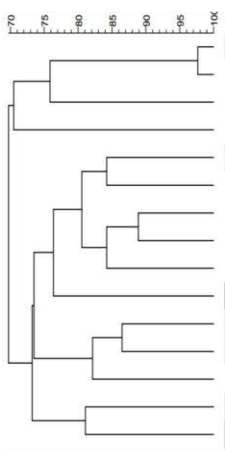

ID	Plasmid profile[a]	Isolation site	Isolation date
JS-61	216, 60	Jiangsu	2015-01-19
JS-64	280	Jiangsu	2015-01-19
FJ-B42	60, 33	Fujian	2014-12-25
SD-137	60	Shandong	2015-03-26
JS-59	244	Jiangsu	2015-01-19
JS-63	216, 60	Jiangsu	2015-01-19
GD-8	33	Guangdong	2014-10-31
JS-B65	60, 33	Jiangsu	2015-01-19
JS-B60	250	Jiangsu	2015-01-19
SD-112	33	Shandong	2015-03-21
FJ-44	250, 33	Fujian	2014-12-25
JS-56	60	Jiangsu	2015-01-19
FJ-B44	33	Fujian	2014-12-25
HN-15	60	Henan	2014-12-16
JS-B73	230	Jiangsu	2015-01-19

Figure 7. 1 XbaI-PFGE cluster analysis of 15 *E. coli* strains from which the *mcr-1* gene was detectable

[a] Plasmid profile refers to the *mcr-1*-bearing plasmids, detailed information of which are presented in **Table 2**. Although strains JS-61 and JS-64 share similar PFGE type, their profiles of *mcr-1*-bearing plasmids are different.

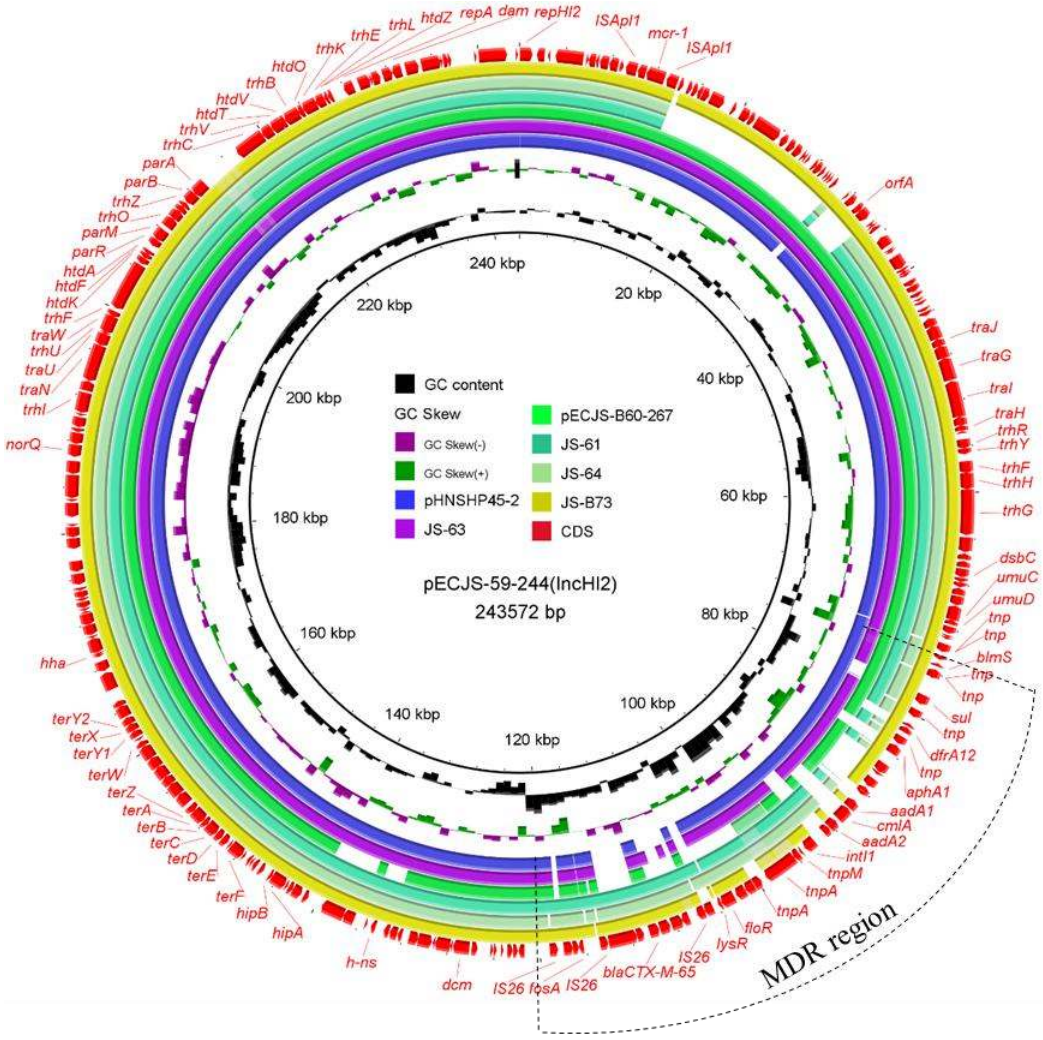

Figure 7. 2 Sequence alignment of IncHI2 *mcr-1* plasmids and WGS contigs in six samples

pECJS-59-244 was used as reference to compare with pHNSHP45-2 (GenBank no. KU341381), pECJS-B60-267 and other WGS data involving IncHI2 contigs detectable in *mcr-1* positive strains. The outer circle with red arrows denotes annotation of reference plasmid. Among the five *mcr-1* IncHI2 strains (JS-44, JS-61, JS-63 and JS64) without complete plasmid sequences, JS-44 exhibits sequence similarity with the reference, but alignment was not successful because of the overall low sequence homology. Note that Tn*6330* is only present in plasmids pECJS-59-244, pECJS-61-230, pECJS-64-280 and pECJS-B73-230. The number of IS*Apl1* repeats is not depicted in this figure. One MDR region was observable in the backbone of all IncHI2 plasmids. Information of the IncHI2 plasmids tested in this study is provided in **Table 1**.

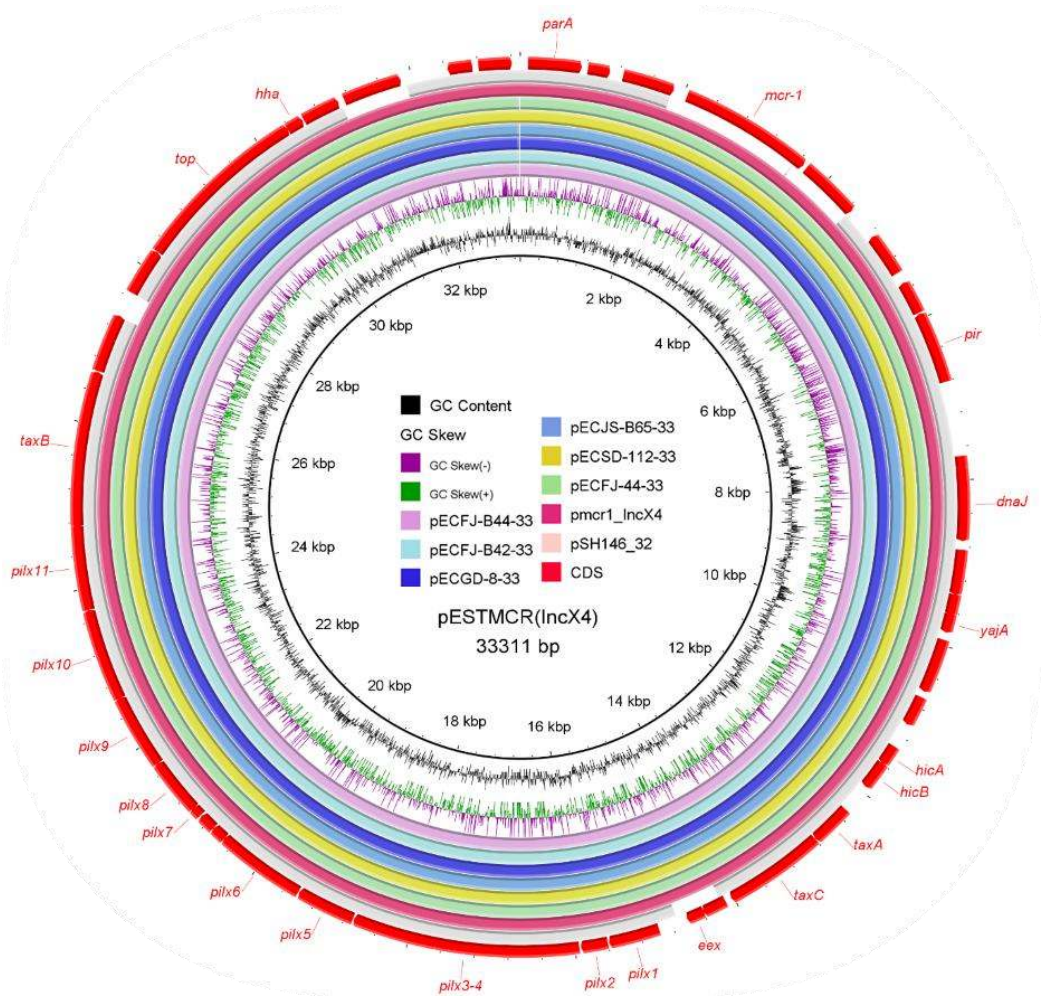

Figure 7. 3 Sequence alignment of IncX4 type *mcr-1*-bearing plasmids

pESTMCR, which was recovered in Estonia with GenBank # KU743383, was used as reference to match with other IncX4 type plasmids with (six plasmids in this study and pmcr1_IncX4, KU761327) and without the *mcr-1* gene (pSH146_32, JX258655). The outer circle with red arrows denotes the annotation of reference sequence. pSH146_32 exhibits a lower degree of sequence homology to the reference sequence when compared to other plasmids, and is depicted by a gray circle instead of the light pink color chosen to represent this plasmid. The figure shows that the six IncX4 plasmids tested in this study and two previously reported IncX4 plasmids (pESTMCR and pmcr1_IncX4) share an extremely high degree of sequence homology. Information of IncX4 plasmids tested in this study is provided in **Table 1**.

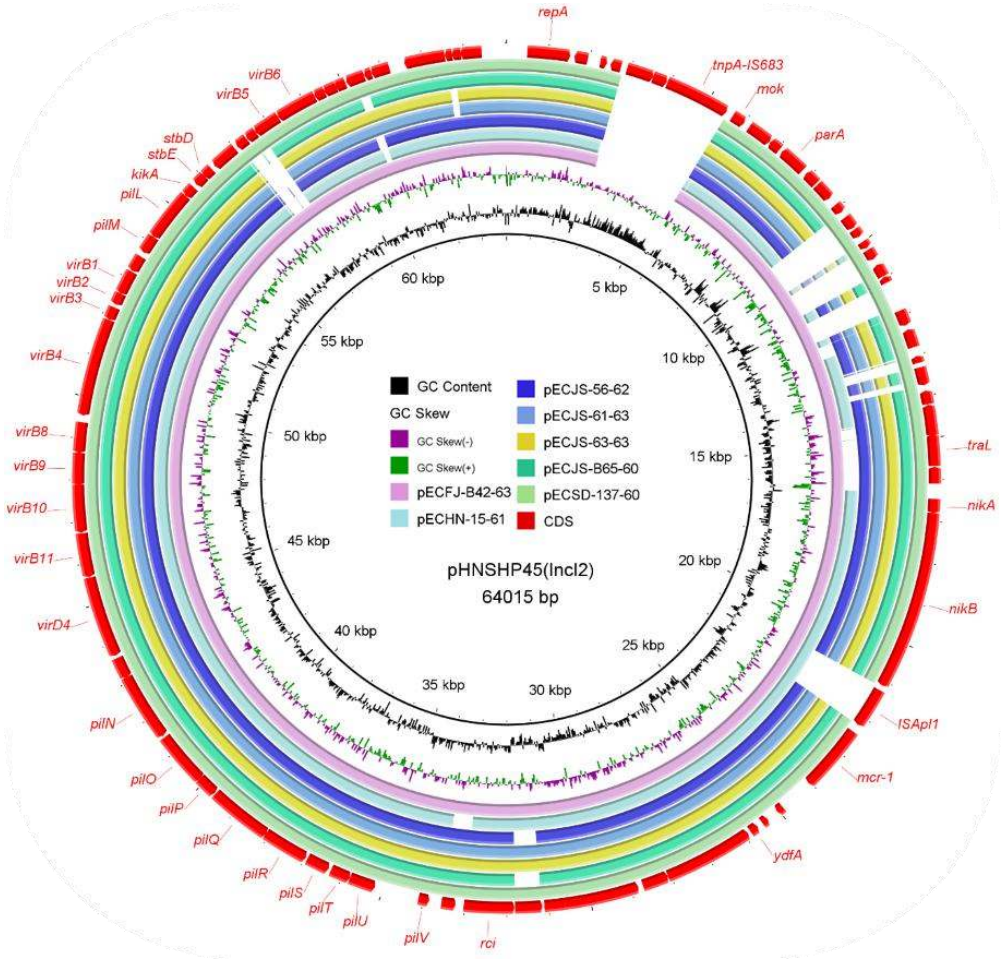

Figure 7. 4 Sequence alignment of seven IncI2 type *mcr-1*-bearing plasmids

pHNSHP45 with GenBank # KP347127 was used as a reference to compare with other *mcr-1*-bearing plasmids which possess the IncI2 replicon. The outer circle with red arrows signifies annotation of the reference sequence. Gaps in the circle refer to plasmid regions which are missing when compared to the reference. The IS*683* element is absent in all the seven IncI2 plasmids tested in this study (See **Table 2** for details). IncI2 plasmids can be categorized into two subtypes based on the presence or absence of IS*Apl1*.

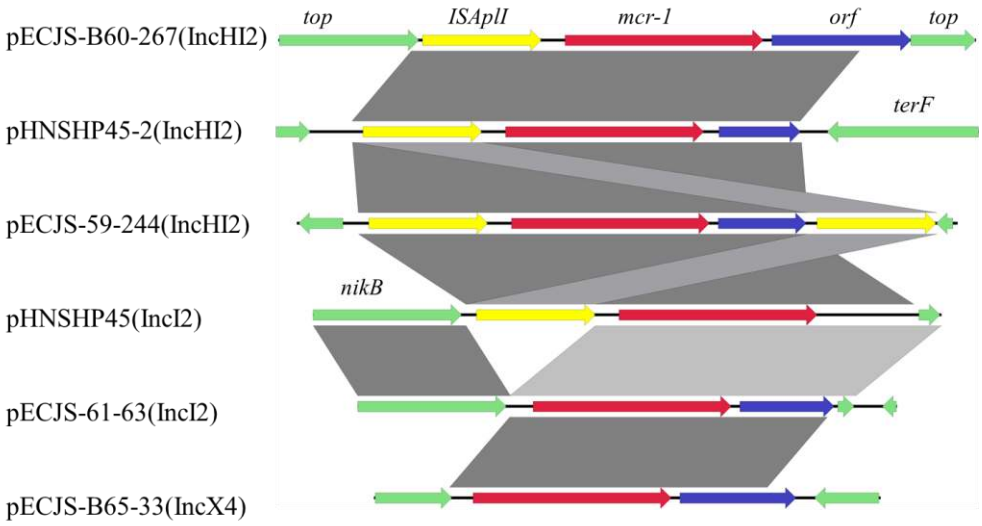

Figure 7. 5 Sequence alignment of plasmids harboring the *mcr-1* gene

CDSs without labels represent hypothetical proteins. The shadow parallelograms denote genetic regions that exhibit sequence homology among different segments. Light shadow denotes regions with a lower level of sequence identity (>99%). Genetic contexts of *mcr-1* in IncHI2 plasmids can be categorized into four types according to the complete sequences available to date. Another plasmid with a new format *mcr-1* gene cassette, namely pSA26-MCR-1, is described in **Figure 7. 7**. IncI2 type plasmids can be divided into two subtypes based on existence or absence of IS*Apl1*. All the IncX4 type plasmids are identical in terms of genetic arrangement in the vicinity of the *mcr-1* gene.

7.3.6 Characterization of circular intermediate

Based on the knowledge that the IS*30* family insertion sequences could form DNA circular intermediate (280) and that IS*Apl1* exhibits similarity with the IS*30* family members (39% identity with IS*30* transposase from *E.coli* NP_414790 in protein sequence), a set of reverse primers targeting *mcr-1* was designed to investigate the potential of IS*Apl1-mcr-1* segment to form a circular form (**Table 7.3**, **Fig. 7.6a**). The PCR products were sequenced by Sanger sequencing to obtain a complete map of the circular intermediate.

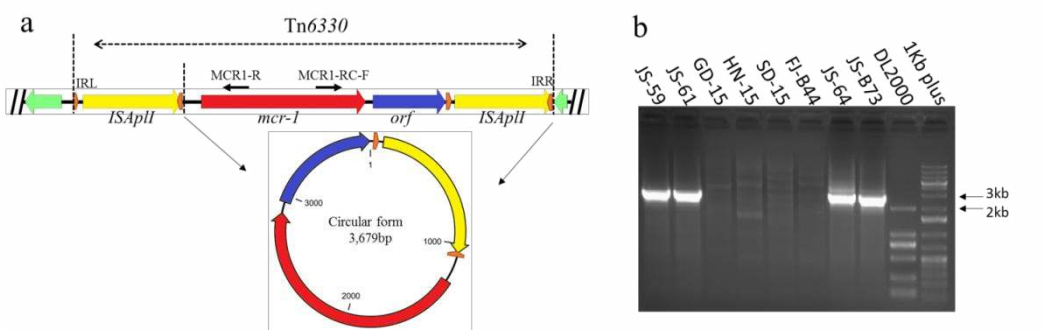

Figure 7. 6 Formation of a circular intermediate by *mcr-1* gene cassette

a) Genetic structure of transposon Tn*6330* (located in pECJS-59-244) and its circular intermediate, which harbors the *mcr-1* gene. b) Gel electrophoresis of PCR amplicons corresponding to the circular intermediate of Tn*6330*, detectable in *mcr-1* positive *E. coli* strains using the reverse primers MCR-RC-F and MCR-R.

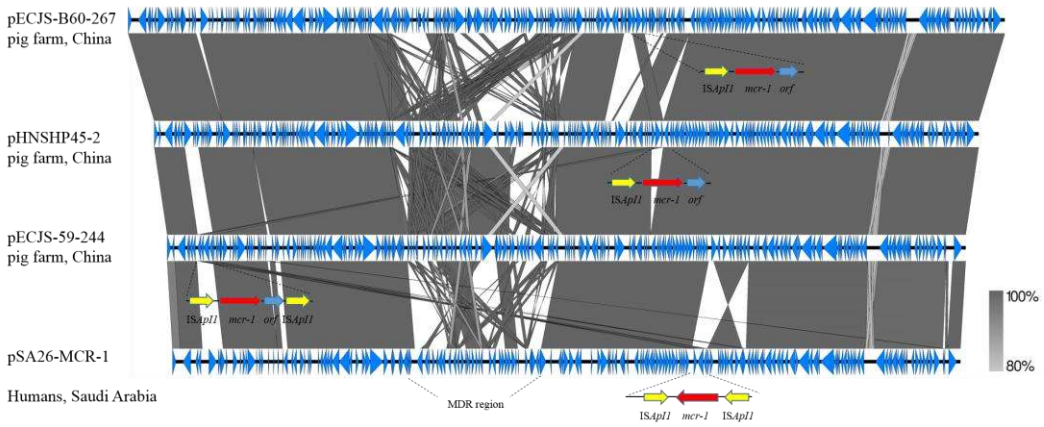

Figure 7. 7 Alignment of four *mcr-1*-bearing IncHI2 plasmids and the respective location of the *mcr-1* gene

The accession numbers are as follows: pECJS-B60-267, KX254341; pHNSHP45-2, KU341381; pECJS-59-244, KX084394; pSA26-MCR-1, KU743384. The color-intensity bar in bottom right-hand corner depicts the degree of sequence homology. A large MDR region located in similar location can be found in all the four IncHI2 plasmids.

To test the stability of Tn*6330*, a pair of reverse primers (MCR1-RC-F ACGCACAGCAATGCCTATGA, MCR1-R

CTTGGTCGGTCTGTAGGG) targeting *mcr-1* was used to test the ability of Tn*6330* to generate circular intermediate (281). Primers Tn-F (GTTCCCGACAGAAGAGGAGC) and Tn-R (ATTGGCGACTGATGGAGTGG) targeting the surrounding sequences of Tn*6330* in HYEC7 were utilized to investigate whether the intact Tn*6330* was consistently present among the test bacterial population. The sequences of PCR products were confirmed by Sanger sequencing.

7.4 RESULTS

7.4.1 Characterization of *mcr-1* positive, ESBL-producing *E. coli*

Among the 97 cefotaxime-resistant *E. coli* strains isolated from fecal samples of pigs in various farms, 35 isolates (36%) were found to harbor the *mcr-1* gene. These *mcr-1* positive strains, which were isolated from pigs in farms located in five geographically divergent provinces of China, were shown to exhibit genetically diverse PFGE types (**Fig. 7.1**). However, strains collected from the same province were generally genetically more related to each other than those obtained from other provinces (data not shown). The MICs of colistin were either 4 or 8 μg/mL for all the *mcr-1* positive strains, with the majority exhibiting resistance to multiple antimicrobial agents except meropenem (**Table 7.1**). To obtain a comprehensive view of the genetic features of *mcr-1*-bearing plasmids in these isolates, 15 *mcr-1*-positive *E. coli* strains of different PFGE types

were selected for further characterization. S1-PFGE and Southern hybridization analysis showed that each of these isolates carried multiple plasmids, among which some were found to harbor more than one *mcr-1*-bearing plasmid. The size of plasmids observed in these isolates ranged from ~33kb - ~280kb, with three major categories being observable: ~33kb, ~60kb and ~216-280kb. Most of the strains were found to harbor one ~33kb or 60kb plasmid, with some, such as strains FJ-B42 and JS-B65, carrying both. Some strains such as JS-B60, JS-64, JS-B73 and JS-59 were also found to carry additional plasmids of 216~280kb in size (**Table 7.3**).

Table 7. 2 Antibiotic susceptibility profiles of 15 *E. coli* strains which harbor the *mcr-1* gene

Strain ID	CLS[a]	AMK	CTX	CIP	KAN	OLA	STR	CRO	TET	CHL	NAL	AMP	MRP	SXT
GD-8	8	＞128	16	1	＞128	16	8	＞16	＞32	4	32	＞64	0.015	＞32
HN-15	4	2	16	8	8	16	32	＞16	16	2	＞64	＞64	0.015	＞32
FJ-44	4	4	8	＞16	32	＞256	128	＞16	＞32	＞64	＞64	＞64	0.015	＞32
JS-56	8	4	>16	>16	64	>256	32	>16	32	>64	>64	>64	0.03	8
JS-59	8	2	16	2	>128	128	8	16	32	＞64	32	>64	0.03	16
JS-61	8	2	>16	>16	2	>256	128	>16	>32	＞64	>64	>64	0.03	2
JS-63	4	2	16	>16	>128	256	>128	16	>32	＞64	>64	>64	0.0075	16
SD-112	8	2	>16	＞16	＞128	256	＞128	>16	32	＞64	>64	＞64	0.03	＞32
SD-137	4	8	>16	>16	64	128	>128	>16	16	>64	>64	>64	0.015	32
FJ-B42	8	0.5	0.25	0.03	＞128	＞256	2	8	32	4	＞64	＞64	≤0.075	＞32
FJ-B44	4	4	8	＞16	32	＞256	128	16	＞32	＞64	＞64	＞64	0.015	＞32
JS-B60	8	2	8	>16	>128	256	32	8	16	>64	>64	>64	0.03	8
JS-B65	8	4	16	>16	64	256	64	>16	32	>64	>64	>64	0.03	8
JS-64	8	2	>16	16	2	128	32	>16	>32	＞64	>64	>64	0.03	0.5
JS-B73	4	2	16	>16	>128	128	4	>16	32	32	32	>64	0.015	16

[a] CLS, colistin; AMK, amikacin; CTX, ceftazidime; CIP, ciprofloxacin; KAN, kanamycin; OLA, olaquindox; STR, streptomycin; CRO, ceftriaxone; TET, tetracycline; CHL, chloramphenicol; NAL, nalidixic acid; AMP, ampicillin; MRP, meropenem; SXT, Trimethoprim-sulfamethoxazole.

Table 7. 3 The sizes and profiles of *mcr-1*-bearing plasmids harbored by 15 ESBL-producing *E. coli* strains

Strains ID	*mcr-1* plasmids [a] (kb)	Other plasmids [a] (kb)	Plasmids with complete sequence [b]	Plasmids with scaffolds [b]	*mcr-1* locus [c]	Circular form
GD-8	33	104；90；60	pECGD-8-33(IncX4)	-	*mcr-1-orf*	-
HN-15	60	120；90；78	pECHN-15-61(IncI2)	-	IS*Apl1*-*mcr-1-orf*	-
FJ-44	250, 33	560；78；60	pECFJ-44-33(IncX4)	pECFJ-44-250	*mcr-1-orf*	-
JS-56	60	33	pECJS-56-62(IncI2)	-	*mcr-1-orf*	-
JS-59	244	90	pECJS-59-244(IncHI2)	-	Tn*6330*	+
JS-61	230, 60	104；	pECJS-61-63(IncI2)	pECJS-61-230	*mcr-1-orf* Tn*6330*	+
JS-63	230, 60	104；33	pECJS-63-63(IncI2)	pECJS-63-230	*mcr-1-orf*	-
SD-112	33	104；78	pECSD-112-33(IncX4)	-	*mcr-1-orf*	-
SD-137	60	138；104；33	pECSD-137-60(IncI2)	-	*mcr-1-orf*	-
FJ-B42	60, 33	138；104	pECFJ-B42-33(IncX4) pECFJ-B42-63(IncI2)	-	*mcr-1-orf*, IS*Apl1*-*mcr-1-orf*	-
FJ-B44	33	480；270；78；60	pECFJ-B44-33(IncX4)	-	*mcr-1-orf*	-
JS-B60	250	560	pECJS-B60-267(IncHI2)	-	IS*Apl1*-*mcr-1-orf*	-
JS-B65	60, 33	90；40	pECJS-B65-33(IncX4) pECJS-B65-60(IncI2)	-	*mcr-1-orf* *mcr-1-orf*	-
JS-64	280	560；104；60	-	pECJS-64-280	Tn*6330*	+
JS-B73	230	100	-	pECJS-B73-230	Tn*6330*	+

[a] The size of the plasmids was determined according to the S1-PFGE results;
[b] Plasmids for which complete sequences have been obtained. Complete sequences were not available in five IncHI2 *mcr-1*-bearing plasmids, for which only the assembly scaffolds were generated. The replicon types of samples were confirmed by PCR using specific primers listed in **Table 1**.
[c] The *mcr-1* locus for pECFJ-44-250 and pECJS-63-230 was unavailable.

7.4.2 Genetic characterization of plasmids harboring the *mcr-1* gene

Plasmids extracted from the 15 *mcr-1*-positive strains were subjected to nucleotide sequencing using the Illumina platform. Raw reads were subjected to *de novo* assembly to obtain contigs for each sample. BLASTN analysis against the resistance genes database using the Illumina contigs showed that plasmids from these 15 strains comprised multiple drug resistance determinants (**Table 7.4**); such finding was consistent with the multidrug-resistant phenotypes observable among the test strains (**Table 7.2**). In addition to *mcr-1*, plasmids derived from most of the strains were found to harbor multiple resistance elements including but not limited to $bla_{\text{CTX-M}}$, bla_{CMY}, bla_{TEM}, *fosA*, *qnrS*, *floR*, and *oqxAB*. However, it should be noted that there is still a slight possibility that some of the resistance genes (**Table 7.4**) were not plasmid-borne, and were presumably located in the chromosome since the plasmid DNA used for high-throughput sequencing could be contaminated by chromosomal DNA, a phenomenon confirmed by other sequencing projects in our laboratory.

Table 7. 4 Distribution of resistance genes among the 15 *mcr-1*-harboring strains by sequence homology

Resistance genes[a]	SD-112	SD-137	HN-15	FJ-44	JS-56	JS-59	JS-61	JS-63	JS-64	GD-8	FJ-B42	FJ-B44	JS-B60	JS-B65	JS-B73
ARR-3_4_FM207631	0	0	0	0	99.34	0	0	0	0	0	0	0	99.18	0	0
QnrD_1_FJ228229	0	0	0	0	0	0	0	0	100	0	0	0	0	0	100
QnrS1_1_AB187515	0	0	0	100	0	100	0	0	0	0	0	100	0	0	0
QnrS2_1_JF261185	0	0	0	0	0	0	0	0	0	0	0	0	100	0	0
aac(3)-IIa_1_X51534	0	0	0	0	0	0	0	0	0	0	99.77	0	0	0	0
aac(3)-IId_1_EU022314	99.88	99.88	99.88	99.74	0	100	0	99.88	0	99.88	0	0	0	0	100
aac(3)-IVa_1_X01385	0	0	0	0	99.75	0	0	99.75	0	0	0	0	0	99.75	0
aac(6)-Ib_1_M21682	0	99.83	0	99.83	0	0	0	0	0	0	99.66	99.83	0	99.83	0
aac(6)Ib-cr_1_DQ303918	0	0	0	0	100	0	0	0	0	0	0	0	100	0	0
aadA1_1_X02340	99.75	0	0	99.75	99.75	99.75	0	89.62	0	0	89.5	99.75	0	0	0
aadA1_3_JQ414041	0	0	0	0	0	0	0	0	0	0	0	0	0	100	0
aadA2_2_JQ364967	0	98.71	0	0	0	0	99.87	0	0	100	0	0	99.87	99.75	0
aadA5_1_AF137361	0	0	100	100	0	0	0	0	0	0	0	100	0	0	0
aph(3)-Ia_1_V00359	99.6	0	0	0	0	100	0	100	0	100	100	0	99.26	0	100
aph(4)-Ia_1_V01499	0	0	0	0	100	0	0	100	0	0	0	0	0	100	0
blaCMY-2_1_X91840	0	0	0	100	0	0	0	0	0	0	100	100	0	0	0
blaCTX-M-14_1_AF252622	100	100	0	0	0	0	0	100	0	0	0	99.2	100	100	0
blaCTX-M-15_23_DQ302097	0	0	100	0	0	0	0	0	0	0	0	0	0	0	0
blaCTX-M-55_2_GQ456159	0	0	0	0	100	0	0	0	0	100	0	0	0	0	99.89
blaCTX-M-65_2_GQ456158	0	0	0	0	0	100	100	0	100	0	0	0	0	0	100
blaCTX-M-79_1_GU125666	0	0	0	0	0	99.62	0	0	0	0	0	0	0	0	0
blaOXA-1_1_J02967	0	0	0	0	0	0	0	0	0	0	0	0	100	0	0

blaTEM-1A_4_HM749966	0	0	0	0	0	0	99.88	0	0	0	0	0	0	0	0
blaTEM-1B_1_JF910132	100	0	0	0	0	100	0	99.88	0	98.6	0	0	100	100	99.77
blaTEM-206_1_KC783461	0	0	99.87	0	99.87	0	0	0	0	0	0	0	0	0	0
blaTEM-209_1_KF240808	0	0	0	100	0	0	0	0	0	0	0	100	0	0	0
catB3_1_AJ009818	0	0	0	0	98.78	0	0	0	0	0	0	0	99.84	0	0
cmlA1_1_M64556	0	0	0	99.92	99.92	99.92	0	99.84	0	99.92	99.92	99.92	0	0	0
cmlA1_2_AB212941	0	99.92	0	0	0	0	0	0	0	0	0	0	0	99.92	0
dfrA12_1_AB571791	0	0	0	0	0	100	0	100	0	100	0	0	100	0	100
dfrA17_1_FJ460238	0	0	100	100	0	0	0	0	0	0	0	100	0	0	0
dfrA1_30_JQ690541	100	0	0	0	0	0	0	0	0	0	0	0	0	0	0
erm(B)_18_X66468	98.95	98.95	0	0	0	0	0	0	0	0	0	0	0	98.95	0
floR_2_AF118107	98.02	98.19	0	98.27	0	98.19	98.19	98.19	98.19	98.11	98.11	98.11	98.19	98.19	98.19
fosA_14_AB522970	0	0	0	0	100	100	100	100	100	100	0	0	100	0	100
lnu(F)_1_EU118119	0	0	0	0	0	0	100	100	100	100	0	0	0	0	0
mcr-1_1_KP347127	100	100	100	100	100	100	100	100	100	100	100	100	100	100	100
mef(B)_1_FJ196385	0	0	0	99.84	0	0	0	100	0	0	0	99.84	0	0	0
mph(A)_1_D16251	0	0	0	0	0	0	0	0	0	0	100	0	0	0	0
mph(A)_2_U36578	99.67	99.67	99.67	0	99.67	0	0	0	0	0	0	99.67	99.67	99.67	99.67
oqxA_1_EU370913	100	99.83	0	99.83	100	100	100	100	0	100	100	99.83	99.91	100	100
oqxB_1_EU370913	99.92	0	0	99.92	100	100	100	100	0	100	0	99.92	99.92	100	100
strA_1_M96392	0	0	0	0	0	0	0	0	0	0	0	0	100	0	0
strA_4_AF321551	100	100	100	100	0	0	100	0	0	0	100	100	0	0	0
strB_1_M96392	100	0	99.88	100	0	0	100	0	0	0	100	97.61	99.88	99.88	0
sul1_2_CP002151	100	0	100	0	100	100	100	0	100	0	0	0	0	0	100
sul2_2_GQ421466	0	99.88	100	100	100	0	99.87	100	0	100	100	100	0	100	0
sul2_6_FN995456	100	0	0	0	0	0	0	0	0	0	0	0	0	0	0
sul3_2_AJ459418	0	0	0	100	0	100	0	100	0	100	100	100	100	0	100

tet(A)_4_AJ517790	100	99.91	100	100	99.92	100	99.92	99.92	99.92	0	99.91	100	99.92	100	100
tet(M)_8_X04388	0	0	0	96.15	0	0	0	0	0	96.15	0	96.15	96.15	0	0

[a] The numbers indicates the percentage of sequence homology between the resistance genes and the contigs of different strains. The number of resistance genes in the strains ranges from 8 (JS-64) to 21(FJ-B44); all test strains were found to harbor at least one bla_{CTX-M} or one bla_{CMY} gene, both of which confer resistance to third-generation cephalosporins. It should be noted that some of these resistance genes may not plasmid-borne since the plasmid DNA used for high-throughput sequencing was slightly contaminated by chromosomal DNA, a phenomenon confirmed by other sequencing projects in our laboratory.

Table 7. 5 Information of 24 IncHI2 type plasmids including four *mcr-1*-bearing and twenty *mcr-1* negative plasmids showing homologous plasmid backbone structure (more than 70% coverage and 98% identity compared with pECJS-B60-267).

Plasmid ID[a]	Accession Number[a]	Isolation Source	Plasmid Size (bp)	Isolation year	Submission Date[b]	Species	Region
pENT-8a4	CP008899	tracheal aspirate	255013	2011	-	*Enterobacter cloacae*	USA
p34977-263	CP012170	Bodily fluid	263138	2009	-	*Enterobacter cloacae*	USA
pKPC-272	CP008825	sink drain	282439	-	2014	*Enterobacter cloacae*	USA
pMRVIM0813	KP975077	Surveillance swab	311662	-	2015	*Enterobacter cloacae*	USA
pEC-IMPQ	EU855788	clinical	318782	-	2008	*Enterobacter cloacae*	Taiwan
pSA26-MCR-1	KU743384	blood	240367	-	2016	*Escherichia coli*	Saudi Arabia
pAPEC-O1-R	DQ517526	turkey with colibacillosis	241387	-	2006	*Escherichia coli*	USA
pECJS-59-244	KX084394	pig feces	243572	2015	-	*Escherichia coli*	China

pHNSHP45-2	KU341381	pig feces	251493	-	2013	*Escherichia coli*	China
pSJ_255	CP011062	pheasant duodenum	255368	2011	-	*Escherichia coli*	China
pECJS-B60-267	KX254341	pig feces	267486	2015	-	*Escherichia coli*	China
pEC-IMP	EU855787	Unknown	272865	-	2008	*Escherichia coli*	China
pEC5207	KT347600	Unknown	272865	-	2015	*Escherichia coli*	China
pGD0503Z13	KR653209	chicken	351717	-	2015	*Escherichia coli*	China
pK26	EF382672	Unknown	269674	-	2007	*Klebsiella pneumoniae*	Taiwan
pH11	CP013215	patient's sputum	284628	2010	-	*Klebsiella pneumoniae*	China
pCAY1151-296	CP011601	Perirectal	295619	2009	-	*Kluyvera intermedia*	USA
pN13-01290	CP012931	turkey meat	236176	2012	-	*Salmonella Heidelberg*	Canada
pRH-R27	LN555650	pig farm	299305	-	2014	*Salmonella Infantis*	Germany
pHK0653	KT334335	stool	244851	2006	-	*Salmonella Typhimurium*	Hong Kong
pHXY0908	KM877269	chicken stool	249144	-	2014	*Salmonella Typhimurium*	China
incHI2	LN794248	blood	300375	-	2015	*Salmonella Typhimurium*	Kenya
pSTm-A54650	LK056646	Unknown	309406	-	2014	*Salmonella Typhimurium*	Sub-Saharan Africa
p1205p1	CP012141	Unknown	248368	-	2015	*Shigella flexneri*	China

[a] All the information was extracted from Genbank database. The plasmids with red labels indicate the four *mcr-1*-bearing IncHI2 type plasmids to date. The *mcr-1* structures among them are depicted in **Fig. 7.7**.
[b] The sequences submission date is shown when strains isolation year information is absent in GenBank records.

The complete plasmid sequences of ~33kb and ~60kb plasmids could be obtained by *in-silico* analysis of the Illumina sequencing data using the corresponding reference sequences (pHNSHP45 and pECJP-B65-33). The ~33kb plasmid, pECGD-8-33, obtained from sample GD-8, was shown to belong to the IncX4 type, comprising 55 CDSs with a size of 33, 307bp, and an overall GC content of 41.84% GC. The complete plasmid sequence of ~60kb plasmid, pECJS-61-63, obtained from sample JS-61, was shown to belong to the IncI2 type and comprise 88 CDSs, with a size of 63, 656bp and a GC content of 42.64%. The complete plasmid sequences of 216-280kb plasmids could not be generated from the Illumina sequencing data. Two representative plasmids, from samples JS-61 and JS-59 respectively were subjected to PacBio sequencing to obtain the complete sequence. The complete sequence of a 216-280kb category plasmid, namely pECJS-59-244 which was derived from sample JS-59, was obtained. It was shown that this plasmid belonged to the IncHI2 type, contained 321 CDSs, and had a size of 243, 572bp, of which the GC content was 46.10%. Another IncHI2 plasmid, pECJS-B60-267, which was obtained from sample JS-B60, was found to comprise a size of 267, 486bp. These two IncHI2 type plasmids were compared to the contigs of IncHI2 plasmids in other samples (**Fig. 7.2**). IncHI2 type plasmids have been reported as genetic elements mediating the transmission of MDR genes (**Table 7.5**). Results of comparative analysis showed that a wide range of resistance genes and genetic elements could be found in a mosaic

MDR region of IncHI2 type plasmids, including integrons, insertion sequences and various resistance gene cassettes. The *mcr-1*-bearing plasmids could be finished with completed sequences successfully by using references of similar type to assist contigs assembly for different samples, with the exception of IncHI2 type plasmids, which contained a large MDR region with numerous insertion sequences. As a result, complete sequences of six IncX4 type, seven IncI2 type and two IncHI2 type plasmids were obtained using this approach (**Table 7.3**).

Plasmids belonging to each of these three types obtained from this study, and genetically similar *mcr-1*-bearing plasmids reported previously, were subjected to comparative analysis. The ~33kb, IncX4 type plasmids harbored by *E. coli* strains isolated from different geological locations of China as well as other countries were found to be almost identical (**Fig. 7.3**). Apart from *mcr-1*, no other resistance genes were detectable; in addition, no IS*Apl1* elements were found to flank the *mcr-1* gene. A genetically homologous, yet *mcr-1* negative plasmid of this type, namely pSH146_32, was previously isolated from a *Salmonella* Heidelberg strain (JX258655), suggesting that the *mcr-1-orf* gene cassette was most likely introduced into this plasmid backbone to form a *mcr-1*-bearing plasmid of this type (**Fig. 7.3**).

The ~60kb, IncI2 type *mcr-1* plasmid was present in 7 out of the 15 samples. Compared to pHNSHP45, which was first reported to

encode the MCR-1 protein (9), an IS*683* region was found to be missing in all the seven IncI2 type plasmids isolated in this study (**Fig. 7.4**). Two of the plasmids were found to contain the same IS*Apl1-mcr-1* cassette as pHNSHP45, whereas another five plasmids lacked the IS*Apl1* gene. The 216-280kb, IncHI2 type plasmids, which harbored a large MDR region, was the most genetically diverse plasmid type (**Fig. 7.2, Fig. 7.7**). Unlike the IncX4 and IncI2 type plasmids, for which the structure and location of the *mcr-1* cassettes were consistent among members of each plasmid type, the insertion site of the *mcr-1* cassette in IncHI2 plasmids were variable and could be categorized into four types, which differed by the truncation status of *orf*, and the orientation and numbers of IS*Apl1* elements (**Fig. 7.5**). Alignment of *mcr-1*-bearing elements revealed the core structure of all known *mcr-1* cassettes, detectable in this and previous studies. Our data showed that the most conserved structure was that of *mcr-1-orf* (the *orf* encodes the putative PAP family transmembrane protein). However, three of the six structures were found to have lost this intact *orf* due to alteration of the last four nucleotides in this element (**Fig. 7.5**). Furthermore, a newly deposited *mcr-1*-bearing IncHI2 plasmid, named pSA26-MCR-1 (KU743384), which was recovered from a NDM-1-producing *E. coli* ST68 strain isolated from a blood sample in a Saudi Arabian patient, was found to harbor a new *mcr-1* genetic architecture in which the second copy of IS*Apl1* is inserted into the *orf* in a reverse manner, indicating that the putative PAP *orf* is not necessary for the evolution of *mcr-1* cassettes. In order to

investigate the prevalence of various resistance genes in IncHI2 plasmids recovered from different sources, another 20 non-*mcr-1* plasmids exhibiting homology to pECJS-B60-267 (coverage >70%, identity >98% by BLASTN in nr database) were extracted. The number of resistance genes in these 24 IncHI2 plasmids (including the four *mcr-1*-bearing plasmids) ranged from 2 to 17 and carbapenemase-encoding genes, such as $bla_{\text{IMP-8}}$, $bla_{\text{KPC-3}}$ and $bla_{\text{VIM-1}}$, were found in five plasmids. Since the insertion site of *mcr-1* in IncHI2 may vary, according to the four complete IncHI2 plasmids (**Fig. 7.7**), we hypothesize that these four plasmids acquired the *mcr-1* gene via different evolutionary routes.

7.4.3 Formation of a circular intermediate containing the *mcr-1* gene cassette

Reverse primers targeting the *mcr-1* gene were used to amplify the putative circular intermediate that harbored the *mcr-1* gene. PCR products with a size of ~2.5kb in length were amplified in four samples harboring the IncHI2 *mcr-1* plasmids (**Fig. 7.6b**). Sequence analysis showed that the circular intermediate was 3, 679bp in size, containing IS*Apl1*, *mcr-1* and one *orf* (**Fig. 7.6a**). After aligning to the pECJS-59-244 sequence, we found that this circular form was 100% homologous to position 173,391-177,069 (KX084394). Notably, the circular intermediate can only be generated when the *mcr-1-orf* was surrounded by IS*Apl1* direct repeats. The four plasmid samples from which the circular intermediate could be amplified were found to contain a *mcr-1* gene cassette flanked by

two intact IS*Apl1*elements. This new composite transposon containing two direct repeats of IS*Apl1* and the *mcr-1* gene, which can form a circular intermediate, was designated Tn*6330*.

7.4.4 Characterization of HYEC7

The *E. coli* strain HYEC7 was found to be resistant to a wide range of antimicrobial agents including ceftriaxone (16μg/mL) and colistin (8μg/mL), but remained susceptible to meropenem. S1-PFGE and hybridization indicated three plasmids existed in HYEC7, and the *mcr-1* gene was located in the smallest plasmid with ca. 90Kb in length (**Fig. 7.8**). Conjugation assay was performed on HYEC7, while colistin resistance phenotype could not be transferred to the recipient strain, even though many tries have been conducted. To characterize the genetic features of *mcr-1*-bearing plasmid and another two plasmids, the complete sequences of these three plasmids, pHYEC7-*mcr1*, pHYEC7-IncHI2 and pHYEC7-110, with sizes of 224,736 bp, 110, 226 bp and 97, 559bp, respectively, were obtained for further analysis.

The complete sequence of the *mcr-1*-bearing plasmid pHYEC7-*mcr1* was found to be 97, 559bp in length, exhibit a GC content of 47.46% and comprise 105 ORFs. BLASTn results showed that it was 98% identical to phage P1 (AF234172) at 72% coverage and P7 (AF503408) at 73% coverage. It exhibited high level homology to the phage-harboring MDR plasmid pKP12226 (KP453775) in

Klebsiella pneumoniae with 98% identity at 79% coverage, as well as the *bla*$_{SHV-2}$-bearing phage RCS47 (FO818745) in *Escherichia coli* with 98% identity at 72% coverage. Apart from the backbone region encoding phage-related proteins, the *mcr-1*-borne transposable element Tn*6330*, characterized by the structure IS*Apl1*-*mcr-1*-*orf*-IS*Apl1*, and a type I restriction-modification system, were also found to have been inserted into the genetically conserved region of the plasmid backbone (**Fig. 7.8**). The presence of Tn*6330* in IncHI2 plasmids and bacterial chromosomes has previously been described (281-283). In this work, we showed that Tn*6330* in this phage-like plasmid could be excised as a circular intermediate, which was detectable in the form of a ~2.5kb amplicon (**Fig. 7.8F**). Hence, two PCR products (ca. 5kb, 1.4kb) could be generated by the primers Tn-F and Tn-R, when genomic DNA of the *E. coli* strain was used as template (**Fig. 7.8C**). DNA sequencing of the two PCR products showed that the 5kb PCR product was the intact Tn*6330*, and that the 1.4kb PCR product consisted of only one copy of IS*Apl1*, which was presumably the plasmid fragment that remained upon excision of the circular intermediate containing *mcr-1*. These data indicate that transposition of Tn*6330* is reversible and dynamic, and that the circular form could readily be excised from the plasmid and regenerate into Tn*6330* by integrating with IS*Apl1* inversely, thereby facilitating its transposition into the backbone of other plasmids which contain the IS*Apl1* element (**Fig. 7.8**). A similar integration and excision mechanism has previously been demonstrated for the IS*30* transposase (284), which is homologous

to IS*Apl1*. Similarly, the recently reported *mcr-2* gene was found to be located in a composite transposon with the structure IS*1595-mcr-2-pap2*-IS*1595*, whose functional role was unknown at present (285). On the other hand, transfer of resistance genes via phage-related elements has previously been reported (105, 286, 287). The RepA protein of pHYEC7-*mcr1* is known to belong to the IncY incompatibility group and exist in P1 and P7 bacteriophages, both of which replicate in their hosts as independent low-copy-number, plasmid-like elements (286). The presence of *mcr-1* in P7-like phage also implies that *mcr-1* is transferable to other bacteria through transduction or insertion into chromosome via its recombination system. Considering that phages are widespread in natural *E. coli* isolates (286), the role of phages or phage-like plasmids in dissemination of *mcr-1* highlights a new concern.

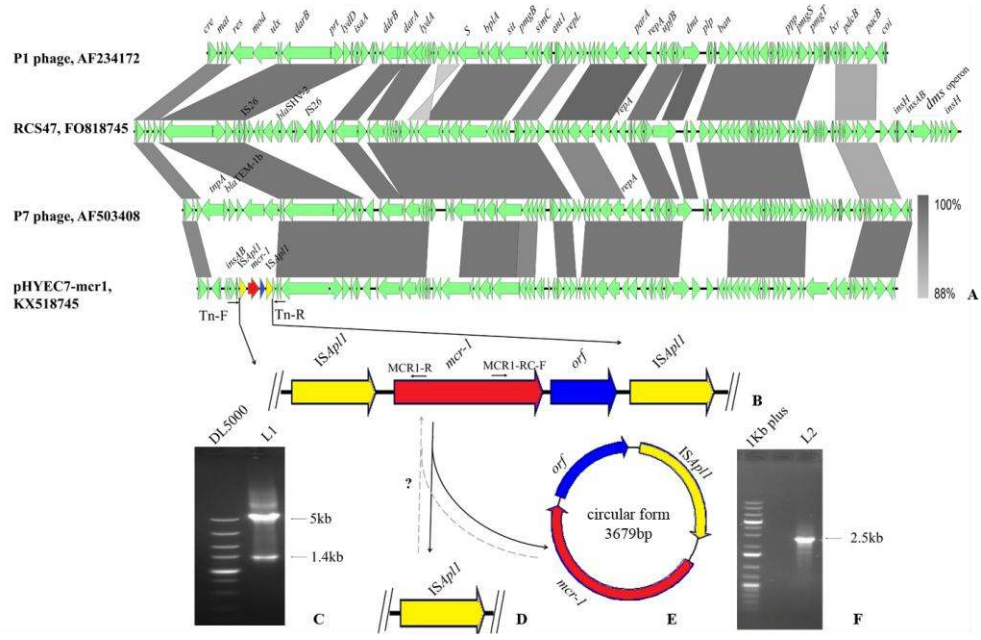

Figure 7. 8 Comparison between bacteriophages and P7-like plasmid pHYEC7-*mcr1*, and schematic of the excision of circular form from Tn*6330*

A, sequence comparison between the plasmid pHYEC7-*mcr1* (97, 559bp) and three structurally similar bacteriophages: P1 phage, bla_{SHV-2}-bearing P1-like RCS47 phages and bla_{TEM-1b}-bearing P7 phage. The legend indicates the degree of homology between different genetic loci; B, the structure of Tn*6330* harbored by pHYEC7-*mcr1*: primers MCR1-R and MCR1-RC-F were used to detect the circular form (E, L2 in F); C, the gel picture of PCR products generated by primers Tn-F and Tn-R targeting surrounding sequences of Tn*6330*; D, schematic representation of the structure of pHYEC7-*mcr1* after excision of the circular form; E, schematic representation of the circular form obtained by sequencing the 2.5kb PCR product; F, the gel pictureof PCR product generated by the primers, MCR1-R and MCR1-RC-F . Approximate locations of primers used are indicated by line arrows.

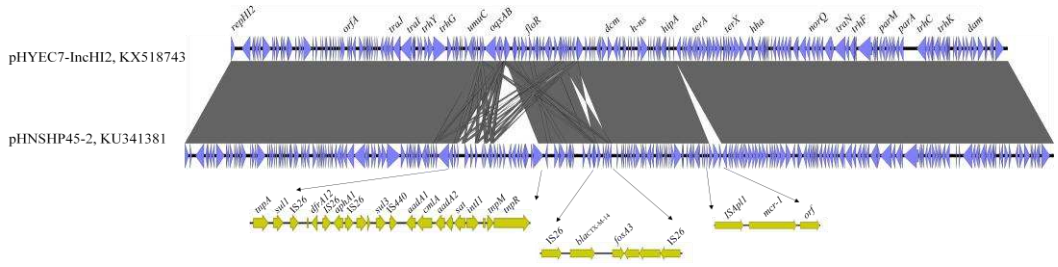

Figure 7. 9 Comparison between pHYEC7-IncHI2 and *mcr-1*-bearing pHNSHP45-2.

The genetic segments below the comparison plot denote the new elements found in pHNSHP45-2 (251, 493bp), the first IncHI2 type plasmid known to harbor *mcr-1*, implying that pHYEC7-IncHI2 (224,736bp) could be a prototype of pHNSHP45-2 which plays an active role in the evolution of IncHI2 plasmids.

Among the three plasmids, the size of the IncHI2 type plasmid pHYEC7-IncHI2 was the largest, with a length of 224,736bp and 266 predicted CDSs. The backbone of this plasmid was almost identical to other structurally similar IncHI2 plasmids, which harbor various antibiotic resistance genes including $bla_{CTX-M-14}$, *fosA3*,

oqxAB, *floR*, *sul2 and* gene cassettes distributed among mobile elements. Compared with the original *mcr-1*-bearing IncHI2 plasmid pHNSHP45-2 (288), three regions in which antibiotic resistance genes were observable were found to exhibit structural difference (**Fig. 7.9**). First, the IS*Apl1-mcr-1-orf* region located between *terF* and the hypothetical CDS was absent in pHYEC7-IncHI2, indicating that *mcr-1* could readily be inserted into this region in IncHI2 plasmids. Second, the fragment IS*26*-$bla_{\text{CTX-M-14}}$-ΔIS*903-fosA3*-IS*26* was reversely inserted in pHYEC7-IncHI2. Third, pHNSHP45-2 was known to harbor a large MDR region of ca. 50kb, whereas in pHYEC7-IncHI2, the complex class 1 integron (ca. 17K) located between IS*26-oqxAB*-IS*26* and *floR* was absent. Based on these findings, we hypothesize that the ESBL-encoding pHYEC7-IncHI2 plasmid could be the prototype of *mcr-1*-bearing IncHI2 plasmids. Because of the existence of *mcr-1*-bearing mobile elements in the HYEC7 strain, the IncHI2 type plasmid pHYEC7-IncHI2 may have the potential to capture *mcr-1* by site-specific recombination, thereby further facilitating the dissemination of *mcr-1* by horizontal gene transfer and creating *mcr-1*-positive IncHI2 plasmids which possess a structure similar to that of pHNSHP45-2. This recombination process enables the non-conjugative plasmid, pHYEC7-*mcr1*, to transfer its *mcr-1*-encoding mobile element to pHYEC7-IncHI2, forming a conjugative *mcr-1*-positive plasmid similar to pHNSHP45-2, which can in turn mediate the transmission of *mcr-1* among different bacterial species.

The third plasmid that the HYEC7 strain harbors, pHYEC7-110, was found to comprise the IncX1 and IncFIB replicons, the *mph* operon, *floR* gene, class 1 integron, *oqxAB* operon and some other resistance gene cassettes bounded by various insertion sequences. It was 110, 226bp in length, in which 143 CDSs were predicted. BLASTn analysis showed that pHYEC7-110 displayed the highest level of homology with the plasmid pSJ_255 found in *E. coli* (NZ_CP011062), with 99% identity at 51% coverage (**Fig. 7.10**), suggesting that the structure of the plasmid was novel. Resistance genes and insertion sequences accounted for more than half of the plasmid. Upon comparison with pHYEC7-IncHI2, it was found that several resistance regions including *oqxAB* and *floR* coexisted in both plasmids. In addition, the *sul3*-associated class 1 integron was found to be present and located between two IS*26* elements in pHYEC7-110, in which a class 1 integron similar to that found in pHNSHP45-2 also existed (**Fig. 7.9**). The recovery of multiple plasmids which harbored structurally similar mobile elements in one host strain implied that genetic exchange between such plasmids was common, and that such plasmids could readily be transferred to other organisms, constituting one major evolution and resistance development route of bacterial pathogens.

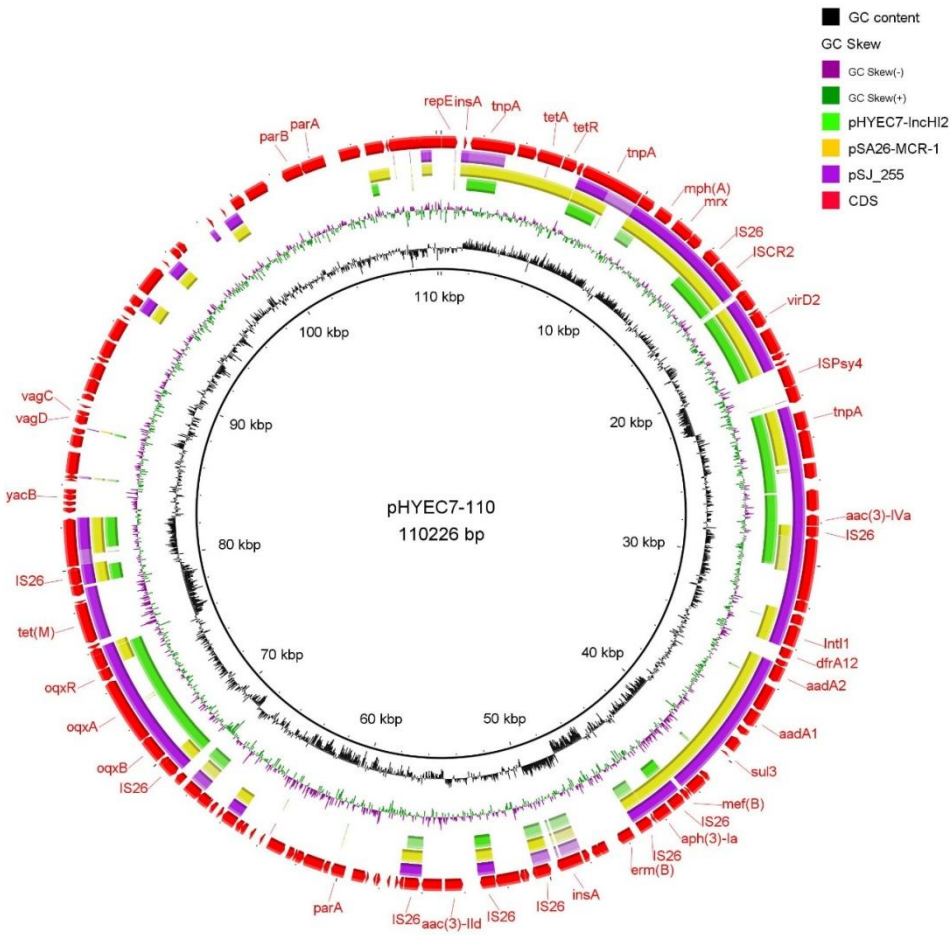

Figure 7. 10 A circular plot of comparison by BRIG depicting details of genetic similarities and differences between pHYEC7-110 and other structurally similar plasmids

The outer ring represents the CDSs of pHYEC7-110, which is used as the reference sequence when performing BLASTn. Three IncHI2 type plasmids exhibiting similarity to pHYEC7-110 were mapped to the reference sequence by BLASTn. The plasmid pSJ-25 (NZ_CP011062) was found in a MDR *E. coli* strain isolated from pheasant duodenum in Fujian Province, China. Another similar plasmid pSA26-MCR-1 (KU743384) was from clinical blood sample in Saudi Arabia.

7.5 DISCUSSION

Since the discovery of the *mcr-1* element in China in late 2015 (9), the mobile colistin resistance determinant has been reported among

different *Enterobacteriaceae* species isolated from various sources in different countries (269, 270, 289). However, there is lack of information regarding the genetic context of plasmids harboring this gene and the underlying transmission mechanisms. In this study, we surveyed the prevalence of the *mcr-1* gene in ESBLs-producing *E.coli* strains isolated from different geological locations in China and conducted comprehensive analysis of the plasmids that harbored the *mcr-1* gene in 15 representative strains. Three major types of plasmids, namely IncX4 (~33kb), IncI2 (~60kb) and IncHI2 (~216-280kb), were detectable, alone or in various combinations, in as few as 15 *E. coli* strains, suggesting that *mcr-1* can be captured by a wide range of mobile genetic elements circulating among bacterial strains of animal origin. Among such plasmids, we noted that the IncX4 type (~33kb) was genetically the least variable, whereas the IncHI2 type (~216-280kb) was the most divergent due to the fact that this type of plasmid contains a MDR region which comprises a variable combination of antibiotic resistance genes. Plasmids of similar backbone but lacking the *mcr-1* gene cassette, such as pHXY0908 and pHK0683, have previously been reported in *Salmonella* spp., suggesting that the formation of this IncH12 type of plasmid is most likely due to the acquisition of *mcr-1* gene cassette by vectors containing such backbone structure (288). In this work, four types of genetic cassettes harboring the *mcr-1* gene have been identified in the IncHI2 type plasmids, suggesting that the *mcr-1* gene may be actively inserted into different genetic loci of the plasmid during dynamic gene

transposition events that commonly occur in animal isolates. Although only four complete *mcr-1*-bearing IncHI2 plasmids are available, the different locations of *mcr-1* in these plasmids, and the prevalence of MDR IncHI2 plasmids in human pathogens, infer that IncHI2 is the most efficient vehicle for disseminating *mcr-1* and other resistance elements including the carbapenemase encoding genes. The clinical significance of this category of plasmid is therefore highlighted by its potential to confer, on a wide range pathogens, phenotypic resistance to carbapenems and colistin, both last-line antibiotics used to treat Gram-negative bacterial infections, Apart from the IncHI2 type of plasmid, the prototype plasmid pSH146_32, which belongs to the IncX4 type (~33kb), has also been found in *Salmonella* Heidelberg, thus further supporting the notion that acquisition of the *mcr-1* gene cassette by specific prototype plasmids plays an important role in the transmission of the colistin resistance element. On the other hand, although no prototype plasmid of IncI2 (~60kb) has been reported previously, two *mcr-1* gene cassettes of different genetic contents, observable in *S. enteric* and *E. coli* strains in England and Wales, could be found through bioinformatics analysis (272), suggesting that insertion of the *mcr-1* gene cassette into this type of plasmid is also a common event and has spread worldwide.

It is known that some members of the insertion sequence family including IS*3*, IS*30*, IS*110*, IS*26* and IS*CR1* utilize circular DNA intermediates that contain accessory genes to undergo gene

translocation, through copy-and-paste or cut-and-paste mechanisms (116, 227, 290, 291). IS*Apl1* is a type of insertion sequence surrounded by a pair of left and right inverted repeats (IRL and IRR), which was first identified in *Actinobacillus pleuropneumoniae*, with the ability to disrupt a range of genes in such species (275). The fact that the *mcr-1* gene is consistently associated with IS*Apl1* and that the *mcr-1* gene cassette may be inserted into different genetic loci in different plasmids, prompted us to hypothesize that *mcr-1* translocation could be mediated through a circular intermediate with the aid of IS*Apl1* (273, 292). In this study, we provided direct evidence that all *mcr-1* gene cassettes containing IS*Apl1-mcr-1-orf* -IS*Apl1*, designated as Tn*6330*, could form a circular intermediate which mediates the insertion of *mcr-1* gene cassette into the IncHI2 plasmid backbone, and possibly other plasmids. In the first study on IS*Apl1*, a circular form harboring only IS*Apl1* was detected without other accessory genes (275). This is in agreement with the fact that no circular form containing *mcr-1* can be detected when only one copy of *ISApl1* is located upstream of *mcr-1*, or in cases where no *ISApl1* exists. With the help of IS*Apl1*, the generation of circular intermediate undoubtedly renders *mcr-1* the ability to be translocated into different plasmid genetic sites. We also notice that the number of IS*Apl1* around *mcr-1* in the IncX4 (0), IncI2 (1 or 0) and IncHI2 (1 or 2) plasmids varies. Notably, another complete *mcr-1*-bearing IncHI2 plasmid, pSA26-MCR-1, was found to harbor three copies of IS*Apl1* (**Fig. 7.7**), two of which flanked *mcr-1* in the form of inverted repeats, constituting

another possible transposable element format. This observation, together with the fact that the degree of genetic similarity between IncX4 and IncI2 types of plasmids is high but IncHI2 type plasmids are genetically divergent, may suggest that Tn*6330* insertion in IncHI2 type is still highly active, yet the loss of IS*Apl1* in *mcr-1* gene cassette in IncX4 and IncI2 types of plasmids renders these plasmids more stable since the *mcr-1* gene cassette in these vectors is no longer transposable. Nevertheless, the molecular mechanisms underlying the formation of the circular intermediate of Tn*6330*, and how it evolves to become a genetically stable fragment in the residing plasmid entail further investigation.

7.6 Conclusion

In conclusion, this study characterized in detail the diverse genetic features of *mcr-1*-bearing plasmids in *E. coli* isolated from food animals, and revealed the presence of a novel transposon Tn*6330* comprising a *mcr-1* gene cassette IS*Apl1-mcr-1-orf*-IS*Apl1,* which may be regarded as the key element responsible for mediating the translocation of *mcr-1* gene cassette into various plasmid backbones through formation of a circular intermediate. Findings in this work therefore provide important insights into the transmission mechanisms of *mcr-1*, and lay the foundation for devising effective intervention approaches aimed at preserving the value of colistin as the last line antimicrobial agent.

Furthermore, the *mcr-1* gene was found in a P7-like plasmid pHYEC7-*mcr1* and shown to exist in the format of the transposon Tn*6330* (IS*Apl1-mcr-1-orf*-IS*Apl1*), which could generate a circular intermediate (IS*Apl1-mcr-1-orf*) by excision from the plasmid. Based on these findings, we propose that Tn*6330* is a key element responsible for transmission of *mcr-1*, the circular intermediate of which may eventually be integrated in various IS*Apl1*-bearing vectors. The finding that Tn*6330* is located in a phage-like plasmid infers that such transposable element may be further disseminated via transduction events. The exact functional mechanism of both the Tn*6330* element and phage-like plasmids in dissemination of the *mcr-1* gene needs to be further investigated.

Chapter Eight: Conclusion and Summary

In conclusion, works described in the first part of this thesis identified a novel class A β-lactamase, *bla*$_{\text{CARB-17}}$, which is responsible for the intrinsic resistance to penicillins in *V. parahaemolyticus*. The regulatory system of this gene, a two component system (TCS), was found conserved in species other than *V.parahaemolyticus*, indicating that such TCS may play a role in regulating the expression of other genes in non-*V.parahaemolyticus* species of the *Vibrios*. Furthermore, we showed that *bla*$_{\text{CARB-17}}$ was an ideal marker gene for molecular detection.

In part two, we found that various ESBLs genes increased in prevalence gradually among the foodborne pathogen *V.parahaemolyticus*. Transmission of ESBLs and AmpC β-lactamase genes via conjugative plasmids (IncA/C, IncQ and novel Inc types plasmids) can mediate the development of extended-spectrum cephalosporins resistance in *V. parahaemolyticus*, thereby posing a potential threat to public health.

Finally, through comparative sequence analysis of *mcr-1*-bearing plasmids, we demonstrated that the colistin resistance determinant was often closely associated with a transposable element which can be actively integrated into various conjugative plasmids. Importantly, a novel transposon Tn*6330*, which contained two

IS*Apl1* elements and could form a circular intermediate by excision, was identified as the key genetic structure that actively mediated the insertion and translocation of the *mcr-1* gene cassette into various plasmid backbones. These findings confirm that *mcr-1* can be disseminated via multiple mobile elements, inferring that such colistin resistance determinant can be readily co-transmitted among a wide range of potential human pathogens, along with other mobile resistance elements.

All in all, according to findings described in this thesis, the threats imposed by antibiotic resistance become more severe via two routes: mobilization of common resistance genes from original bacterial host to new species, and emergence of new mobile resistance genes in clinical pathogens. To cope with the issues, further studies on the molecular evolution of resistance genes and its vehicles including plasmids or other mobile elements should be conducted to shed light on efforts to devise new measures to curb the global dissemination of antibiotic resistance-encoding genetic elements among bacterial pathogens.

References

1. Cohen ML. 2000. Changing patterns of infectious disease. Nature 406:762-767.
2. Ventola CL. 2015. The antibiotic resistance crisis: part 1: causes and threats. P T 40:277-283.
3. Rossolini GM, Arena F, Pecile P, Pollini S. 2014. Update on the antibiotic resistance crisis. Curr Opin Pharmacol 18:56-60.
4. Eurosurveillance editorial t. 2015. WHO member states adopt global action plan on antimicrobial resistance. Euro Surveill 20.
5. Farrar J, Davies S. 2016. Wellcome Trust: Report released on antibiotic resistance. Nature 537:167.
6. WHO. 2015. Global action plan on antimicrobial resistance. http://www.who.int/antimicrobial-resistance/global-action-plan/en/.
7. Walsh TR, Toleman MA. 2012. The emergence of pan-resistant Gram-negative pathogens merits a rapid global political response. J Antimicrob Chemother 67:1-3.
8. Hawkey PM. 2015. Multidrug-resistant Gram-negative bacteria: a product of globalization. J Hosp Infect 89:241-247.
9. Liu YY, Wang Y, Walsh TR, Yi LX, Zhang R, Spencer J, Doi Y, Tian G, Dong B, Huang X, Yu LF, Gu D, Ren H, Chen X, Lv L, He D, Zhou H, Liang Z, Liu JH, Shen J. 2015. Emergence of plasmid-mediated colistin resistance mechanism MCR-1 in animals and human beings in China: a microbiological and molecular biological study. Lancet Infect Dis 16:161-168.
10. Liakopoulos A, Mevius DJ, Olsen B, Bonnedahl J. 2016. The colistin resistance mcr-1 gene is going wild. J Antimicrob Chemother doi:10.1093/jac/dkw262.
11. Salter SJ. 2014. The food-borne identity. Nat Rev Microbiol 12:533.
12. McLinden T, Sargeant JM, Thomas MK, Papadopoulos A, Fazil A. 2014. Component costs of foodborne illness: a scoping review. BMC Public Health 14:509.
13. Scallan E, Hoekstra RM, Angulo FJ, Tauxe RV, Widdowson MA, Roy SL, Jones JL, Griffin PM. 2011. Foodborne Illness

Acquired in the United States-Major Pathogens. Emerg Infect Dis 17:7-15.

14. WHO. 2015. WHO's first ever global estimates of foodborne diseases find children under 5 account for almost one third of deaths. http://www.who.int/mediacentre/news/releases/2015/foodborne-disease-estimates/en/.
15. Liu X, Chen Y, Wang X, Ji R. 2004. [Foodborne disease outbreaks in China from 1992 to 2001 national foodborne disease surveillance system]. Wei Sheng Yan Jiu 33:725-727.
16. Centre for Health Protection. 2011. Scientific Committee on Enteric Infections and Foodborne Diseases Food poisoning associated with Vibrio parahaemolyticus in Hong Kong—current situation and recommendations. http://www.chp.gov.hk/files/pdf/Food_Poisoning_Associated_with_Vibrio_parahaemolyticus_in_Hong%20Kong_Current_Situation_and_Recommendations.pdf.
17. Doyle ME. 2015. Multidrug-Resistant Pathogens in the Food Supply. Foodborne Pathog Dis 12:261-279.
18. Elmahdi S, DaSilva LV, Parveen S. 2016. Antibiotic resistance of Vibrio parahaemolyticus and Vibrio vulnificus in various countries: A review. Food Microbiol 57:128-134.
19. Clatworthy AE, Pierson E, Hung DT. 2007. Targeting virulence: a new paradigm for antimicrobial therapy. Nat Chem Biol 3:541-548.
20. Caburlotto G, Gennari M, Ghidini V, Tafi M, Lleo MM. 2010. Serological and molecular characterization of Vibrio parahaemolyticus marine strains carrying pandemic genetic markers. ISME J 4:1071-1074.
21. Ottaviani D, Leoni F, Serra R, Serracca L, Decastelli L, Rocchegiani E, Masini L, Canonico C, Talevi G, Carraturo A. 2012. Nontoxigenic Vibrio parahaemolyticus Strains Causing Acute Gastroenteritis. J Clin Microbiol 50:4141-4143.
22. Coutard F, Crassous P, Droguet M, Gobin E, Colwell RR, Pommepuy M, Hervio-Heath D. 2007. Recovery in culture of viable but nonculturable Vibrio parahaemolyticus: regrowth or resuscitation? ISME J 1:111-120.
23. Su YC, Liu C. 2007. Vibrio parahaemolyticus: a concern of seafood safety. Food Microbiol 24:549-558.

24. Ritchie JM, Rui H, Zhou X, Iida T, Kodoma T, Ito S, Davis BM, Bronson RT, Waldor MK. 2012. Inflammation and disintegration of intestinal villi in an experimental model for Vibrio parahaemolyticus-induced diarrhea. PLoS Pathog 8:e1002593.
25. McCarter L, Silverman M. 1990. Surface-induced swarmer cell differentiation of Vibrio parahaemolyticus. Mol Microbiol 4:1057-1062.
26. Nair GB, Ramamurthy T, Bhattacharya SK, Dutta B, Takeda Y, Sack DA. 2007. Global dissemination of Vibrio parahaemolyticus serotype O3:K6 and its serovariants. Clin Microbiol Rev 20:39-48.
27. Martinez-Urtaza J, Baker-Austin C, Jones JL, Newton AE, Gonzalez-Aviles GD, DePaola A. 2013. Spread of Pacific Northwest Vibrio parahaemolyticus strain. N Engl J Med 369:1573-1574.
28. Cost Estimates of Foodborne Illnesses. http://www.ers.usda.gov/data-products/cost-estimates-of-foodborne-illnesses.aspx.
29. Liu M, Chen S. 2013. Draft Genome Sequence of Vibrio parahaemolyticus V110, Isolated from Shrimp in Hong Kong. Genome Announc 1(3).
30. Jones JL, Ludeke CH, Bowers JC, DeRosia-Banick K, Carey DH, Hastback W. 2014. Abundance of Vibrio cholerae, V. vulnificus, and V. parahaemolyticus in oysters (Crassostrea virginica) and clams (Mercenaria mercenaria) from Long Island sound. Appl Environ Microbiol 80:7667-7672.
31. Baker-Austin C, Stockley L, Rangdale R, Martinez-Urtaza J. 2010. Environmental occurrence and clinical impact of Vibrio vulnificus and Vibrio parahaemolyticus: a European perspective. Environ Microbiol Rep 2:7-18.
32. Okada N, Iida T, Park KS, Goto N, Yasunaga T, Hiyoshi H, Matsuda S, Kodama T, Honda T. 2009. Identification and characterization of a novel type III secretion system in trh-positive Vibrio parahaemolyticus strain TH3996 reveal genetic lineage and diversity of pathogenic machinery beyond the species level. Infect Immun 77:904-913.
33. Saito S, Iwade Y, Tokuoka E, Nishio T, Otomo Y, Araki E, Konuma H, Nakagawa H, Tanaka H, Sugiyama K, Hasegawa A, Sugita-Konishi Y, Hara-Kudo Y. 2015. Epidemiological

evidence of lesser role of thermostable direct hemolysin (TDH)-related hemolysin (TRH) than TDH on Vibrio parahaemolyticus pathogenicity. Foodborne Pathog Dis 12:131-138.

34. Mizunoe Y, Wai SN, Ishikawa T, Takade A, Yoshida S. 2000. Resuscitation of viable but nonculturable cells of Vibrio parahaemolyticus induced at low temperature under starvation. FEMS Microbiol Lett 186:115-120.
35. Duan JY, Su YC. 2005. Occurrence of Vibrio parahaemolyticus in two oregon oyster-growing bays. J Food Sci 70:M58-M63.
36. Zhao F, Zhou DQ, Cao HH, Ma LP, Jiang YH. 2011. Distribution, serological and molecular characterization of Vibrio parahaemolyticus from shellfish in the eastern coast of China. Food Control 22:1095-1100.
37. Li Y, Xie X, Shi X, Lin Y, Qiu Y, Mou J, Chen Q, Lu Y, Zhou L, Jiang M, Sun H, Ma H, Cheng J, Hu Q. 2014. Vibrio parahaemolyticus, Southern Coastal Region of China, 2007-2012. Emerg Infect Dis 20:685-688.
38. Ma C, Deng X, Ke C, He D, Liang Z, Li W, Ke B, Li B, Zhang Y, Ng L, Cui Z. 2014. Epidemiology and etiology characteristics of foodborne outbreaks caused by Vibrio parahaemolyticus during 2008-2010 in Guangdong province, China. Foodborne Pathog Dis 11:21-29.
39. Holmes AH, Moore LS, Sundsfjord A, Steinbakk M, Regmi S, Karkey A, Guerin PJ, Piddock LJ. 2016. Understanding the mechanisms and drivers of antimicrobial resistance. Lancet 387:176-187.
40. Blair JM, Webber MA, Baylay AJ, Ogbolu DO, Piddock LJ. 2015. Molecular mechanisms of antibiotic resistance. Nat Rev Microbiol 13:42-51.
41. Gerardin Y, Springer M, Kishony R. 2016. A competitive trade-off limits the selective advantage of increased antibiotic production. Nat Microbiol 1:16175.
42. Cox G, Wright GD. 2013. Intrinsic antibiotic resistance: mechanisms, origins, challenges and solutions. Int J Med Microbiol 303:287-292.
43. van Hoek AH, Mevius D, Guerra B, Mullany P, Roberts AP, Aarts HJ. 2011. Acquired antibiotic resistance genes: an overview. Front Microbiol 2:203.

44. Zgurskaya HI, Lopez CA, Gnanakaran S. 2015. Permeability Barrier of Gram-Negative Cell Envelopes and Approaches To Bypass It. ACS Infect Dis 1:512-522.
45. Tamber S, Hancock RE. 2003. On the mechanism of solute uptake in Pseudomonas. Front Biosci 8:s472-483.
46. Piddock LJ. 2006. Clinically relevant chromosomally encoded multidrug resistance efflux pumps in bacteria. Clin Microbiol Rev 19:382-402.
47. Piddock LJ. 2006. Multidrug-resistance efflux pumps - not just for resistance. Nat Rev Microbiol 4:629-636.
48. Sun J, Deng Z, Yan A. 2014. Bacterial multidrug efflux pumps: mechanisms, physiology and pharmacological exploitations. Biochem Biophys Res Commun 453:254-267.
49. Randall CP, Mariner KR, Chopra I, O'Neill AJ. 2013. The Target of Daptomycin Is Absent from Escherichia coli and Other Gram-Negative Pathogens. Antimicrob Agents Chemother 57:637-639.
50. Poirel L, Nordmann P. 2006. Carbapenem resistance in Acinetobacter baumannii: mechanisms and epidemiology. Clin Microbiol Infect 12:826-836.
51. Olivares J, Bernardini A, Garcia-Leon G, Corona F, M BS, Martinez JL. 2013. The intrinsic resistome of bacterial pathogens. Front Microbiol 4:103.
52. Kong KF, Schneper L, Mathee K. 2010. Beta-lactam antibiotics: from antibiosis to resistance and bacteriology. APMIS 118:1-36.
53. Bush K, Bradford PA. 2016. beta-Lactams and beta-Lactamase Inhibitors: An Overview. Cold Spring Harb Perspect Med 6.
54. Rice LB. 2012. Mechanisms of resistance and clinical relevance of resistance to beta-lactams, glycopeptides, and fluoroquinolones. Mayo Clin Proc 87:198-208.
55. Bush K, Jacoby GA. 2010. Updated functional classification of beta-lactamases. Antimicrob Agents Chemother 54:969-976.
56. Jacoby GA. 2009. AmpC beta-lactamases. Clin Microbiol Rev 22:161-182.
57. Marsik FJ, Nambiar S. 2011. Review of carbapenemases and AmpC-beta lactamases. Pediatr Infect Dis J 30:1094-1095.

58. Ghafourian S, Sadeghifard N, Soheili S, Sekawi Z. 2015. Extended Spectrum Beta-lactamases: Definition, Classification and Epidemiology. Curr Issues Mol Biol 17:11-21.
59. Bush K. 2013. The ABCD's of beta-lactamase nomenclature. J Infect Chemother 19:549-559.
60. Schwarz S, Kehrenberg C, Doublet B, Cloeckaert A. 2004. Molecular basis of bacterial resistance to chloramphenicol and florfenicol. FEMS Microbiol Rev 28:519-542.
61. Shen J, Wang Y, Schwarz S. 2013. Presence and dissemination of the multiresistance gene cfr in Gram-positive and Gram-negative bacteria. J Antimicrob Chemother 68:1697-1706.
62. Fabrega A, Madurga S, Giralt E, Vila J. 2009. Mechanism of action of and resistance to quinolones. Microb Biotechnol 2:40-61.
63. Ruiz J, Pons MJ, Gomes C. 2012. Transferable mechanisms of quinolone resistance. Int J Antimicrob Agents 40:196-203.
64. Yamane K, Wachino J, Suzuki S, Kimura K, Shibata N, Kato H, Shibayama K, Konda T, Arakawa Y. 2007. New plasmid-mediated fluoroquinolone efflux pump, QepA, found in an Escherichia coli clinical isolate. Antimicrob Agents Chemother 51:3354-3360.
65. Ho PL, Ng KY, Lo WU, Law PY, Lai ELY, Wang Y, Chow KH. 2016. Plasmid-Mediated OqxAB Is an Important Mechanism for Nitrofurantoin Resistance in Escherichia coli. Antimicrob Agents Chemother 60:537-543.
66. Hansen LH, Jensen LB, Sorensen HI, Sorensen SJ. 2007. Substrate specificity of the OqxAB multidrug resistance pump in Escherichia coli and selected enteric bacteria. J Antimicrob Chemother 60:145-147.
67. Rodriguez-Martinez JM, Cano ME, Velasco C, Martinez-Martinez L, Pascual A. 2011. Plasmid-mediated quinolone resistance: an update. J Infect Chemother 17:149-182.
68. Warburton PJ, Ciric L, Lerner A, Seville LA, Roberts AP, Mullany P, Allan E. 2013. TetAB46, a predicted heterodimeric ABC transporter conferring tetracycline resistance in Streptococcus australis isolated from the oral cavity. J Antimicrob Chemother 68:17-22.

69. You Y, Hilpert M, Ward MJ. 2013. Identification of Tet45, a tetracycline efflux pump, from a poultry-litter-exposed soil isolate and persistence of tet(45) in the soil. J Antimicrob Chemother 68:1962-1969.
70. Roberts MC. 2005. Update on acquired tetracycline resistance genes. FEMS Microbiol Lett 245:195-203.
71. Garneau-Tsodikova S, Labby KJ. 2016. Mechanisms of Resistance to Aminoglycoside Antibiotics: Overview and Perspectives. Medchemcomm 7:11-27.
72. Yang J, Ye L, Wang W, Luo Y, Zhang Y, Han L. 2011. Diverse prevalence of 16S rRNA methylase genes armA and rmtB amongst clinical multidrug-resistant Escherichia coli and Klebsiella pneumoniae isolates. Int J Antimicrob Agents 38:348-351.
73. Rahman M, Prasad KN, Pathak A, Pati BK, Singh A, Ovejero CM, Ahmad S, Gonzalez-Zorn B. 2015. RmtC and RmtF 16S rRNA Methyltransferase in NDM-1-Producing Pseudomonas aeruginosa. Emerg Infect Dis 21:2059-2062.
74. Bueno MF, Francisco GR, O'Hara JA, de Oliveira Garcia D, Doi Y. 2013. Coproduction of 16S rRNA methyltransferase RmtD or RmtG with KPC-2 and CTX-M group extended-spectrum beta-lactamases in Klebsiella pneumoniae. Antimicrob Agents Chemother 57:2397-2400.
75. Ramirez MS, Tolmasky ME. 2010. Aminoglycoside modifying enzymes. Drug Resist Updat 13:151-171.
76. Roberts MC. 2008. Update on macrolide-lincosamide-streptogramin, ketolide, and oxazolidinone resistance genes. FEMS Microbiol Lett 282:147-159.
77. Weisblum B. 1995. Erythromycin resistance by ribosome modification. Antimicrob Agents Chemother 39:577-585.
78. Roberts MC. 2011. Environmental macrolide-lincosamide-streptogramin and tetracycline resistant bacteria. Front Microbiol 2:40.
79. Wang Y, Lv Y, Cai J, Schwarz S, Cui L, Hu Z, Zhang R, Li J, Zhao Q, He T, Wang D, Wang Z, Shen Y, Li Y, Fessler AT, Wu C, Yu H, Deng X, Xia X, Shen J. 2015. A novel gene, optrA, that confers transferable resistance to oxazolidinones and phenicols and its presence in Enterococcus faecalis and Enterococcus faecium of human and animal origin. J Antimicrob Chemother 70:2182-2190.

80. Perreten V, Boerlin P. 2003. A new sulfonamide resistance gene (sul3) in Escherichia coli is widespread in the pig population of Switzerland. Antimicrob Agents Chemother 47:1169-1172.
81. Skold O. 2001. Resistance to trimethoprim and sulfonamides. Vet Res 32:261-273.
82. Shin HW, Lim J, Kim S, Kim J, Kwon GC, Koo SH. 2015. Characterization of Trimethoprim-Sulfamethoxazole Resistance Genes and Their Relatedness to Class 1 Integron and Insertion Sequence Common Region in Gram-Negative Bacilli. J Microbiol Biotechnol 25:137-142.
83. Byrne-Bailey KG, Gaze WH, Kay P, Boxall ABA, Hawkey PM, Wellington EMH. 2009. Prevalence of Sulfonamide Resistance Genes in Bacterial Isolates from Manured Agricultural Soils and Pig Slurry in the United Kingdom. Antimicrob Agents Chemother 53:696-702.
84. Levings RS, Lightfoot D, Elbourne LD, Djordjevic SP, Hall RM. 2006. New integron-associated gene cassette encoding a trimethoprim-resistant DfrB-type dihydrofolate reductase. Antimicrob Agents Chemother 50:2863-2865.
85. Nurjadi D, Olalekan AO, Layer F, Shittu AO, Alabi A, Ghebremedhin B, Schaumburg F, Hofmann-Eifler J, Van Genderen PJ, Caumes E, Fleck R, Mockenhaupt FP, Herrmann M, Kern WV, Abdulla S, Grobusch MP, Kremsner PG, Wolz C, Zanger P. 2014. Emergence of trimethoprim resistance gene dfrG in Staphylococcus aureus causing human infection and colonization in sub-Saharan Africa and its import to Europe. J Antimicrob Chemother 69:2361-2368.
86. Liu M, Wong MH, Chen S. 2013. Molecular characterisation of a multidrug resistance conjugative plasmid from Vibrio parahaemolyticus. Int J Antimicrob Agents 42:575-579.
87. Han F, Walker RD, Janes ME, Prinyawiwatkul W, Ge B. 2007. Antimicrobial susceptibilities of Vibrio parahaemolyticus and Vibrio vulnificus isolates from Louisiana Gulf and retail raw oysters. Appl Environ Microbiol 73:7096-7098.
88. Melo LMR, Almeida D, Hofer E, Dos Reis CM, Theophilo GN, Santos AF, Vieira RH. 2011. Antibiotic resistance of Vibrio parahaemolyticus isolated from pond-reared

Litopenaeus vannamei marketed in natal, brazil. Braz J Microbiol 42:1463-1469.
89. Lagana P, Caruso G, Minutoli E, Zaccone R, Santi D. 2011. Susceptibility to antibiotics of Vibrio spp. and Photobacterium damsela ssp. piscicida strains isolated from Italian aquaculture farms. New Microbiol 34:53-63.
90. Jiang Y, Yao L, Li F, Tan Z, Zhai Y, Wang L. 2014. Characterization of antimicrobial resistance of Vibrio parahaemolyticus from cultured sea cucumbers (Apostichopus japonicas). Lett Appl Microbiol 59:147-154.
91. Wong MHY, Liu M, Wan HY, Chen S. 2012. Characterization of Extended-Spectrum-beta-Lactamase-Producing Vibrio parahaemolyticus. Antimicrob Agents Chemother 56:4026-4028.
92. Paterson DL, Bonomo RA. 2005. Extended-spectrum beta-lactamases: a clinical update. Clin Microbiol Rev 18:657-686.
93. Bradford PA. 2001. Extended-spectrum beta-lactamases in the 21st century: Characterization, epidemiology, and detection of this important resistance threat. Clin Microbiol Rev 14:933-951.
94. Bae IK, Jang SJ, Kim J, Jeong SH, Cho B, Lee K. 2011. Interspecies Dissemination of the bla Gene Encoding PER-1 Extended-Spectrum beta-Lactamase. Antimicrobial Agents and Chemotherapy 55:1305-1307.
95. Danel F, Hall IMC, Gur D, Akalin HE, Livermore DM. 1995. Transferable Production of Per-1 Beta-Lactamase in Pseudomonas-Aeruginosa. J Antimicrob Chemother 35:281-294.
96. Bonnin RA, Potron A, Poirel L, Lecuyer H, Neri R, Nordmann P. 2011. PER-7, an extended-spectrum beta-lactamase with increased activity toward broad-spectrum cephalosporins in Acinetobacter baumannii. Antimicrob Agents Chemother 55:2424-2427.
97. Celenza G, Pellegrini C, Caccamo M, Segatore B, Amicosante G, Perilli M. 2006. Spread of bla(CTX-M-type) and bla(PER-2) beta-lactamase genes in clinical isolates from Bolivian hospitals. J Antimicrob Chemother 57:975-978.
98. Ruggiero M, Kerff F, Herman R, Sapunaric F, Galleni M, Gutkind G, Charlier P, Sauvage E, Power P. 2014. Crystal Structure of the Extended-Spectrum beta-Lactamase PER-2

and Insights into the Role of Specific Residues in the Interaction with beta-Lactams and beta-Lactamase Inhibitors. Antimicrob Agents Chemother 58:5994-6002.

99. Zong ZY. 2014. The Complex Genetic Context of bla(PER-1) Flanked by Miniature Inverted-Repeat Transposable Elements in Acinetobacter johnsonii. Plos One 9.
100. Poirel L, Cabanne L, Vahaboglu H, Nordmann P. 2005. Genetic environment and expression of the extended-spectrum beta-lactamase bla(PER-1) gene in gram-negative bacteria. Antimicrobial Agents and Chemotherapy 49:1708-1713.
101. Sidjabat HE, Seah KY, Coleman L, Sartor A, Derrington P, Heney C, Faoagali J, Nimmo GR, Paterson DL. 2014. Expansive spread of IncI1 plasmids carrying blaCMY-2 amongst Escherichia coli. Int J Antimicrob Agents 44:203-208.
102. Verdet C, Gautier V, Chachaty E, Ronco E, Hidri N, Decre D, Arlet G. 2009. Genetic context of plasmid-carried blaCMY-2-like genes in Enterobacteriaceae. Antimicrob Agents Chemother 53:4002-4006.
103. Muniesa M, Colomer-Lluch M, Jofre J. 2013. Could bacteriophages transfer antibiotic resistance genes from environmental bacteria to human-body associated bacterial populations? Mob Genet Elements 3:e25847.
104. Muniesa M, Colomer-Lluch M, Jofre J. 2013. Potential impact of environmental bacteriophages in spreading antibiotic resistance genes. Future Microbiol 8:739-751.
105. Brown-Jaque M, Calero-Caceres W, Muniesa M. 2015. Transfer of antibiotic-resistance genes via phage-related mobile elements. Plasmid 79:1-7.
106. Johnston C, Martin B, Fichant G, Polard P, Claverys JP. 2014. Bacterial transformation: distribution, shared mechanisms and divergent control. Nat Rev Microbiol 12:181-196.
107. Overballe-Petersen S, Harms K, Orlando LA, Mayar JV, Rasmussen S, Dahl TW, Rosing MT, Poole AM, Sicheritz-Ponten T, Brunak S, Inselmann S, de Vries J, Wackernagel W, Pybus OG, Nielsen R, Johnsen PJ, Nielsen KM, Willerslev E. 2013. Bacterial natural transformation by highly fragmented and damaged DNA. Proc Natl Acad Sci U S A 110:19860-19865.

108. Domingues S, Harms K, Fricke WF, Johnsen PJ, da Silva GJ, Nielsen KM. 2012. Natural Transformation Facilitates Transfer of Transposons, Integrons and Gene Cassettes between Bacterial Species. PLoS Pathog 8.
109. Shintani M, Sanchez ZK, Kimbara K. 2015. Genomics of microbial plasmids: classification and identification based on replication and transfer systems and host taxonomy. Front Microbiol 6:242.
110. Garcillan-Barcia MP, Alvarado A, de la Cruz F. 2011. Identification of bacterial plasmids based on mobility and plasmid population biology. FEMS Microbiol Rev 35:936-956.
111. Smillie C, Garcillan-Barcia MP, Francia MV, Rocha EPC, de la Cruz F. 2010. Mobility of Plasmids. Microbiol Mol Biol Rev 74:434-452.
112. Svara F, Rankin DJ. 2011. The evolution of plasmid-carried antibiotic resistance. BMC Evol Biol 11:130.
113. Bennett PM. 2008. Plasmid encoded antibiotic resistance: acquisition and transfer of antibiotic resistance genes in bacteria. Br J Pharmacol 153 Suppl 1:S347-357.
114. Garcillan-Barcia MP, Francia MV, de la Cruz F. 2009. The diversity of conjugative relaxases and its application in plasmid classification. FEMS Microbiol Rev 33:657-687.
115. Siguier P, Gourbeyre E, Varani A, Ton-Hoang B, Chandler M. 2015. Everyman's Guide to Bacterial Insertion Sequences. Microbiol Spectr 3:MDNA3-0030-2014.
116. Siguier P, Gourbeyre E, Chandler M. 2014. Bacterial insertion sequences: their genomic impact and diversity. FEMS Microbiol Rev 38:865-891.
117. Kichenaradja P, Siguier P, Perochon J, Chandler M. 2010. ISbrowser: an extension of ISfinder for visualizing insertion sequences in prokaryotic genomes. Nucleic Acids Res 38:D62-68.
118. Roberts AP, Chandler M, Courvalin P, Guedon G, Mullany P, Pembroke T, Rood JI, Smith CJ, Summers AO, Tsuda M, Berg DE. 2008. Revised nomenclature for transposable genetic elements. Plasmid 60:167-173.
119. Gillings MR. 2014. Integrons: past, present, and future. Microbiol Mol Biol Rev 78:257-277.

120. Partridge SR, Tsafnat G, Coiera E, Iredell JR. 2009. Gene cassettes and cassette arrays in mobile resistance integrons. FEMS Microbiol Rev 33:757-784.
121. Moura A, Soares M, Pereira C, Leitao N, Henriques I, Correia A. 2009. INTEGRALL: a database and search engine for integrons, integrases and gene cassettes. Bioinformatics 25:1096-1098.
122. Mazel D. 2006. Integrons: agents of bacterial evolution. Nat Rev Microbiol 4:608-620.
123. Deng Y, Bao X, Ji L, Chen L, Liu J, Miao J, Chen D, Bian H, Li Y, Yu G. 2015. Resistance integrons: class 1, 2 and 3 integrons. Ann Clin Microbiol Antimicrob 14:45.
124. Wozniak RA, Waldor MK. 2010. Integrative and conjugative elements: mosaic mobile genetic elements enabling dynamic lateral gene flow. Nat Rev Microbiol 8:552-563.
125. Carraro N, Burrus V. 2014. Biology of Three ICE Families: SXT/R391, ICEBs1, and ICESt1/ICESt3. Microbiol Spectr 2.
126. Wozniak RAF, Fouts DE, Spagnoletti M, Colombo MM, Ceccarelli D, Garriss G, Dery C, Burrus V, Waldor MK. 2009. Comparative ICE Genomics: Insights into the Evolution of the SXT/R391 Family of ICEs. PLoS Genet 5.
127. Johnson CM, Grossman AD. 2015. Integrative and Conjugative Elements (ICEs): What They Do and How They Work. Annu Rev Genet 49:577-601.
128. Carraro N, Poulin D, Burrus V. 2015. Replication and Active Partition of Integrative and Conjugative Elements (ICEs) of the SXT/R391 Family: The Line between ICEs and Conjugative Plasmids Is Getting Thinner. PLoS Genet 11:e1005298.
129. Seth-Smith H, Croucher NJ. 2009. Genome watch: breaking the ICE. Nat Rev Microbiol 7:328-329.
130. Bellanger X, Payot S, Leblond-Bourget N, Guedon G. 2014. Conjugative and mobilizable genomic islands in bacteria: evolution and diversity. FEMS Microbiol Rev 38:720-760.
131. Juhas M, van der Meer JR, Gaillard M, Harding RM, Hood DW, Crook DW. 2009. Genomic islands: tools of bacterial horizontal gene transfer and evolution. FEMS Microbiol Rev 33:376-393.
132. Loman NJ, Pallen MJ. 2015. Twenty years of bacterial genome sequencing. Nat Rev Microbiol 13:787-794.

133. van Dijk EL, Auger H, Jaszczyszyn Y, Thermes C. 2014. Ten years of next-generation sequencing technology. Trends Genet 30:418-426.
134. Goodwin S, McPherson JD, McCombie WR. 2016. Coming of age: ten years of next-generation sequencing technologies. Nat Rev Genet 17:333-351.
135. Didelot X, Bowden R, Wilson DJ, Peto TE, Crook DW. 2012. Transforming clinical microbiology with bacterial genome sequencing. Nat Rev Genet 13:601-612.
136. Punina NV, Makridakis NM, Remnev MA, Topunov AF. 2015. Whole-genome sequencing targets drug-resistant bacterial infections. Hum Genomics 9:19.
137. Salipante SJ, SenGupta DJ, Cummings LA, Land TA, Hoogestraat DR, Cookson BT. 2015. Application of whole-genome sequencing for bacterial strain typing in molecular epidemiology. J Clin Microbiol 53:1072-1079.
138. Palmer AC, Kishony R. 2013. Understanding, predicting and manipulating the genotypic evolution of antibiotic resistance. Nat Rev Genet 14:243-248.
139. Piddock LJ. 2016. Assess drug-resistance phenotypes, not just genotypes. Nat Microbiol 1:16120.
140. Ashton PM, Nair S, Dallman T, Rubino S, Rabsch W, Mwaigwisya S, Wain J, O'Grady J. 2015. MinION nanopore sequencing identifies the position and structure of a bacterial antibiotic resistance island. Nat Biotechnol 33:296-300.
141. Conlan S, Thomas PJ, Deming C, Park M, Lau AF, Dekker JP, Snitkin ES, Clark TA, Luong K, Song Y, Tsai YC, Boitano M, Dayal J, Brooks SY, Schmidt B, Young AC, Thomas JW, Bouffard GG, Blakesley RW, Program NCS, Mullikin JC, Korlach J, Henderson DK, Frank KM, Palmore TN, Segre JA. 2014. Single-molecule sequencing to track plasmid diversity of hospital-associated carbapenemase-producing Enterobacteriaceae. Sci Transl Med 6:254ra126.
142. Scott L, McGee P, Walsh C, Fanning S, Sweeney T, Blanco J, Karczmarczyk M, Earley B, Leonard N, Sheridan JJ. 2009. Detection of numerous verotoxigenic E. coli serotypes, with multiple antibiotic resistance from cattle faeces and soil. Vet Microbiol 134:288-293.
143. Wong MH, Liu M, Wan HY, Chen S. 2012. Characterization of extended-spectrum-beta-lactamase-producing Vibrio

parahaemolyticus. Antimicrob Agents Chemother 56:4026-4028.
144. Li L, Wang Q, Zhang H, Yang M, Khan MI, Zhou X. 2016. Sensor histidine kinase is a beta-lactam receptor and induces resistance to beta-lactam antibiotics. Proc Natl Acad Sci U S A 113:1648-1653.
145. CLSI. 2013. Performance Standards for Antimicrobial Susceptibility Testing. CLSI document M100-S23. Clinical and Laboratory Standards Institute, Wayne, PA.
146. Moali C, Anne C, Lamotte-Brasseur J, Groslambert S, Devreese B, Van Beeumen J, Galleni M, Frere JM. 2003. Analysis of the importance of the metallo-beta-lactamase active site loop in substrate binding and catalysis. Chem Biol 10:319-329.
147. Nasu H, Iida T, Sugahara T, Yamaichi Y, Park KS, Yokoyama K, Makino K, Shinagawa H, Honda T. 2000. A filamentous phage associated with recent pandemic Vibrio parahaemolyticus O3:K6 strains. J Clin Microbiol 38:2156-2161.
148. Makino K, Oshima K, Kurokawa K, Yokoyama K, Uda T, Tagomori K, Iijima Y, Najima M, Nakano M, Yamashita A, Kubota Y, Kimura S, Yasunaga T, Honda T, Shinagawa H, Hattori M, Iida T. 2003. Genome sequence of Vibrio parahaemolyticus: a pathogenic mechanism distinct from that of V cholerae. Lancet 361:743-749.
149. Partridge SR, Brown HJ, Hall RM. 2002. Characterization and movement of the class 1 integron known as Tn2521 and Tn1405. Antimicrob Agents Chemother 46:1288-1294.
150. Choury D, Szajnert MF, Joly-Guillou ML, Azibi K, Delpech M, Paul G. 2000. Nucleotide sequence of the bla(RTG-2) (CARB-5) gene and phylogeny of a new group of carbenicillinases. Antimicrob Agents Chemother 44:1070-1074.
151. Melano R, Petroni A, Garutti A, Saka HA, Mange L, Pasteran F, Rapoport M, Rossi A, Galas M. 2002. New carbenicillin-hydrolyzing beta-lactamase (CARB-7) from Vibrio cholerae non-O1, non-O139 strains encoded by the VCR region of the V. cholerae genome. Antimicrob Agents Chemother 46:2162-2168.

152. Philippon AM, Paul GC, Thabaut AP, Jacoby GA. 1986. Properties of a novel carbenicillin-hydrolyzing beta-lactamase (CARB-4) specified by an IncP-2 plasmid from Pseudomonas aeruginosa. Antimicrob Agents Chemother 29:519-520.
153. Potron A, Poirel L, Croize J, Chanteperdrix V, Nordmann P. 2009. Genetic and biochemical characterization of the first extended-spectrum CARB-type beta-lactamase, RTG-4, from Acinetobacter baumannii. Antimicrob Agents Chemother 53:3010-3016.
154. Jensen RV, Depasquale SM, Harbolick EA, Hong T, Kernell AL, Kruchko DH, Modise T, Smith CE, McCarter LL, Stevens AM. 2013. Complete Genome Sequence of Prepandemic Vibrio parahaemolyticus BB22OP. Genome Announc 1(1).
155. Kalburge SS, Polson SW, Boyd Crotty K, Katz L, Turnsek M, Tarr CL, Martinez-Urtaza J, Boyd EF. 2014. Complete Genome Sequence of Vibrio parahaemolyticus Environmental Strain UCM-V493. Genome Announc 2(2).
156. Gomez-Jimenez S, Noriega-Orozco L, Sotelo-Mundo RR, Cantu-Robles VA, Cobian-Guemes AG, Cota-Verdugo RG, Gamez-Alejo LA, Del Pozo-Yauner L, Guevara-Hernandez E, Garcia-Orozco KD, Lopez-Zavala AA, Ochoa-Leyva A. 2014. High-Quality Draft Genomes of Two Vibrio parahaemolyticus Strains Aid in Understanding Acute Hepatopancreatic Necrosis Disease of Cultured Shrimps in Mexico. Genome Announc 2(4).
157. Gomez-Gil B, Soto-Rodriguez S, Lozano R, Betancourt-Lozano M. 2014. Draft Genome Sequence of Vibrio parahaemolyticus Strain M0605, Which Causes Severe Mortalities of Shrimps in Mexico. Genome Announc 2(2).
158. Kondo H, Tinwongger S, Proespraiwong P, Mavichak R, Unajak S, Nozaki R, Hirono I. 2014. Draft Genome Sequences of Six Strains of Vibrio parahaemolyticus Isolated from Early Mortality Syndrome/Acute Hepatopancreatic Necrosis Disease Shrimp in Thailand. Genome Announc 2(2).
159. Haendiges J, Timme R, Allard M, Myers RA, Payne J, Brown EW, Evans P, Gonzalez-Escalona N. 2014. Draft Genome Sequences of Clinical Vibrio parahaemolyticus Strains Isolated in Maryland (2010 to 2013). Genome Announc 2(4).

160. Lachapelle J, Dufresne J, Levesque RC. 1991. Characterization of the blaCARB-3 gene encoding the carbenicillinase-3 beta-lactamase of Pseudomonas aeruginosa. Gene 102:7-12.
161. Petroni A, Melano RG, Saka HA, Garutti A, Mange L, Pasteran F, Rapoport M, Miranda M, Faccone D, Rossi A, Hoffman PS, Galas MF. 2004. CARB-9, a carbenicillinase encoded in the VCR region of Vibrio cholerae non-O1, non-O139 belongs to a family of cassette-encoded beta-lactamases. Antimicrob Agents Chemother 48:4042-4046.
162. Takahashi I, Tsukamoto K, Harada M, Sawai T. 1983. Carbenicillin-hydrolyzing penicillinases of Proteus mirabilis and the PSE-type penicillinases of Pseudomonas aeruginosa. Microbiol Immunol 27:995-1004.
163. Mammeri H, Poirel L, Mangeney N, Nordmann P. 2003. Chromosomal integration of a cephalosporinase gene from Acinetobacter baumannii into Oligella urethralis as a source of acquired resistance to beta-lactams. Antimicrob Agents Chemother 47:1536-1542.
164. Teo JW, Suwanto A, Poh CL. 2000. Novel beta-lactamase genes from two environmental isolates of Vibrio harveyi. Antimicrob Agents Chemother 44:1309-1314.
165. Chiou J, Li R, Chen S. 2015. CARB-17 family of beta-lactamases mediates intrinsic resistance to penicillins in Vibrio parahaemolyticus. Antimicrob Agents Chemother 59:3593-3595.
166. Capra EJ, Laub MT. 2012. Evolution of two-component signal transduction systems. Annu Rev Microbiol 66:325-347.
167. Li RC, Chiou JC, Chan EWC, Chen S. 2016. A Novel PCR-Based Approach for Accurate Identification of Vibrio parahaemolyticus. Front Microbiol 7:44.
168. Qi M, Sun FJ, Caetano-Anolles G, Zhao Y. 2010. Comparative genomic and phylogenetic analyses reveal the evolution of the core two-component signal transduction systems in enterobacteria. J Mol Evol 70:167-180.
169. Felsenstein J. 1985. Confidence-Limits on Phylogenies - an Approach Using the Bootstrap. Evolution 39:783-791.
170. Tamura K, Nei M, Kumar S. 2004. Prospects for inferring very large phylogenies by using the neighbor-joining method. Proc Natl Acad Sci U S A 101:11030-11035.

171. Tamura K, Stecher G, Peterson D, Filipski A, Kumar S. 2013. MEGA6: Molecular Evolutionary Genetics Analysis Version 6.0. Mol Biol Evol 30:2725-2729.
172. Sawabe T, Ogura Y, Matsumura Y, Feng G, Amin AR, Mino S, Nakagawa S, Sawabe T, Kumar R, Fukui Y, Satomi M, Matsushima R, Thompson FL, Gomez-Gil B, Christen R, Maruyama F, Kurokawa K, Hayashi T. 2013. Updating the Vibrio clades defined by multilocus sequence phylogeny: proposal of eight new clades, and the description of Vibrio tritonius sp. nov. Front Microbiol 4:414.
173. Di Pinto A, Terio V, Novello L, Tantillo G. 2011. Comparison between thiosulphate-citrate-bile salt sucrose (TCBS) agar and CHROMagar Vibrio for isolating Vibrio parahaemolyticus. Food Control 22:124-127.
174. Izumiya H, Matsumoto K, Yahiro S, Lee J, Morita M, Yamamoto S, Arakawa E, Ohnishi M. 2011. Multiplex PCR assay for identification of three major pathogenic Vibrio spp., Vibrio cholerae, Vibrio parahaemolyticus, and Vibrio vulnificus. Mol Cell Probes 25:174-176.
175. Bej AK, Patterson DP, Brasher CW, Vickery MCL, Jones DD, Kaysner CA. 1999. Detection of total and hemolysin-producing Vibrio parahaemolyticus in shellfish using multiplex PCR amplification of tl, tdh and trh. J Microbiol Methods 36:215-225.
176. Bauer A, Rorvik LM. 2007. A novel multiplex PCR for the identification of Vibrio parahaemolyticus, Vibrio cholerae and Vibrio vulnificus. Lett Appl Microbiol 45:371-375.
177. Neogi SB, Chowdhury N, Asakura M, Hinenoya A, Haldar S, Saidi SM, Kogure K, Lara RJ, Yamasaki S. 2010. A highly sensitive and specific multiplex PCR assay for simultaneous detection of Vibrio cholerae, Vibrio parahaemolyticus and Vibrio vulnificus. Lett Appl Microbiol 51:293-300.
178. Ward LN, Bej AK. 2006. Detection of Vibrio parahaemolyticus in shellfish by use of multiplexed real-time PCR with TaqMan fluorescent probes. Appl Environ Microbiol 72:2031-2042.
179. Liu B, He XH, Chen WY, Yu SJ, Shi CL, Zhou XJ, Chen J, Wang DP, Shi XM. 2012. Development of a real time PCR assay for rapid detection of Vibrio parahaemolyticus from seafood. Protein & Cell 3:204-212.

180. Vinothkumar K, Bhardwaj AK, Ramamurthy T, Niyogi SK. 2013. Triplex PCR assay for the rapid identification of 3 major Vibrio species, Vibrio cholerae, Vibrio parahaemolyticus, and Vibrio fluvialis. Diagn Microbiol Infect Dis 76:526-528.
181. Turton JF, Woodford N, Glover J, Yarde S, Kaufmann ME, Pitt TL. 2006. Identification of Acinetobacter baumannii by detection of the blaOXA-51-like carbapenemase gene intrinsic to this species. J Clin Microbiol 44:2974-2976.
182. Chiou J, Li R, Chen S. 2015. CARB-17 family of beta-lactamases mediated intrinsic resistance to penicillins in Vibrio parahaemolyticus. Antimicrob Agents Chemother 59:3593-3595.
183. Thompson CC, Thompson FL, Vicente ACP, Swings J. 2007. Phylogenetic analysis of vibrios and related species by means of atpA gene sequences. Int J Syst Evol Microbiol 57:2480-2484.
184. Xie ZY, Hu CQ, Chen C, Zhang LP, Ren CH. 2005. Investigation of seven Vibrio virulence genes among Vibrio alginolyticus and Vibrio parahaemolyticus strains from the coastal mariculture systems in Guangdong, China. Lett Appl Microbiol 41:202-207.
185. Klein SL, West CKG, Mejia DM, Lovell CR. 2014. Genes Similar to the Vibrio parahaemolyticus Virulence-Related Genes tdh, tlh, and vscC2 Occur in Other Vibrionaceae Species Isolated from a Pristine Estuary. Appl Environ Microbiol 80:595-602.
186. Dickinson G, Lim KY, Jiang SC. 2013. Quantitative Microbial Risk Assessment of Pathogenic Vibrios in Marine Recreational Waters of Southern California. Appl Environ Microbiol 79:294-302.
187. Kim YB, Okuda J, Matsumoto C, Takahashi N, Hashimoto S, Nishibuchi M. 1999. Identification of Vibrio parahaemolyticus strains at the species level by PCR targeted to the toxR gene. J Clin Microbiol 37:1173-1177.
188. Chen W, Xie Y, Xu J, Wang Q, Gu M, Yang J, Zhou M, Wang D, Shi C, Shi X. 2012. Molecular typing of Vibrio parahaemolyticus isolates from the middle-east coastline of China. Int J Food Microbiol 153:402-412.

189. Sani NA, Ariyawansa S, Babji AS, Hashim JK. 2013. The risk assessment of Vibrio parahaemolyticus in cooked black tiger shrimps (Penaeus monodon) in Malaysia. Food Control 31:546-552.
190. Gutierrez West CK, Klein SL, Lovell CR. 2013. High frequency of virulence factor genes tdh, trh, and tlh in Vibrio parahaemolyticus strains isolated from a pristine estuary. Appl Environ Microbiol 79:2247-2252.
191. Tsai SE, Jong KJ, Tey YH, Yu WT, Chiou CS, Lee YS, Wong HC. 2013. Molecular characterization of clinical and environmental Vibrio parahaemolyticus isolates in Taiwan. Int J Food Microbiol 165:18-26.
192. Paydar M, Teh CSJ, Thong KL. 2013. Prevalence and characterisation of potentially virulent Vibrio parahaemolyticus in seafood in Malaysia using conventional methods, PCR and REP-PCR. Food Control 32:13-18.
193. CLSI. 2005. Methods for Antimicrobial Dilution and Disk Susceptibility Testing of Infrequently Isolated or Fastidious Bacteria; Proposed Guideline. CLSI document M45-P, Wayne, PA: Clinical and Laboratory Standards Institute.
194. CLSI. 2014. Performance Standards for Antimicrobial Susceptibility Testing ; Twenty-third informational supplement. CLSI document M100-S23, Wayne, PA: Clinical and Laboratory Standards Institute.
195. Dallenne C, Da Costa A, Decre D, Favier C, Arlet G. 2010. Development of a set of multiplex PCR assays for the detection of genes encoding important beta-lactamases in Enterobacteriaceae. J Antimicrob Chemother 65:490-495.
196. Carattoli A, Bertini A, Villa L, Falbo V, Hopkins KL, Threlfall EJ. 2005. Identification of plasmids by PCR-based replicon typing. J Microbiol Methods 63:219-228.
197. Verdet C, Gautier V, Chachaty E, Ronco E, Hidri N, Decre D, Arlet G. 2009. Genetic Context of Plasmid-Carried bla(CMY-2)-Like Genes in Enterobacteriaceae. Antimicrob Agents Chemother 53:4002-4006.
198. Khan AA, Cheng CM, Van KT, West CS, Nawaz MS, Khan SA. 2006. Characterization of class 1 integron resistance gene cassettes in Salmonella enterica serovars Oslo and Bareily from imported seafood. J Antimicrob Chemother 58:1308-1310.

199. Bortolaia V, Hansen KH, Nielsen CA, Fritsche TR, Guardabassi L. 2014. High diversity of plasmids harbouring blaCMY-2 among clinical Escherichia coli isolates from humans and companion animals in the upper Midwestern USA. J Antimicrob Chemother 69:1492-1496.
200. Wiesner M, Calva E, Fernandez-Mora M, Cevallos MA, Campos F, Zaidi MB, Silva C. 2011. Salmonella Typhimurium ST213 is associated with two types of IncA/C plasmids carrying multiple resistance determinants. BMC Microbiol 11:9.
201. Call DR, Singer RS, Meng D, Broschat SL, Orfe LH, Anderson JM, Herndon DR, Kappmeyer LS, Daniels JB, Besser TE. 2010. blaCMY-2-positive IncA/C plasmids from Escherichia coli and Salmonella enterica are a distinct component of a larger lineage of plasmids. Antimicrob Agents Chemother 54:590-596.
202. Borjesson S, Jernberg C, Brolund A, Edquist P, Finn M, Landen A, Olsson-Liljequist B, Tegmark Wisell K, Bengtsson B, Englund S. 2013. Characterization of plasmid-mediated AmpC-producing E. coli from Swedish broilers and association with human clinical isolates. Clin Microbiol Infect 19:E309-311.
203. Giles WP, Benson AK, Olson ME, Hutkins RW, Whichard JM, Winokur PL, Fey PD. 2004. DNA sequence analysis of regions surrounding blaCMY-2 from multiple Salmonella plasmid backbones. Antimicrob Agents Chemother 48:2845-2852.
204. Zong Z, Partridge SR, Iredell JR. 2009. A blaVEB-1 variant, blaVEB-6, associated with repeated elements in a complex genetic structure. Antimicrob Agents Chemother 53:1693-1697.
205. Poirel L, Naas T, Guibert M, Chaibi EB, Labia R, Nordmann P. 1999. Molecular and biochemical characterization of VEB-1, a novel class A extended-spectrum beta-lactamase encoded by an Escherichia coli integron gene. Antimicrob Agents Chemother 43:573-581.
206. Lahiri SD, Alm RA. 2016. Identification of Novel VEB beta-Lactamase Enzymes and Their Impact on Avibactam Inhibition. Antimicrob Agents Chemother 60:3183-3186.

207. Woodford N, Zhang J, Kaufmann ME, Yarde S, Tomas Mdel M, Faris C, Vardhan MS, Dawson S, Cotterill SL, Livermore DM. 2008. Detection of Pseudomonas aeruginosa isolates producing VEB-type extended-spectrum beta-lactamases in the United Kingdom. J Antimicrob Chemother 62:1265-1268.
208. Naas T, Bogaerts P, Bauraing C, Degheldre Y, Glupczynski Y, Nordmann P. 2006. Emergence of PER and VEB extended-spectrum beta-lactamases in Acinetobacter baumannii in Belgium. J Antimicrob Chemother 58:178-182.
209. CLSI. 2010. Methods for antimicrobial dilution and disk susceptibility testing of infrequently isolated or fastidious bacteria; approved guideline, 2nd ed. CLSI document M45-A2:Clinical and Laboratory Standards Institute, Wayne, PA.
210. Xie M, Lin D, Chen K, Chan EW, Yao W, Chen S. 2016. Molecular Characterization of Escherichia coli Strains Isolated from Retail Meat That Harbor blaCTX-M and fosA3 Genes. Antimicrob Agents Chemother 60:2450-2455.
211. Alikhan NF, Petty NK, Ben Zakour NL, Beatson SA. 2011. BLAST Ring Image Generator (BRIG): simple prokaryote genome comparisons. BMC Genomics 12:402.
212. Vallenet D, Nordmann P, Barbe V, Poirel L, Mangenot S, Bataille E, Dossat C, Gas S, Kreimeyer A, Lenoble P, Oztas S, Poulain J, Segurens B, Robert C, Abergel C, Claverie JM, Raoult D, Medigue C, Weissenbach J, Cruveiller S. 2008. Comparative analysis of Acinetobacters: three genomes for three lifestyles. PLoS One 3:e1805.
213. Maurya AP, Das Talukdar A, Chanda DD, Chakravarty A, Bhattacharjee A. 2014. Integron-Borne Transmission of VEB-1 Extended-Spectrum beta-Lactamase in Pseudomonas aeruginosa in a Tertiary Care Hospital in India. Antimicrob Agents Chemother 58:6966-6969.
214. Naas T, Aubert D, Lambert T, Nordmann P. 2006. Complex genetic structures with repeated elements, a sul-type class 1 integron, and the bla(VEB) extended-spectrum beta-lactamase gene. Antimicrob Agents Chemother 50:1745-1752.
215. Ye L, Li R, Lin D, Zhou Y, Fu A, Ding Q, Chan EW, Yao W, Chen S. 2016. Characterization of an IncA/C Multidrug Resistance Plasmid in Vibrio alginolyticus. Antimicrob Agents Chemother 60:3232-3235.

216. Xia R, Guo X, Zhang Y, Xu H. 2010. qnrVC-like gene located in a novel complex class 1 integron harboring the ISCR1 element in an Aeromonas punctata strain from an aquatic environment in Shandong Province, China. Antimicrob Agents Chemother 54:3471-3474.
217. Loftie-Eaton W, Rawlings DE. 2012. Diversity, biology and evolution of IncQ-family plasmids. Plasmid 67:15-34.
218. Ito H, Ishii H, Akiba M. 2004. Analysis of the complete nucleotide sequence of an Actinobacillus pleuropneumoniae streptomycin-sulfonamide resistance plasmid, pMS260. Plasmid 51:41-47.
219. Smalla K, Jechalke S, Top EM. 2015. Plasmid Detection, Characterization, and Ecology. Microbiol Spectr 3.
220. Cain AK, Hall RM. 2013. Evolution of IncHI1 plasmids: Two distinct lineages. Plasmid 70:201-208.
221. Carattoli A. 2009. Resistance plasmid families in Enterobacteriaceae. Antimicrob Agents Chemother 53:2227-2238.
222. Alvarado A, Garcillan-Barcia MP, de la Cruz F. 2012. A degenerate primer MOB typing (DPMT) method to classify gamma-proteobacterial plasmids in clinical and environmental settings. PLoS One 7:e40438.
223. Cabello FC, Godfrey HP, Buschmann AH, Dolz HJ. 2016. Aquaculture as yet another environmental gateway to the development and globalisation of antimicrobial resistance. Lancet Infect Dis 16:E127-E133.
224. Poirel L, Cattoir V, Nordmann P. 2012. Plasmid-Mediated Quinolone Resistance; Interactions between Human, Animal, and Environmental Ecologies. Front Microbiol 3:24.
225. Nonaka L, Maruyama F, Miyamoto M, Miyakoshi M, Kurokawa K, Masuda M. 2012. Novel Conjugative Transferable Multiple Drug Resistance Plasmid pAQU1 from Photobacterium damselae subsp damselae Isolated from Marine Aquaculture Environment. Microbes Environ 27:263-272.
226. Nonaka L, Maruyama F, Onishi Y, Kobayashi T, Ogura Y, Hayashi T, Suzuki S, Masuda M. 2014. Various pAQU plasmids possibly contribute to disseminate tetracycline resistance gene tet(M) among marine bacterial community. Front Microbiol 5.

227. Li R, Wong MH, Zhou Y, Chan EW, Chen S. 2015. Complete nucleotide sequence of a conjugative plasmid carrying blaPER-1. Antimicrob Agents Chemother 59:3582-3584.
228. Marti E, Variatza E, Balcazar JL. 2014. The role of aquatic ecosystems as reservoirs of antibiotic resistance. Trends Microbiol 22:36-41.
229. Li R, Lin D, Chen K, Wong MH, Chen S. 2015. First detection of AmpC beta-lactamase blaCMY-2 on a conjugative IncA/C plasmid in Vibrio parahaemolyticus of food origin. Antimicrob Agents Chemother 59:4106-4111.
230. Overbeek R, Olson R, Pusch GD, Olsen GJ, Davis JJ, Disz T, Edwards RA, Gerdes S, Parrello B, Shukla M, Vonstein V, Wattam AR, Xia FF, Stevens R. 2014. The SEED and the Rapid Annotation of microbial genomes using Subsystems Technology (RAST). Nucleic Acids Res 42:D206-D214.
231. Darling AE, Treangen TJ, Messeguer X, Perna NT. 2007. Analyzing patterns of microbial evolution using the mauve genome alignment system. Methods Mol Biol 396:135-152.
232. Bankevich A, Nurk S, Antipov D, Gurevich AA, Dvorkin M, Kulikov AS, Lesin VM, Nikolenko SI, Pham S, Prjibelski AD, Pyshkin AV, Sirotkin AV, Vyahhi N, Tesler G, Alekseyev MA, Pevzner PA. 2012. SPAdes: a new genome assembly algorithm and its applications to single-cell sequencing. J Comput Biol 19:455-477.
233. Sullivan MJ, Petty NK, Beatson SA. 2011. Easyfig: a genome comparison visualizer. Bioinformatics 27:1009-1010.
234. Carattoli A, Zankari E, Garcia-Fernandez A, Larsen MV, Lund O, Villa L, Aarestrup FM, Hasman H. 2014. In Silico Detection and Typing of Plasmids using PlasmidFinder and Plasmid Multilocus Sequence Typing. Antimicrob Agents Chemother 58:3895-3903.
235. Seemann T. 2014. Prokka: rapid prokaryotic genome annotation. Bioinformatics 30:2068-2069.
236. Page AJ, Cummins CA, Hunt M, Wong VK, Reuter S, Holden MT, Fookes M, Falush D, Keane JA, Parkhill J. 2015. Roary: rapid large-scale prokaryote pan genome analysis. Bioinformatics 31:3691-3693.

237. Garcillan-Barcia MP, Francia MV, de la Cruz F. 2009. The diversity of conjugative relaxases and its application in plasmid classification. FEMS Microbiol Rev 33:657-687.
238. Dallenne C, Da Costa A, Decre D, Favier C, Arlet G. 2010. Development of a set of multiplex PCR assays for the detection of genes encoding important beta-lactamases in Enterobacteriaceae. J Antimicrob Chemother 65:490-495.
239. Poirel L, Cabanne L, Vahaboglu H, Nordmann P. 2005. Genetic environment and expression of the extended-spectrum beta-lactamase blaPER-1 gene in gram-negative bacteria. Antimicrob Agents Chemother 49:1708-1713.
240. Zong Z. 2014. The complex genetic context of blaPER-1 flanked by miniature inverted-repeat transposable elements in Acinetobacter johnsonii. PLoS One 9:e90046.
241. Zhao JY, Mu XD, Zhu YQ, Xi L, Xiao Z. 2015. Identification of an integron containing the quinolone resistance gene qnrA1 in Shewanella xiamenensis. FEMS Microbiol Lett 362:fnv146.
242. Wu J, Xie L, Zhang F, Ni Y, Sun J. 2015. Molecular characterization of ISCR1-mediated blaPER-1 in a non-O1, non-O139 Vibrio cholerae strain from China. Antimicrob Agents Chemother doi:10.1128/AAC.00166-15.
243. Wang R, Yu D, Yue J, Kan B. 2016. Variations in SXT elements in epidemic Vibrio cholerae O1 El Tor strains in China. Sci Rep 6:22733.
244. Chalmers R, Sewitz S, Lipkow K, Crellin P. 2000. Complete nucleotide sequence of Tn10. J Bacteriol 182:2970-2972.
245. Doublet B, Schwarz S, Kehrenberg C, Cloeckaert A. 2005. Florfenicol resistance gene floR is part of a novel transposon. Antimicrob Agents Chemother 49:2106-2108.
246. Barraud O, Ploy MC. 2015. Diversity of Class 1 Integron Gene Cassette Rearrangements Selected under Antibiotic Pressure. J Bacteriol 197:2171-2178.
247. del Castillo CS, Hikima J, Jang HB, Nho SW, Jung TS, Wongtavatchai J, Kondo H, Hirono I, Takeyama H, Aoki T. 2013. Comparative Sequence Analysis of a Multidrug-Resistant Plasmid from Aeromonas hydrophila. Antimicrob Agents Chemother 57:120-129.
248. Yuan J, Yamaichi Y, Waldor MK. 2011. The three vibrio cholerae chromosome II-encoded ParE toxins degrade

chromosome I following loss of chromosome II. J Bacteriol 193:611-619.
249. Toleman MA, Bennett PM, Walsh TR. 2006. ISCR elements: Novel gene-capturing systems of the 21st century? Microbiol Mol Biol Rev 70:296-316.
250. Chen YT, Liao TL, Liu YM, Lauderdale TL, Yan JJ, Tsai SF. 2009. Mobilization of qnrB2 and ISCR1 in plasmids. Antimicrob Agents Chemother 53:1235-1237.
251. Nordmann P, Ronco E, Naas T, Duport C, Michel-Briand Y, Labia R. 1993. Characterization of a novel extended-spectrum beta-lactamase from Pseudomonas aeruginosa. Antimicrob Agents Chemother 37:962-969.
252. Xia RR, Guo XH, Zhang YZ, Xu H. 2010. qnrVC-Like Gene Located in a Novel Complex Class 1 Integron Harboring the ISCR1 Element in an Aeromonas punctata Strain from an Aquatic Environment in Shandong Province, China. Antimicrob Agents Chemother 54:3471-3474.
253. Wang FP, Wu KH, Sun JJ, Wang Q, Chen Q, Yu SY, Rui YY. 2012. Novel ISCR1-linked resistance genes found in multidrug-resistant Gram-negative bacteria in southern China. Int J Antimicrob Agents 40:404-408.
254. Toleman MA, Bennett PM, Walsh TR. 2006. Common regions e.g. orf513 and antibiotic resistance: IS91-like elements evolving complex class 1 integrons. J Antimicrob Chemother 58:1-6.
255. Toleman MA, Walsh TR. 2011. Combinatorial events of insertion sequences and ICE in Gram-negative bacteria. FEMS Microbiol Rev 35:912-935.
256. Connor TR, Owen SV, Langridge G, Connell S, Nair S, Reuter S, Dallman TJ, Corander J, Tabing KC, Le Hello S, Fookes M, Doublet B, Zhou Z, Feltwell T, Ellington MJ, Herrera S, Gilmour M, Cloeckaert A, Achtman M, Parkhill J, Wain J, De Pinna E, Weill FX, Peters T, Thomson N. 2016. What's in a Name? Species-Wide Whole-Genome Sequencing Resolves Invasive and Noninvasive Lineages of Salmonella enterica Serotype Paratyphi B. MBio 7.
257. Xie L, Wu J, Zhang F, Han L, Guo X, Ni Y, Sun J. 2016. Molecular Epidemiology and Genetic Characteristics of Various blaPER Genes in Shanghai, China. Antimicrob Agents Chemother 60:3849-3853.

258. Toleman MA, Bennett PM, Walsh TR. 2006. ISCR elements: novel gene-capturing systems of the 21st century? Microbiol Mol Biol Rev 70:296-316.
259. Vilacoba E, Almuzara M, Gulone L, Traglia GM, Figueroa SA, Sly G, Fernandez A, Centron D, Ramirez MS. 2013. Emergence and spread of plasmid-borne tet(B)::ISCR2 in minocycline-resistant Acinetobacter baumannii isolates. Antimicrob Agents Chemother 57:651-654.
260. Arpin C, Thabet L, Yassine H, Messadi AA, Boukadida J, Dubois V, Coulange-Mayonnove L, Andre C, Quentin C. 2012. Evolution of an incompatibility group IncA/C plasmid harboring blaCMY-16 and qnrA6 genes and its transfer through three clones of Providencia stuartii during a two-year outbreak in a Tunisian burn unit. Antimicrob Agents Chemother 56:1342-1349.
261. Loftie-Eaton W, Yano H, Burleigh S, Simmons RS, Hughes JM, Rogers LM, Hunter SS, Settles ML, Forney LJ, Ponciano JM, Top EM. 2016. Evolutionary Paths That Expand Plasmid Host-Range: Implications for Spread of Antibiotic Resistance. Mol Biol Evol 33:885-897.
262. Cain AK, Hall RM. 2012. Evolution of IncHI2 plasmids via acquisition of transposons carrying antibiotic resistance determinants. J Antimicrob Chemother 67:1121-1127.
263. Norrby SR, Nord CE, Finch R, European Society of Clinical M, Infectious D. 2005. Lack of development of new antimicrobial drugs: a potential serious threat to public health. Lancet Infect Dis 5:115-119.
264. Falagas ME, Rafailidis PI, Matthaiou DK. 2010. Resistance to polymyxins: Mechanisms, frequency and treatment options. Drug Resist Updat 13:132-138.
265. Falagas ME, Kasiakou SK. 2005. Colistin: the revival of polymyxins for the management of multidrug-resistant gram-negative bacterial infections. Clin Infect Dis 40:1333-1341.
266. Falagas ME, Kasiakou SK. 2006. Toxicity of polymyxins: a systematic review of the evidence from old and recent studies. Crit Care 10:R27.
267. Olaitan AO, Morand S, Rolain JM. 2014. Mechanisms of polymyxin resistance: acquired and intrinsic resistance in bacteria. Front Microbiol 5:643.

268. Liu YY, Wang Y, Walsh TR, Yi LX, Zhang R, Spencer J, Doi Y, Tian G, Dong B, Huang X, Yu LF, Gu D, Ren H, Chen X, Lv L, He D, Zhou H, Liang Z, Liu JH, Shen J. 2016. Emergence of plasmid-mediated colistin resistance mechanism MCR-1 in animals and human beings in China: a microbiological and molecular biological study. Lancet Infect Dis 16:161-168.
269. Ye H, Li Y, Li Z, Gao R, Zhang H, Wen R, Gao GF, Hu Q, Feng Y. 2016. Diversified mcr-1-Harbouring Plasmid Reservoirs Confer Resistance to Colistin in Human Gut Microbiota. MBio 7.
270. Rapoport M, Faccone D, Pasteran F, Ceriana P, Albornoz E, Petroni A, Group MCR, Corso A. 2016. mcr-1-mediated colistin resistance in human infections caused by Escherichia coli: First description in Latin America. Antimicrob Agents Chemother 60:4412-4413.
271. Shen Z, Wang Y, Shen Y, Shen J, Wu C. 2016. Early emergence of mcr-1 in Escherichia coli from food-producing animals. Lancet Infect Dis 16:293.
272. Doumith M, Godbole G, Ashton P, Larkin L, Dallman T, Day M, Day M, Muller-Pebody B, Ellington MJ, de Pinna E, Johnson AP, Hopkins KL, Woodford N. 2016. Detection of the plasmid-mediated mcr-1 gene conferring colistin resistance in human and food isolates of Salmonella enterica and Escherichia coli in England and Wales. J Antimicrob Chemother doi:10.1093/jac/dkw093.
273. Li A, Yang Y, Miao M, Chavda KD, Mediavilla JR, Xie X, Feng P, Tang YW, Kreiswirth BN, Chen L, Du H. 2016. Complete sequences of mcr-1-harboring plasmids from extended spectrum beta-lactamase (ESBL)- and carbapenemase-producing Enterobacteriaceae (CPE). Antimicrob Agents Chemother 60:4351-4354.
274. Malhotra-Kumar S, Xavier BB, Das AJ, Lammens C, Butaye P, Goossens H. 2016. Colistin resistance gene mcr-1 harboured on a multidrug resistant plasmid. Lancet Infect Dis 16:283-284.
275. Tegetmeyer HE, Jones SC, Langford PR, Baltes N. 2008. ISApl1, a novel insertion element of Actinobacillus pleuropneumoniae, prevents ApxIV-based serological

detection of serotype 7 strain AP76. Vet Microbiol 128:342-353.
276. Institute CaLS. Performance Standards for Antimicrobial Susceptibility Testing: Twenty-fourth Informational Supplement M100-S24. CLSI, Wayne, PA, USA, 2014.
277. Luo R, Liu B, Xie Y, Li Z, Huang W, Yuan J, He G, Chen Y, Pan Q, Liu Y, Tang J, Wu G, Zhang H, Shi Y, Liu Y, Yu C, Wang B, Lu Y, Han C, Cheung DW, Yiu SM, Peng S, Xiaoqian Z, Liu G, Liao X, Li Y, Yang H, Wang J, Lam TW, Wang J. 2012. SOAPdenovo2: an empirically improved memory-efficient short-read de novo assembler. Gigascience 1:18.
278. Zankari E, Hasman H, Cosentino S, Vestergaard M, Rasmussen S, Lund O, Aarestrup FM, Larsen MV. 2012. Identification of acquired antimicrobial resistance genes. J Antimicrob Chemother 67:2640-2644.
279. Carattoli A, Zankari E, Garcia-Fernandez A, Voldby Larsen M, Lund O, Villa L, Moller Aarestrup F, Hasman H. 2014. In silico detection and typing of plasmids using PlasmidFinder and plasmid multilocus sequence typing. Antimicrob Agents Chemother 58:3895-3903.
280. Kiss J, Olasz F. 1999. Formation and transposition of the covalently closed IS30 circle: the relation between tandem dimers and monomeric circles. Mol. Microbiol 34:37-52.
281. Li R, Xie M, Zhang J, Yang Z, Liu L, Liu X, Zheng Z, Chan EW-C, Chen S. 2016. Genetic characterization of mcr-1-bearing plasmids to depict molecular mechanisms underlying dissemination of the colistin resistance determinant. J Antimicrob Chemother 72:393-401.
282. Zurfluh K, Klumpp J, Nuesch-Inderbinen M, Stephan R. 2016. Full-length nucleotide sequences of mcr-1 harboring plasmids isolated from extended-spectrum beta-lactamase (ESBL)-producing Escherichia coli of different origins. Antimicrob Agents Chemother 60:5589-5591.
283. Yu H, Qu F, Shan B, Huang B, Jia W, Chen C, Li A, Miao M, Zhang X, Bao C, Xu Y, Chavda KD, Tang YW, Kreiswirth BN, Du H, Chen L. 2016. Detection of mcr-1 colistin resistance gene in carbapenem-resistant Enterobacteriaceae (CRE) from different hospitals in China. Antimicrob Agents Chemother 60:5033-5035.

284. Kiss J, Szabo M, Olasz F. 2003. Site-specific recombination by the DDE family member mobile element IS30 transposase. Proc Natl Acad Sci U S A 100:15000-15005.
285. Xavier BB, Lammens C, Ruhal R, Kumar-Singh S, Butaye P, Goossens H, Malhotra-Kumar S. 2016. Identification of a novel plasmid-mediated colistin-resistance gene, mcr-2, in Escherichia coli, Belgium, June 2016. Euro Surveill 21.
286. Billard-Pomares T, Fouteau S, Jacquet ME, Roche D, Barbe V, Castellanos M, Bouet JY, Cruveiller S, Medigue C, Blanco J, Clermont O, Denamur E, Branger C. 2014. Characterization of a P1-like bacteriophage carrying an SHV-2 extended-spectrum beta-lactamase from an Escherichia coli strain. Antimicrob Agents Chemother 58:6550-6557.
287. Shin J, Ko KS. 2015. A Plasmid Bearing the bla(CTX-M-15) Gene and Phage P1-Like Sequences from a Sequence Type 11 Klebsiella pneumoniae Isolate. Antimicrob Agents Chemother 59:6608-6610.
288. Zhi C, Lv L, Yu LF, Doi Y, Liu JH. 2016. Dissemination of the mcr-1 colistin resistance gene. Lancet Infect Dis 16:292-293.
289. Elnahriry SS, Khalifa HO, Soliman AM, Ahmed AM, Hussein AM, Shimamoto T, Shimamoto T. 2016. Emergence of Plasmid-Mediated Colistin Resistance Gene mcr-1 in a Clinical Escherichia coli Isolate from Egypt. Antimicrob Agents Chemother 60:3249-3250.
290. He S, Hickman AB, Varani AM, Siguier P, Chandler M, Dekker JP, Dyda F. 2015. Insertion Sequence IS26 Reorganizes Plasmids in Clinically Isolated Multidrug-Resistant Bacteria by Replicative Transposition. MBio 6:e00762.
291. Olasz F, Farkas T, Kiss J, Arini A, Arber W. 1997. Terminal inverted repeats of insertion sequence IS30 serve as targets for transposition. J Bacteriol 179:7551-7558.
292. Petrillo M, Angers-Loustau A, Kreysa J. 2016. Possible genetic events producing colistin resistance gene mcr-1. Lancet Infect Dis 16:280.